modelling of the diffusion of gases through membranes of novel polyimides

Evert Smit

MODELLING OF THE DIFFUSION OF GASES THROUGH MEMBRANES OF NOVEL POLYIMIDES

PROEFSCHRIFT

ter verkrijging van
de graad van doctor aan de Universiteit Twente,
op gezag van de rector magnificus
prof. dr. ir. J.H.A. de Smit
volgens besluit van het College van Dekanen
in het openbaar te verdedigen
op woensdag 19 juni 1991 te 14.00 uur

door

EVERT SMIT

geboren op 11 juli 1961 te Delft

Dit proefschrift is goedgekeurd door de promotor prof. dr. C.A. Smolders.
Assistent-promotor: dr. ing. M.H.V. Mulder.

VOORWOORD

Onder de schitterende begeleiding van Paul Kamps ben ik in 1987 in het kader van een BRITE project aan de UT gestart. Samen met de assistenten Herman en Robert is toen eigenlijk al het fundament gelegd voor het onderzoek zoals dat in dit boekje beschreven staat. Veel van het echte werk is verricht door mijn doctoraal/bijvak studenten Bernard-Jan, Jan en Henri. Maar niet alleen tijdens werkuren heb ik veel plezier van en met hen gehad. Eventueel onder het genot van een drankje zijn vele zaken ook buiten de werksfeer de revue gepasseerd. In dat zelfde kader wil ik ook mijn kamergenoten Remko en Ingrid en die hele fantastische vakgroep bedanken.
Werken in een grote organisatie als de UT vergt een soepele samenwerking. "Onze" secretaresses Bartie, Julia en Annemieke, de portiers (m/v), de kantine-dames, John Heeks, Jan Heezen: we kunnen het echt niet zonder jullie. Samenwerking met de groep van prof. Feil, en in het bijzonder met Hans van Eerden, Sybolt Harkema en Wim Briels heeft een grote invloed gehad op mijn proefschrift, zoals de oplettende lezer zal opvallen. Maar samenwerking strekt verder: de medewerkers van het HF-NMR centrum aan de K.U. Nijmegen die mij enorm geholpen hebben bij het uitwerken van mijn ideëen over het gebruik van vaste-stof NMR bij mijn onderzoek. Jammer dat er niet iets moois is uitgekomen, dat is zeker niet hun schuld. Met Joop Bitter (voorheen KSLA) heb ik vele geanimeerde en zinvolle gesprekken gehad. With our modern communication methods cooperation can easily be made world-wide. I am very grateful for the exchange of information, thoughts, and very *hot* data with Hisao Takeuchi of Mitsubishi Kasei Corp., Japan. We will be in touch!

Als dan alles opgeschreven moet worden blijkt eigenlijk pas goed waarom je niet zonder een goed promoter als Kees Smolders kunt. Of de assistent-promotor Marcel Mulder. Ingo Blume heeft als laatste "screener", gewaardeerde gesprekspartner en wandelende membraan-encyclopedie een duidelijk stempel op mijn werk gedrukt. In goede tijden en slechte tijden heeft Thonie van den Boomgaard mij bijgestaan. Ja, en mijn paranimfen Mariska en Sylvia zullen dat zeker ook voor, tijdens en na de promotie-plechtigheid doen.
En dan komt het op het uitgeven van het boekje aan. Dat het zo is als het nu voor U ligt is te danken aan de lay-out capaciteiten van Fons Haenraets. In (nachtelijk) stress-sessies is het toch nog goed gekomen. De kunst in het boekje is van Saskia van der Linden. Ik ben er erg verguld mee.

De warmte, belangstelling, het geduld en de kookkunst van mijn vrienden en vriendinnen hebben me in de schrijfperiode in leven gehouden. Maar ook daarbuiten kan ik niet zonder ze overleven! En hier is een extra dank voor Judith op zijn plaats. Mijn ouders en oma horen zeker thuis in dit dankwoord (wat eigenlijk een betere titel zou zijn), voor alle enthousiasme en stimulering. Zonder hen zou ik niet zijn wie ik ben.

Evert

This thesis was entirely written and typeset on Apple Macintosh, using Nisus (wordprocessing and lay-out), Canvas (drawing), ChemIntosh (chemical structures drawing), Expressionist (mathematical formulas), WingZ (spreadsheet) and CricketGraph (charting). Printing was done on a Hewlett-Packard DeskWriter using ATM. The body-font is New Century Schoolbook, headers and figure titles are in Stone Sans.

Smit, Evert
Modelling of the diffusion of gases through membranes of novel polyimides/ Evert Smit. - [S.l. : s.n.]. - Ill.
Proefschrift Enschede. - Met lit. opg.
ISBN 90-9004246-6
Trefw.: gasdiffusie / polymeren

Druk: Krips Repro, Meppel

Cover and other art: Saskia van der Linden

opgedragen aan *Felis domestica*

CONTENTS

CHAPTER ONE

INTRODUCTION

CHAPTER TWO

GAS TRANSPORT THROUGH A POLYMER MATRIX

CHAPTER THREE

POLYMER STRUCTURE AND DIFFUSION

CHAPTER FOUR

AN ADVANCED MATRIX MODEL FOR THE DIFFUSION OF GASES THROUGH POLYMERIC MEMBRANES

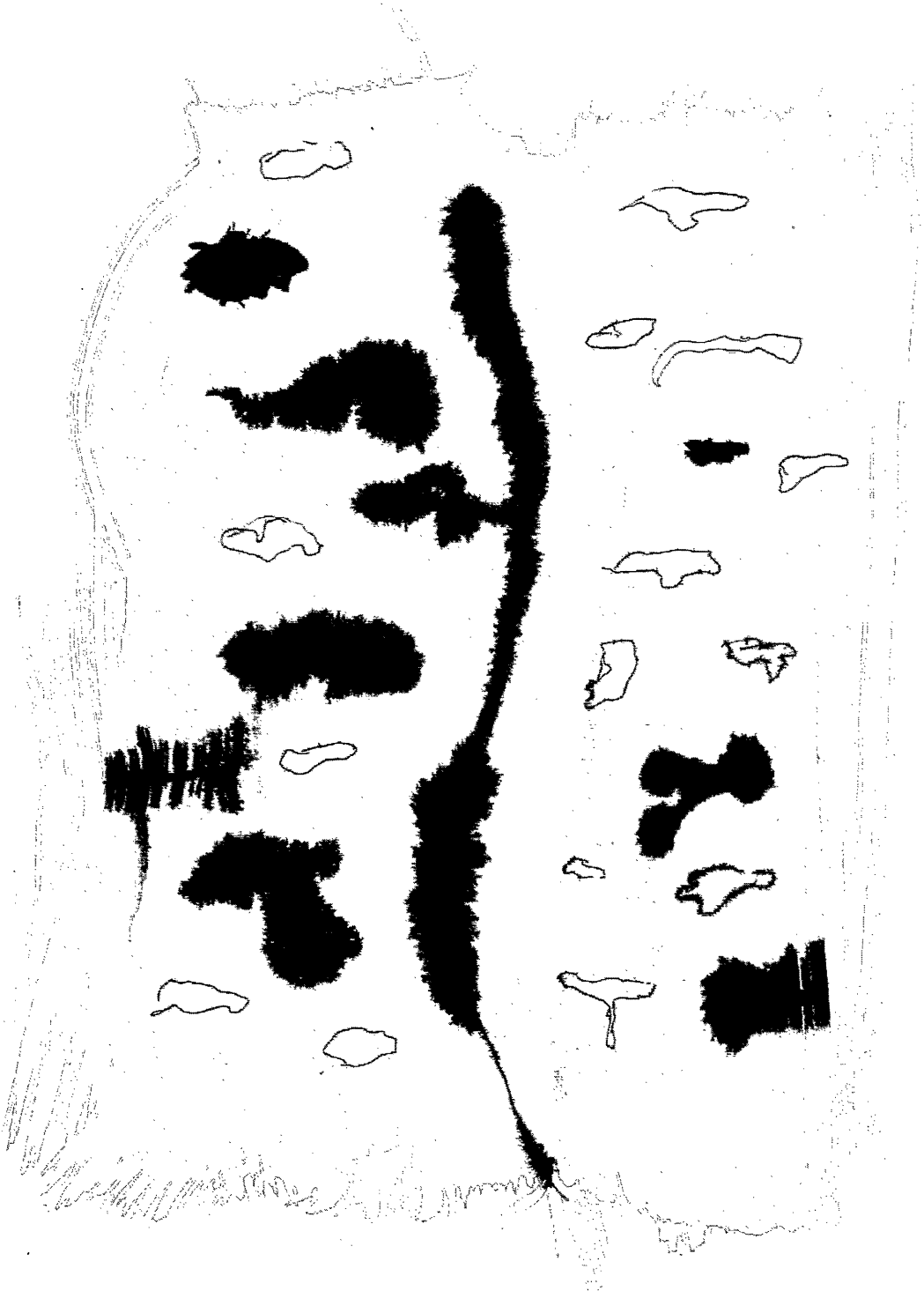

CHAPTER ONE
INTRODUCTION

Membranes for gas separation

CONTENTS

1.1 General introduction: Membranes for gas separation

What is a membrane? This simple question is not very easily answered as can be deduced from the editorial discussions in the principal journal on membranes, the *Journal of Membrane Science* [1,2]. Editor H.K. Lonsdale could not find a satisfactory definition in the *Webster's New Collegiate Dictionary*: "Membrane. 1. A thin soft pliable sheet or layer of animal or plant origin. 2. A piece of parchement forming part of a roll." Nor could it be found in the *McGraw-Hill Dictionary of Scientific and Technical Terms (2nd ed.)*: "Membrane [Chem. Eng.] 1. The medium through which the fluid stream is passed for purposes of filtration. 2. The ion-exchange medium used in dialysis, diffusion, osmosis and reverse osmosis, and electrodialysis. [Histol.] A thin layer of tissue...".

It will be clear that membranes deserve a much more comprehensive definition, since the areas in which they can be, *and are* used is growing day after day. In response to Lonsdale's question for the perfect definition the most appropriate one to my opinion, albeit not short, was given by J.A. Quinn of the University of Pennsylvania [2]:

> "A membrane is an interphase. It has distinct physicochemical properties and it is bounded by two surfaces, each of which joins it to a contiguous bulk phase. Generally it is "thin" – in the sense that it has a large ratio of surface area to volume; as its thickness approaches molecular dimensions the interphase becomes an interface. The special separative/barrier/contacting properties of membranes derive from the fact that an interphase can communicate simultaneously with its two adjacent phases; this permits the establishment and maintenance of gradients across the membrane and allows exchange to occur at both surfaces."

What stands out from the given definitions is that "a membrane isn't just an object in the abstract, but its definition must embody its function" (H.K. Lonsdale [2]).

Besides discussing the benefits of membranes for gas separation we will also summarize alternative processes to separate gas mixtures.

1.2 What is the mechanism of gas separation by membranes?

This is indeed the main question raised in this thesis. A large number of research activities throughout the world is devoted to solve this problem [see reviews 3-7], each lifting a small corner of the veil.
Membranes for the separation of gases can be considered to *act as molecular sieves*. This view is of course somewhat too simple, but may be suitable as a first order approach. The membrane can distinguish, by some mechanism ultimately to be clarified, between (gas) molecules of different size, shape and/or polarity/polarizability. For example, most polymers discriminate reasonably well between carbon dioxide and methane. When a mixture of these gases is brought under pressure in contact with a thin film of, for instance, one of the polyimides studied in this thesis, CO_2 typically passes the membrane about 50 times faster then CH_4. The *permeability* for carbon dioxide is 50 times higher than for methane, so the *selectivity* is said to be 50. Since the gas molecules do not differ very much in size (the Van der Waals volume of CO_2 is 70.9Å^3 and of CH_4 71.0Å^3 [8]), but noticeably in polarizability, one is tempted to take this single property directly responsible for the large difference in permeability. But the explanations are not that simple. Why do CH_4 molecules, while being larger than N_2 molecules (65.0 Å^3 [8]), and of comparable polarizability, still move faster through most polymers studied? And why is this general behavior reversed in 6FDA-based polyimides [9], the group of polyimides studied most intensively in this thesis?

At first the basic aspects of gas separation will be described. The permeability $\mathbb{P}$ of a gas through a polymer is controlled by the product of two distinctly different parameters, the *solubility* $\mathbb{S}$ and the *diffusivity* $\mathbb{D}$. Wrobleski formulated this relation already in 1879 [10]:

$$\mathbb{P} = \mathbb{S} \cdot \mathbb{D}$$

The solubility is mainly determined by the ease of condensation. This can be related to the location of the critical point. The higher the condensability, the larger the sorption will be. The second parameter, the *diffusivity* $\mathbb{D}$ (actually the mobility in the direction of the pressure-, or concentration-gradient) contributes equally to the total permeability. The faster the gas molecules can move through the polymer under unit gradient, the higher $\mathbb{P}$ will be.
In figure 1.1 the process of sorption, diffusion and desorption is shown schematically. An effective separation is based on the cooperative differences in $\mathbb{S}$ and $\mathbb{D}$ of the gases.

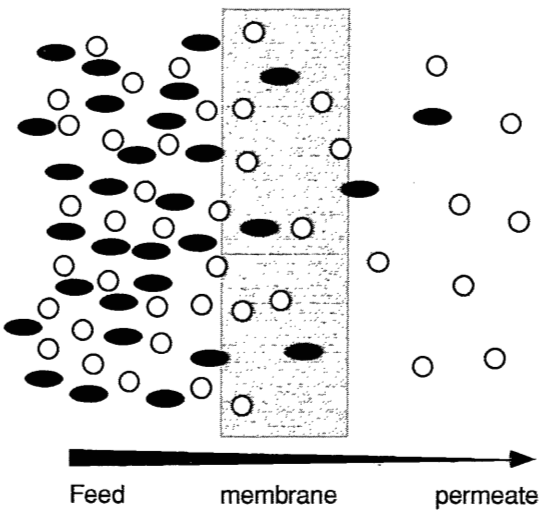

FIGURE 1.1: PERMEATION OF GASES: SORPTION AT THE FEED INTERFACE, DIFFUSION THROUGH THE MEMBRANE, DESORPTION AT THE OPPOSITE INTERFACE

Excellent reviews on the mechanism of *permeation* are numerous [e.g. 3,4,7]. Since our research concentrates on the process of diffusion we will refrain from reciting general permeation models here.

The diffusivity (mobility) of the gas through a polymer is described in literature mainly on the basis of the *statistical model* for transport, based on the free volume theory of DiBenedetto [11]. The constraints of creating fluctuations in local packing density constitute the rate determining

factor. These fluctuations cause the formation of free volume or even micro-voids in the polymer. If an interstice which is large enough is formed near a gas molecule there is a probability to advance into it, thereby effectively moving onward. It is possible to form complete pathways, along which the gas molecules can move (almost like the micro-channels in zeolites). The probability to create a free volume element large enough to accommodate a gas molecule is directly related to the diffusivity. The size of the penetrant is also a factor which determines $\mathbb{D}$.
A more sophisticated form of this model is the *site-change model* [12,13]. The fluctuations within the polymer material are due to the thermal energy. Locally, the (cooperative) thermal motion allows chain segments to change their position, and gas molecules can then be transferred. This site-change is an activated process, because an energy barrier has to be overcome. The size of the gas molecule directly influences the transport rate: more segments must move to allow a larger gas molecule to pass (a larger local free volume is needed), and consequently a larger amount of energy is required.
In this thesis the gas transport will be described at a molecular scale on the basis of these models.

1.3 A survey of gas separation techniques and possible applications

A number of possible applications for gas separation are described in review articles [14-16], and only a few will be mentioned here.
Most applications can be found in the chemical industry, where often gaseous process streams have to be purified by separation of the produced components. Also for the production of pure compounds gas separation is essential. Examples are the recovery of hydrogen from ammonia and water-gas, the oxygen or nitrogen enrichment from air, the drying of process gases, and the production of purge nitrogen or CO_2 in enhanced oil recovery. Natural gas sweetening (removal of acidic gases like CO_2 and H_2S, see figure 1.2) is of major interest for commercial gas winning.

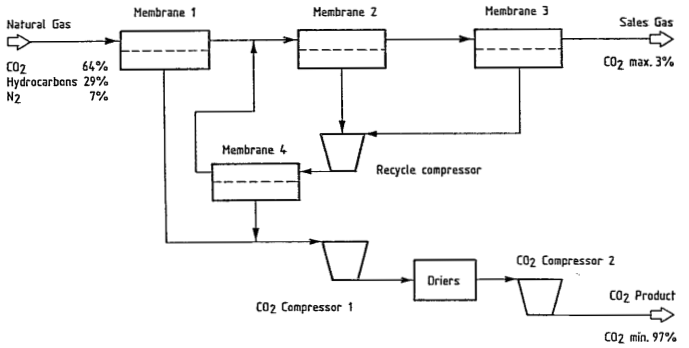

FIGURE 1.2: NATURAL GAS SWEETENING PROCESS USING MEMBRANE TECHNOLOGY [14]

Gas separation under severe operation conditions like high pressures and high temperatures is necessary in natural gas sweetening, so the separation method employed must be robust here.

Another question may arise while reading this chapter: why using *membranes* for gas separation? It is a fact that membranes are being used more frequently in the (industrial) gas separation field. The main reason for this fact is the increasingly competitive properties of membrane separation if compared to conventional separation methods like cryogenic distillation and pressure swing adsorption (PSA) [14,15].
There are four mature methods for the commercial separation of gases.

1. Cryogenic distillation

The separation is based on the difference in boiling point of the (liquefied) gases. This is a very well established technique. The installation design can be compact, the production capacity is typically 100 tons per m^3 of installation per day. Furthermore the operation is continuous, and, not unimportant: the scale-up of the installation is simple. The purity of the products is high to very high, which is not always required. The low operation temperature and high energy consumption are disadvantageous points.

2. Absorption (e.g. in treatment of sour gas with amine)
This process is moderately selective, especially for chemically active compounds. The operation temperature lies in a convenient range, while the process can be made continuous. A more recent development involves the use of molten salt, especially for high grade purity gases. An example is [17]:

$$2\ NaNO_2 + O_2 \xrightarrow{+\Delta T} 2\ NaNO_3 \xrightarrow{-\Delta T} 2\ NaNO_2 + O_2$$

This latter example is a highly energy consuming, thus expensive technique, and a proper heat-exchange design is necessary.

3. Adsorption (particularly PSA)
In pressure swing adsorption (PSA) the gas mixture is pressurized over a specific sorbent. Separation is achieved because of different rates of adsorption. Before equilibrium has been reached the process is stopped and the gases are desorbed by decreasing the pressure, see figure 1.3.

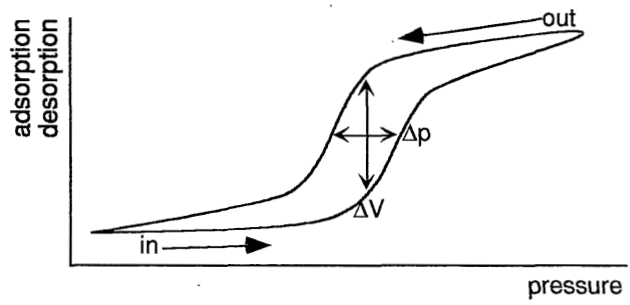

FIGURE 1.3: SCHEMATIC REPRESENTATION OF THE MECHANISM OF PRESSURE SWING ADSORPTION

The technique is also suited for the removal of trace amounts of high boiling contaminants, which will adsorb more strongly on the adsorbent. The purity obtained can be very high, the energy consumption is relatively low. The losses due to the necessary regeneration of the adsorbent can be significant, however. A typical PSA installation is shown schematically in figure 1.4:

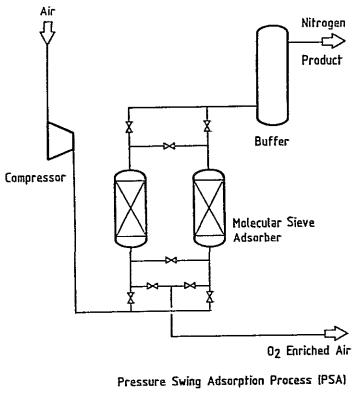

FIGURE 1.4: PRESSURE SWING ADSORPTION INSTALLATION (SCHEMATICALLY) [14]

PSA is a cyclic, semi-continuous process.

4. Membrane based gas separations

The membrane separation process is fairly specific and favors active gases like CO_2. It is best suited for small to medium scale use and is most attractive if only medium purity is needed. In figure 1.5 a typical membrane separation set-up is shown.

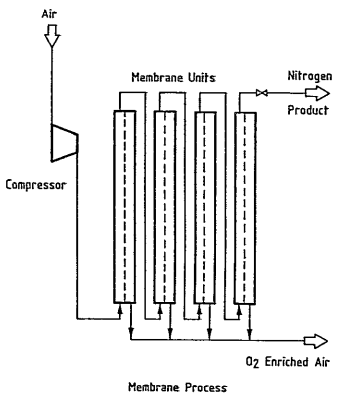

FIGURE 1.5: TYPICAL MEMBRANE INSTALLATION (COUNTER CURRENT FLOW) [14]

In general the feed pressure is adjustable and can range from low (air separation) to high (dictated in e.g. natural gas sweetening). It is a continuous process, but not very suitable for large scale separation and high purity product gas requirements. The simplicity of operation and

the absence of a recycling step are very beneficial.
According to Haselden [17] the membrane process can be considered to be comparable to PSA: a pressure driven sorption into the membrane at the feed side, and low pressure desorption at the permeate side, but with the advantage of the elimination of the recycling step.

Conclusion
Membranes are only one of the options for gas separation installations, and not applicable in all situations.

1.4 When are membranes profitable for gas separation?

The main question that remains to be answered is: which qualities make membranes advantageous in the field of gas separation? J.A. Quinn states [2]: "When viewed as a contacting device a membrane has an additional degree of freedom over conventional bulk phase separations which have but one bounding surface and it is this feature which is unique to membranes." We might expect the membranes to be the Golden Fleece in gas separation. But the competitive techniques as mentioned in § 1.3 are well-established in the chemical industry, and each of them have their own characteristics. Membrane-based separation is a comparatively new technique, partly still in the developing stage. In figure 1.6 this is shown in a schematic manner. This graph was drawn on the blackboard during an informal session at the 5th BOC-Priestley conference in Birmingham, September 19-21, 1989. The G-factor stems from the outcry *gee*, expressing the state of exaltation of the industry for a specific method.

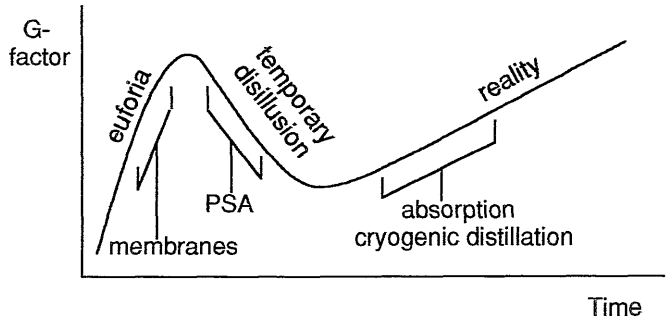

FIGURE 1.6: STAGES OF EVOLUTION OF DIFFERENT SEPARATION TECHNIQUES

Membranes are most likely to be used in new installations when they are supposed to be at least as good as the competitive techniques. At present membranes are mainly applied in medium scale plants which require only moderate purity. But large scale operations will undoubtedly be realized on short term since much effort is put in membrane research and module design nowadays. A comparison of the various processes in the production of nitrogen is shown in the next graph.

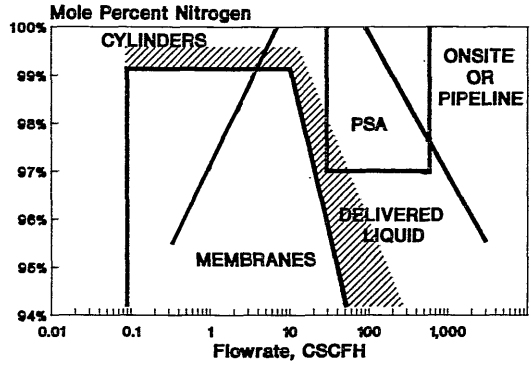

FIGURE 1.7: COMPARISON BETWEEN DIFFERENT SEPARATION PROCESSES FOR NITROGEN ENRICHMENT [16]

This graph indicates the possible commercial scale for membrane installations (taken from [16]). Similar graphs can be made for other gas production or purifying processes.

1.5 Research objectives and choice of the polymers

The study described in this thesis aims to relate physicochemical polymer properties to transport of gases through dense homogeneous membranes of two particular series of *polyimides*, based on 6FDA and SiDA dianhydride units, see figure 1.8.

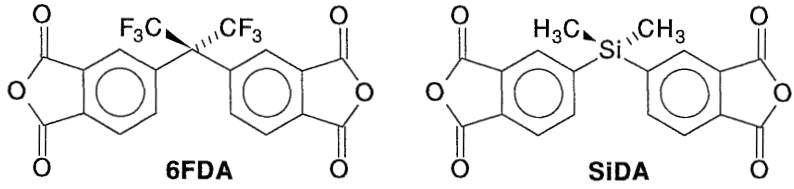

FIGURE 1.8: CHEMICAL STRUCTURES OF 6FDA- AND SIDA-UNITS IN THE POLYIMIDES STUDIED

These dianhydrides were coupled to a series of diamines, to give structures as exemplified in figure 1.9.

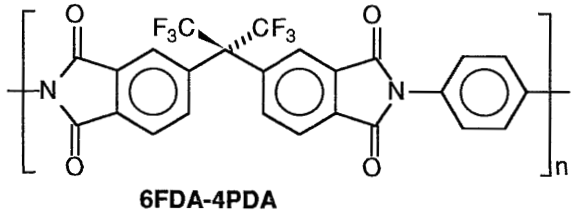

FIGURE 1.9: A POLYIMIDE CHEMICAL STRUCTURE (6FDA-4PDA)

The polymer series were chosen on the basis of various criteria. The first was the possible application in commercial systems. Polymers for this purpose should combine a high permeability with a high selectivity. From literature it is known that polymers are needed with a high chain rigidity. This kind of stiff polymers has a high mobility (diffusivity-) selectivity [9,18,19]. The objective is to fine-tune ('calibrate') the packing density to generate a polymer matrix with a narrow distribution in the free volume, comparable to molecular sieves. This will result in a high permeability selectivity. For this reason rubbery polymers are less suitable, although they show in general a much higher intrinsic permeability.
To understand the underlying processes in the separation of gases, which

is the fundamental topic of this research, more parameters than chain rigidity and packing density have to be considered. In order to obtain more information on permselectivity of polymers the relation between the molecular structure of the polymer and the diffusion- and permeation rate of small gas molecules (CO_2 and CH_4) was evaluated. The aim is to determine which of the structural parameters influences the transport of the gas molecules in a polymer membrane. Or even better, to be able to estimate these on forehand. Therefore we need to know exactly which parameters of a polymer influence the gas permeation (eventually: under actual process conditions). If we understand these factors it will help us to develop new materials in a more systematical way.

For our study *polyimides* were chosen because it is known from literature [19-21] that these polymers exhibit excellent thermal, chemical and mechanical properties, combined with good gas separation abilities and good processability.
Especially the 6FDA-polyimides (the 6FDA monomeric unit was displayed in figure 1.8) have excellent characteristics: a very high glass transition temperature (above 300°C), a high CO_2 permeability (up to 60 Barrer) and a high CO_2/CH_4-selectivity (generally over 35). These values are higher than of most other polymers, as can be seen from figure 1.10.

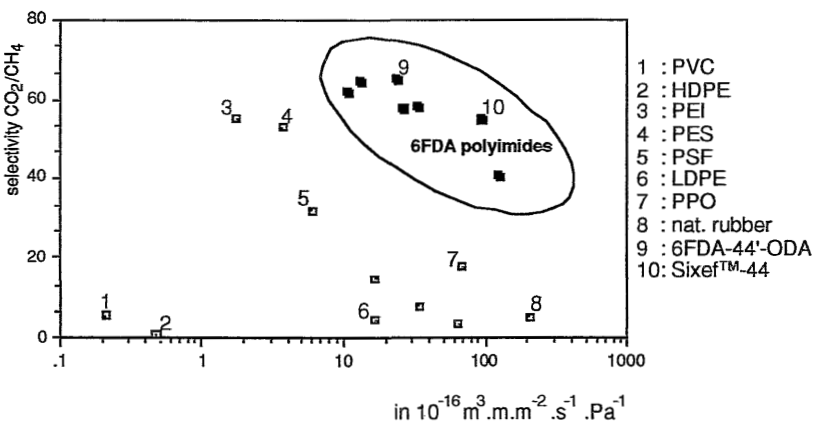

FIGURE 1.10: COMPARISON OF 6FDA-POLYIMIDES WITH COMMON POLYMERS

Furthermore, the polymer series chosen have a very versatile chemistry. The large, rigid 6FDA and SiDA dianhydride units have the advantage over other dianhydrides such as pyromellitic dianhydride (PMDA) or benzophenone tetracarboxylic dianhydride (BTDA) that soluble polyimides are obtained from which membranes can be prepared by phase inversion processes.
It is clear that the 6FDA-based polyimides have very promising properties, making them interesting for both fundamental scientific investigation and for industrial gas separation. All this makes these polyimides the choice *par excellence* for our study. For reasons of comparison, and to study the effect of small and precisely defined structural changes in the polymer backbone introduced by the dianhydride as well as the diamine, the second series was based on the silicon containing dianhydride SiDA (see figure 1.8).

The structures of all polyimides synthesized are given in Appendix C of Chapter 3. The two polyimide series both have the same general polymer properties necessary for a subtle systematic study: a high glass transition temperature, hence a large chain stiffness and a rather low packing density. Some effect of this is to be found back in the inter-chain interaction as reflected by the cohesive energy density (CED, see Chapters 2 and 3). Small structural variations show a broad range of experimental gas permeation and diffusion data. The results will be interpreted in terms of the structural differences (Chapters 2 and 3).

1.6 Relating polymer properties to chemical structure

This thesis will describe a study regarding some of the factors governing membrane behavior, especially its chemical structure–permeation relationship. It certainly will not give the definite answer(s) because a large number of parameters influence the membrane separation properties; these properties are:

- type of polymer; its chemical structure, chain rigidity, packing density (distribution), inter-chain interactions; these also influence the gas diffusivity and solubility
- type of gas or vapor mixture to be separated: condensability, molecular size, polarizability and polarity
- upstream pressure, also in relation to the feed mixture
- upstream/downstream pressure ratio
- operating temperature
- membrane architecture: symmetric (flat sheet), asymmetric (flat sheet or hollow fibre), composite (type of support, or toplayer coating)
- membrane dimensions: top layer thickness, support layer thickness
- state and history of the membrane: (pre-)swelling, temperature/pressure-history, aging
- additives in the membrane: plasticizers, anti-plasticizers

and equally important:

- module and process design

A number of these parameters influence each other, thereby indicating that the modelling of the separation/permeation mechanism is rather complex. It is not possible (yet, and it is doubtful that it will ever be), and not feasible, to present the absolute model. Hence this thesis will deal only with a few elements in the list of parameters that determine the membrane properties, namely those related to the fundamental aspects of *diffusivity* of CO_2 and CH_4 through dense polyimide membranes belonging to the two homologous series. The emphasis lies on the relation between the chemical structure and the gas diffusivity at moderate (5 Bar), constant upstream and negligible downstream pressure. We will attempt to visualize the polymer matrix at a molecular scale (the concept will be explained in Chapter 2), and try to deduce the parameters that directly influence the diffusivity of gas molecules through this matrix. The model of the matrix will be constructed in two ways: by classical methods (Chapters 2 and 3) and by *computer aided molecular modelling* (CAMM, Chapter 4). The computational method is a very promising

technique being utilized more and more frequently [22-24]. The reason is that powerful computers are becoming available at lower costs, and the computer programs are ever so more 'user friendly' by utilization of a graphical user interface. Hence, there is nothing that keeps the membranologist from using this technique anymore. With computer simulations it is possible to gain further insight in processes at a scale that cannot be envisioned in another way. However: one should be very careful in drawing the right conclusions from the data. It should be very well contemplated what was put into the computer model (by assumptions and empirical data), and what is actually generated. This point will be made clear in Chapters 3 and 4.

Literature

(1) Lonsdale, H.K., *J. Membr. Sci.*, **1987**, 34(2), 125

(2) Lonsdale, H.K., *J. Membr. Sci.*, **1989**, 43, 1

(3) Matson, S.L., Lopez, J. and Quinn, J.A., *Chem. Eng. Sci.*, **1983**, 38(4), 503

(4) Aminabhavi, T.M., Aithal, S.U. and Shuklu, S.S., *J.M.S.-Rev. Macromol. Chem. Phys.*, **1988**, C28 (3&4), 421

(5) Dugar'yan, S.G.(†), Yampol'skii, Yu.P. and Plate, N.A., *Russ. Chem. Rev.*, **1988**, 57(6), 549

(6) Chalykh, A.E., Zlobin, V.B., *Russ. Chem. Rev.*, **1988**, 57(6), 504

(7) Vieth, W.R., Howell, J.M. and Hsieh, J.H., *J. Membr. Sci.*, **1976**, 1, 177

(8) *Handbook of Chemistry and Physics*, Weast, R.C. and Astle, M.J., ed., CRC Press Inc., 59th edition **1979**, p. D-230

(9) Kim, T.H., Koros, W.J., Husk, G.R. & O'Brien, K.C., *J. Appl. Polym. Sci.*, **1987**, 34, 1767

(10) Wroblewski, S. von, Wied. Ann. Phys.,**1879**, 8, 29

(11) DiBenedetto, A.T., *J. Polym. Sci.*, **1963**, A1, 3477

(12) Bonart, R., Owen, A.J. & Paulus, I., *Coll. Polym. Sci.*, **1985**, 263, 435

(13) Pongratz, W., Ph.D. Thesis, University of Regensburg, Germany, **1990**

(14) Baldus, W. and D. Tillman, D., in: *Membranes in Gas Separation and Enrichment*, RSC special publication 62, **1987**, p. 26-42

(15) Baker, R.W. and Blume, I., *Chemtech*, **1986** ,16, 232

(16) Spillman, R.W., *Chem. Eng. Prog.*, **1989**, 85(1), 41

(17) Haselden,G.G., paper presented at the 5th BOC-Priestley conference in Birmingham, September 19-21, **1989**

(18) Kim, T.H., Koros, W.J. and Husk, G.R., *J. Membr. Sci.,* **1989**, 46, 43

(19) Kim, T.H., Ph.D. Dissertation, University of Texas at Austin, **1988**

(20) Hayes, R.A., U.S. Patents 4,717,394, **1988**, 4,838,900, **1989**

(21) Stern, S.A., Mi, Y., Tamamoto, H. and St. Clair, A.K., *J.Polym. Sci., Polym. Phys.*, **1989**, 17, 1887

(22) Sonnenburg, J., Gao, J. and Weiner, J.H., *Macromolecules*, **1990**, 23, 4653

(23) Takeuchi, H. & Okazaki, K., *J. Chem. Phys.*, **1990**, 92(2), 5643

(24) Shah, V.M., Stern, S.A. & Ludovice, P.J., *Macromolecules*, **1989**, 22, 4660

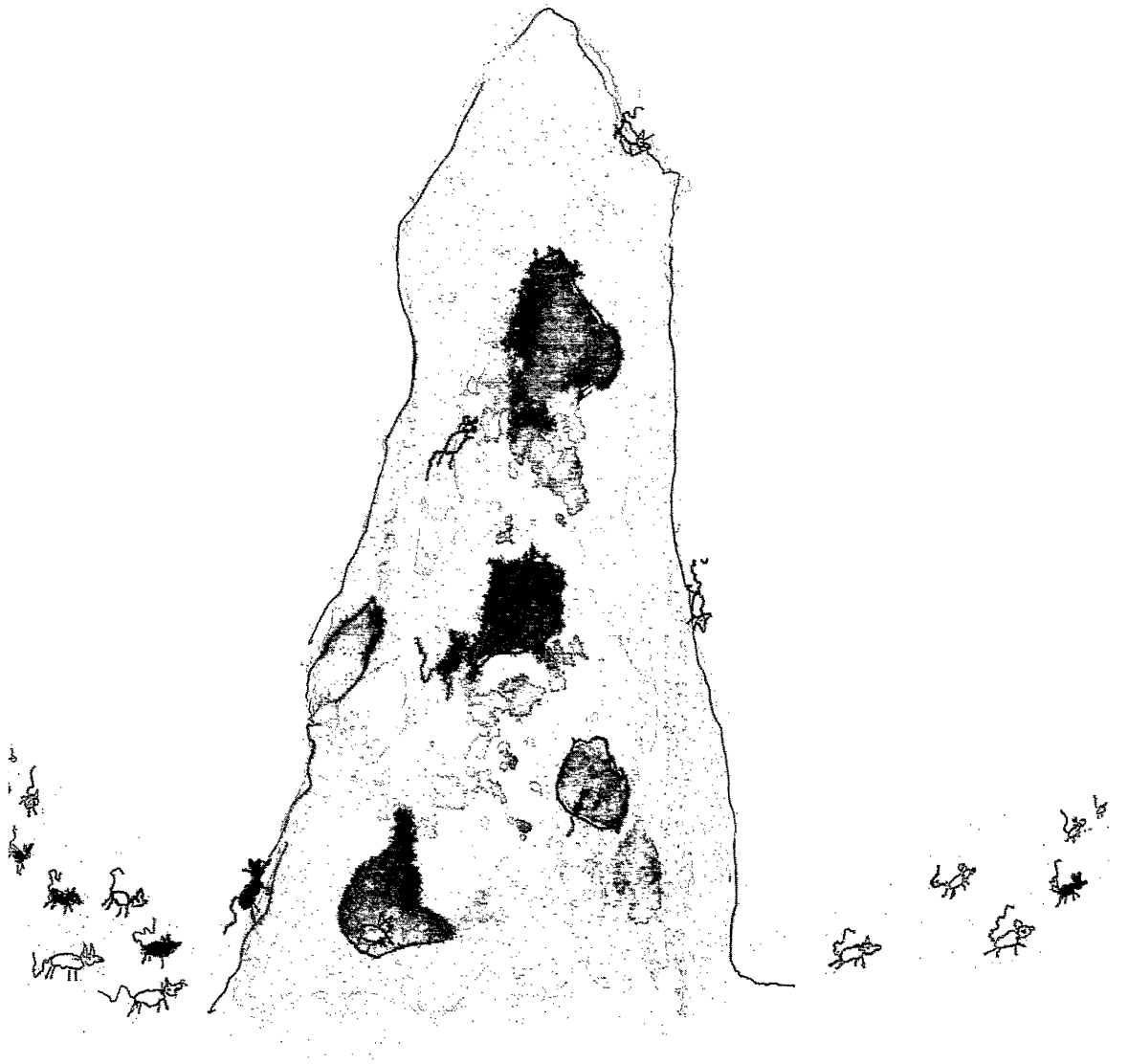

CHAPTER TWO

GAS TRANSPORT THROUGH A POLYMER MATRIX

Development of a molecular model of the polymer matrix

CONTENTS

2.1 Introduction

Why is the permeability of a certain type of gas through a certain polymer membrane higher than through another polymer? This is one of the main questions raised in this thesis. Several models have been proposed to explain the diffusion behavior of small molecules in polymers. These models can be classified as:

1. Molecular or matrix models [1-5] or as
2. Free volume models [6-8].

The matrix model relates the diffusivity of a penetrant molecule to specific polymer-penetrant interactions, and to the change in the matrix that is caused by this interaction. Polymer matrix parameters such as the flexibility of the polymer chains and matrix structure are main parameters limiting the rate of diffusion.
In the free volume model the fractional free volume present in the polymer matrix, and the size and shape of the gas molecule are the rate-determining parameters.
Since these models describe the same phenomena the theories should have corresponding backgrounds.
In order to explain the results obtained with newly synthesized polyimides, a combination of the matrix and the free volume model was followed which is described in this chapter. In the next chapter the detailed elaboration is presented.

The need for a more profound consideration of the different models was based on the first remarkable results using recently synthesized 6FDA-based polyimides. It appeared that the permeability (P) of the 6FDA polyimides, measured at room temperature, was related to the heat capacity jump ΔC_p at the glass transition temperature of these polymers (these parameters and their determination are further described below).

An increase in the permeability $\mathbb{P}$ was accompanied by a drop in the ΔC_p at T_g. By plotting log $\mathbb{P}$ versus ΔC_p a straight line was obtained as shown in figure 2.1.

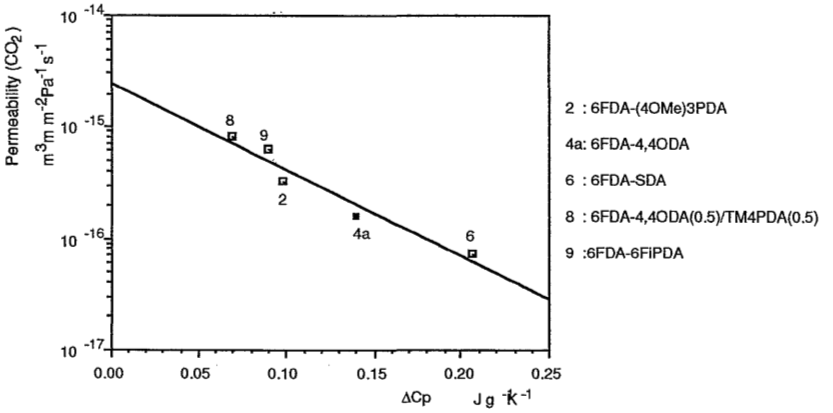

FIGURE 2.1: A LINEAR RELATION BETWEEN LOG $\mathbb{P}$ AND ΔC_p FOR SOME 6FDA POLYIMIDES

An example of the heat capacity jump at the glass transition temperature as measured with differential scanning calorimetry (DSC) is given in figure 2.2.

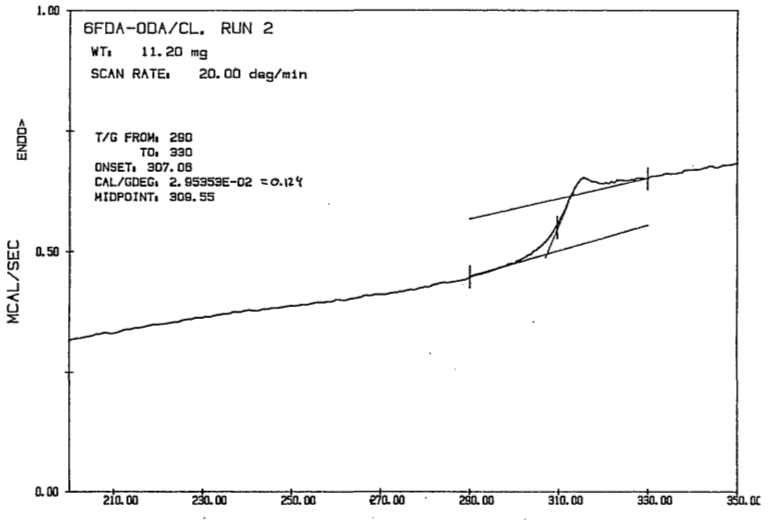

FIGURE 2.2: EXAMPLE OF A DSC GRAPH SHOWING THE ENTHALPY JUMP AT THE GLASS TRANSITION TEMPERATURE

What is the basis of the unexpected relation between the parameters ΔC_p and the permeability, which seem at first sight to refer to completely different processes? To discuss this further, both parameters will be considered in more detail.
The permeability can be divided into a sorption and a diffusion part. In this work the diffusivity $\mathbb{D}$ of a small penetrant (gas molecule) through a wide range of structurally closely related amorphous polyimides has been studied. From these observations it became clear that there is still a need for a more fundamental understanding of the *molecular mechanism* of diffusion of a gas molecule through a (glassy) polymer membrane. Ultimately, the aim is to look directly into the matrix, to actually spot the motions of the chains and the gas molecules which accompany the diffusion process. Since this is impossible, we need an accurate molecular model. The most advanced technique to accomplish this is *computer aided molecular modelling* (CAMM). This new method will be described in detail in Chapter 4.

In this chapter the objective is to visualize the factors that influence the diffusion of gases in an amorphous glassy polymer. At the origin lies the basic molecular structure of the polymer. Based on this structure an advanced model will be developed that takes into account the permeability related factors. These factors are then related to molecular processes occurring during the glass transition. In the next chapter the results are given and discussed using various polyimides, and further refinements for the model are given.

2.2 The polymer matrix: organization of the polymer chains

An amorphous polymer matrix is built up by a random organization of the chains. The matrix is considered as the sum of four sub–organizations, analogous to the terminology commonly used in biochemistry.

The first and most basic level is the **primary structure**, which is the chemical and electronic structure of the segmental units which are building the polymer chains.

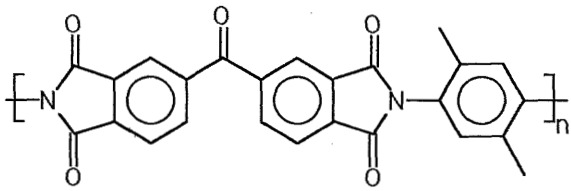

FIGURE 2.3: CHEMICAL STRUCTURE OF THE POLYMER

The primary structure dictates to a great extent the rotational freedom and packing ability inside the matrix. The cohesive energy density (CED, see § 2.3.6) and chain rigidity also depend largely on the electron density and electron distribution in the chain.

In the next level, the secondary structure or chain folding structure, the conformation of the chain is determined by the ability of the chain segments to move with respect to each other.

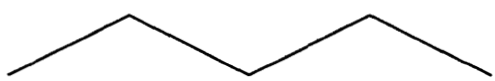

FIGURE 2.4: CHAIN FOLDING

This mobility-ability will be strongly temperature dependent, and is also set by the primary structure of the polymer.

The following level, the **tertiary structure**, represents the way in which the (folded) chains are packed to form a polymer matrix *in equilibrium*.

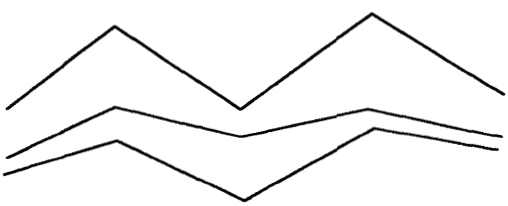

FIGURE 2.5: CHAIN PACKING TO FORM THE MATRIX

Apart from the dependence on the primary and secondary structure, the inter-chain (Lennard-Jones and electrostatic) attractions establish this

organization of the polymer chains. The chains cannot pack infinitely close, because of the Lennard-Jones repulsion and the rigidity of the chains. This results in a certain amount of non-occupied volume.

The last level of organization, the **quarternary structure**, is the most complex level. It displays the actual *non-equilibrium* state of the polymer matrix. Groups of chains arrange at more or less random locations in the matrix, like in the equilibrium state, while at other places they divide and open up to form voids in the matrix.

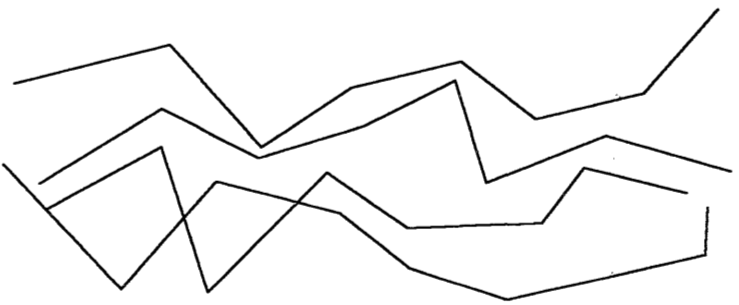

FIGURE 2.6: NON EQUILIBRIUM PACKING: LOCAL DENSITY- AND PACKING-FLUCTUATIONS

This state of the matrix is especially important in the case of glassy polymers, like the polyimides studied here. One of the major causes for the anomalous behavior of glassy polymers is the *excess free volume*, the result of the inability of the matrix to pack most efficiently, hence the existence of voids. Because of the large consequences for the transport of penetrants, the non-equilibrium state will be discussed in detail later. The actual organization of the chains will determine many of the polymer properties, such as the relaxation phenomenon. This relaxation is known to be related to the diffusivity of small molecules through polymers. This knowledge provides us with the links that will help explain the encountered relationship between $\mathbb{P}$ and ΔC_p.

2.3 A detailed look into the polymer matrix

For the gas transport the simple transport model proposed by Brandt [9] and Meares [10] will be used, and the effect of each organization level will be investigated.

When a gas molecule moves through a polymer matrix, the rate of diffusion can be limited by several factors. The main question is, what is the rate-determining factor.
First, a penetrant can move more or less freely within a domain given by some free volume element (hole), if this is large enough to accommodate the molecule. The movement of the gas molecules in the holes is very fast, much faster than could be expected from the effective diffusion coefficient [2]; this movement will certainly not be the rate-limiting step.
Secondly, to allow an effective motion in the direction of the concentration gradient, the penetrant has to overcome barriers imposed by polymer chains. The gas molecule moves from hole to hole through tunnels that open up in the direct neighborhood of it (see figure 2.7A). The opening of a void (of a specific size) in a glassy polymer has already been the subject of many studies [2,10-12], as has been the dependence of diffusion thereon. The opening of the tunnel is accomplished by (cooperative) thermal motion of some polymer segments.
The proposed diffusion model is quite similar to the cooperative site-change model used for explaining polymer relaxation behavior [13,14]. In glassy polymers the translational motion of polymer segments is restricted. Energy is required to move a few segments of the polymer chains in the matrix, in order to allow a translational movement of a penetrant. To some extent the process shown in figure 2.7A can be compared with a chemical reaction, according to the activated complex theory of Eyring, which is shown schematically in figure 2.7B.

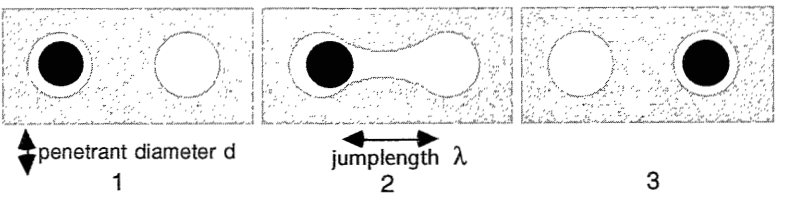

FIGURE 2.7A: OPENING AND CLOSING OF A TUNNEL IN THE MATRIX IN THE DIFFUSION PROCESS

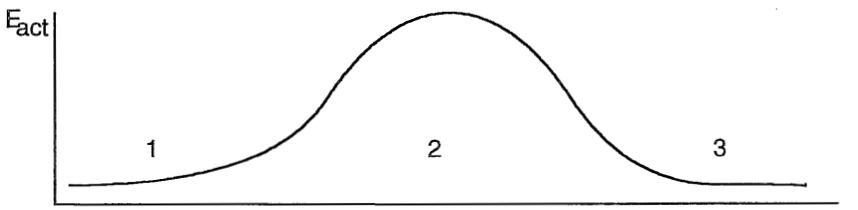

FIGURE 2.7B: OPENING OF THE TUNNEL IS AN ACTIVATED PROCESS

In order to pass through the potential energy maximum, adequate energy is needed to form situation 2. In the case of diffusion through a polymer, this is the activation energy of void formation E_h, the hole formation energy as defined by Meares [10]. For a penetrant to move on, a pathway has to be opened at least of the size of the penetrant, as was shown by Chen and Edin [11]. After opening up of the constriction a diffusional jump can be performed (see figure 2.7A). Since the movement of a single gas molecule is much faster than the movement of a (small) part of the polymer chain, the hole formation will be the rate-limiting step in the diffusion process [2,15].

2.3.1 Effect of the primary and secondary structure: chain rigidity

The chain rigidity is one of the most important properties of a polymer which is responsible for many of its bulk-properties, as stated by Privalko [16]. The chain stiffness is often expressed as the steric factor σ [17].

Within one class of polymers a linear relationship exists between σ and T_g [18]. However σ is not a single variable controlling T_g, different polymer classes show different dependencies (see figure 2.8).

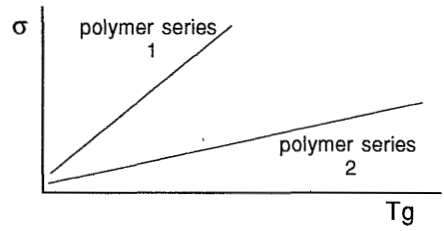

FIGURE 2.8: RELATION BETWEEN GLASS TRANSITION TEMPERATURE AND CHAIN RIGIDITY FOR DIFFERENT POLYMER CLASSES

The polymers within one class have a similarity in their primary structures. The 6FDA- or SiDA-based series of polyimides prepared for this study (see Chapter 3) have very similar chain backbones within each series. Therefore we may assume that for these two series of polyimides a linear relationship will exist between T_g and σ. Hence the T_g can be considered to be a convenient measure for the chain rigidity.

The chain rigidity influences the gas transport in two opposite ways:

- Stiffer chains hinder the ease of formation of new holes. Hence the overall chain mobility and thus the frequency of the creation of a hole will be lower. This will result in a decreased diffusivity.

- Stiffer chains hinder the efficient packing of the polymer matrix. This can be visualized by a 'spaghetti'-model as depicted in figure 2.9. The stiffer polymer chain will create relatively more large holes, and often also a higher overall free volume. Hence the diffusivity will be enhanced.

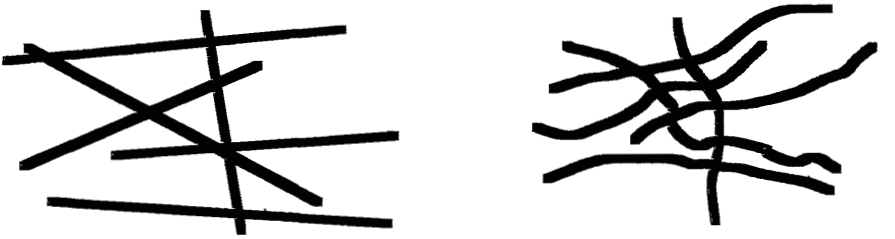

FIGURE 2.9: CHAIN RIGIDITY AFFECTING PACKING DENSITY

Another important side-effect of the lower packing density of the stiffer polymer type is the reduction of the inter-segment attractions. It is known that within one class of glassy polymers the ΔC_p (which is linearly related to the cohesive energy density (CED) as will be shown later) and T_g are inversely related: the product $\Delta C_p \cdot T_g$ is almost a constant [19]. This way a higher T_g will be accompanied by a smaller CED.
The overall effect of stiffer polymer chains will often be an enhanced diffusivity due to a greater free volume (with a broader distribution, see § 2.3.3-2.3.5), and thus the permeability will be higher.

The glass transition temperature is an indication for the presence of a highly rigid polymer chain. The glass transition temperatures of all 6FDA-polyimides are high, mostly well over 300°C, whereas the SiDA polyimides have a somewhat lower T_g, suggesting a more flexible backbone.
An interesting observation is that the glass transition temperatures of the meta-substituted polyimides are always significantly lower than the para-homologues (or isomers) as shown in Table 2.1

Table 2.1: Glass transition temperatures of some *meta*- and *para*-substituted 6FDA polyimides.

meta		*para*	
6FDA-3,3'DAPS	264°C	6FDA-4,4'DAPS	320°C
6FDA-3PDA	305°C	6FDA-4PDA	350°C
6FDA-3,4'ODA	269°C	6FDA-4,4'ODA	303°C.

The same observations were reported by Chern et al. [20] and Sykes [21] for different classes of polymers. This must be due to the more flexible polymer chains of the meta-substituted polyimides. In Chapter 3 a more detailed discussion and a possible explanation for this phenomenon will be given.

2.3.2 Effect of the tertiary and quaternary structure: packing density

The packing density of the matrix is certainly a very important parameter determining the permeability of a gas: the lower the packing density the more easily gases will diffuse. One of the reasons of the high permeability of 6FDA-polyimides are the large trifluoromethyl groups which inhibit dense packing, as shown schematically in figure 2.10.

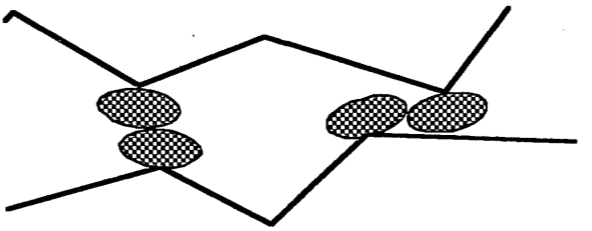

FIGURE 2.10: BULKY SIDE GROUPS INHIBIT DENSE PACKING

However, inter-molecular forces, chain rigidity and polymer history must also be taken into account when considering the packing density.

Askadskii [22] shows a way to determine accurately the packing density of a polymer. His method is in principle a refined group contribution method. By adding the volume increments of each atom (which depends on its direct surroundings) the total volume of a polymeric repeat unit can be calculated:

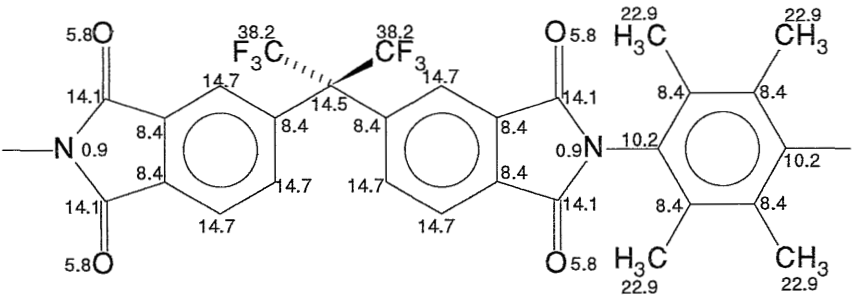

FIGURE 2.11: EXAMPLE OF THE VOLUME (Å3) OF INDIVIDUAL ATOMS/GROUPS IN A REPEAT UNIT OF 6FDA-TME4PDA

From the actual bulk density of the polymer and the calculated Van der Waals volume of the polymer molecules the packing coefficient K (the part of the volume which is occupied) can be determined:

$$K = \frac{N_a \sum_i \Delta V_i}{M / \rho} \qquad [2.1]$$

- K : Molecular packing coefficient
- N_a : Avogadro's number
- ΔV_i : Van der Waals volume of each atom
- M : Molecular mass repeat unit
- ρ : Bulk density of the polymer

For most amorphous polymers this packing coefficient K is 0.68 [22]. Hence 32% of the polymer matrix consists of not occupied or free volume.

The 6FDA- and SiDA-polyimides have somewhat lower packing densities, around 0.65, see §3.3.2. This relatively low overall packing density is often used in explaining the high permeability of the 6FDA polyimides [1,23-25]. But, as will be shown next, the *distribution* of the free volume over smaller and larger holes is also very important in determining the rate of gas diffusion.

2.3.3 Free volume distribution and the polymer structure

A polymer differs very much from 'ordinary' organic or inorganic substances. Due to its long chain (making it almost a one-dimensional molecule) the bulk phase of a polymer will generally not be able to create a fully ordered, highly relaxed structure. The chains become entangled, prohibiting further ordering. A complex primary structure as of the 6FDA and SiDA polyimides will further hinder the relaxation of the chains to form a densely packed structure.
In an *amorphous* polymer (structure) the chains will not be ordered (the amorphous phase will of course lack a melting point). As a consequence non-relaxed areas in the matrix will be formed. Because the chains will not pack as closely as possible, extra space in the matrix is created: an *excess free volume*.

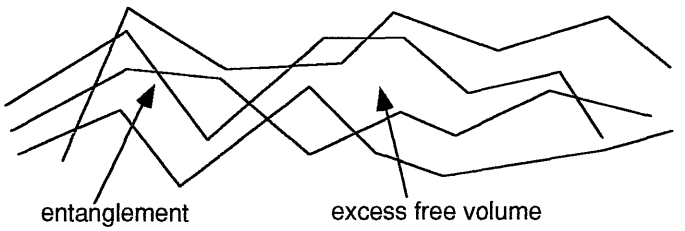

FIGURE 2.12: EXCESS FREE VOLUME IN THE AMORPHOUS POLYMER MATRIX

This phenomenon of excess free volume, or for simplicity just free volume, which is typical for glassy polymers, is very important in gas diffusion through membranes as will be shown.

A polymer in the glassy state again differs very much in physical proper-

ties from the same polymer in the rubbery state. The main reason is the almost complete restriction in translational mobility of the chain segments in the glassy state [6,19,26]. The thermal energy necessary for the translational motions is not available below the glass transition temperature. The polymer matrix is effectively 'frozen in' at T_g. However, below T_g the structure may contain more free volume than could be expected from the difference in thermal expansion coefficient. The thermal expansion coefficient of the glass (actually a supercooled liquid) is lower than that of the rubber (a liquid state). The 'extra' free volume in the glassy state is responsible for the unusual diffusion, sorption and hence permeation behavior of glasses [6].

An even more important parameter with respect to diffusion is the *distribution of the free volume* (FVD, Free Volume Distribution). Two polymers with the same overall free volume (or the same packing density) can still differ in the FVD. The total amount of empty space in the polymer can largely be determined by small holes, or be distributed over a wider range of holes of different sizes. The effect of the distribution may be dominating as will be shown in the next paragraphs.

A very important question now arises: what factors determine the distribution curve?

2.3.4 A model for describing the Free Volume Distribution

Two factors determine the free volume distribution in the polymer matrix. First the available thermal energy allows holes to exist larger than interstitial space (as holes in crystalline areas). Secondly compression of the surroundings of a hole inhibit the formation of larger holes, which means these are less probable. The strongly reduced mobility of chain segments in the frozen glassy state contributes to the preservation of holes, and broadens the FVD as will be explained below.

Volume is an "extensive property" like energy, which means that the volume (or energy) for the whole system is equal to the sum of the vol-

umes (or energies) for the individual parts of the system. "Intensive properties", such as pressure and temperature, are not additive: in a homogeneous system the pressure and temperature of any part is the same as that of the whole system.

For extensive properties (denoted with E here) the distribution of particles among all possible energy levels N_i (e.g. the molecules, but of course also the parts without molecules, the holes) can be described by a Boltzmann distribution [see e.g. 28]:

$$N_i = \vartheta \cdot e^{-E_i/kT} \qquad (2.2)$$
$$\text{and} \quad \Sigma N_i = N_{total}$$

The pre-exponential factor ϑ has the same value for every quantum state (it is however not a constant, it does depend on temperature). It is easy to see that the hole-volume distribution in a polymer matrix, which is the distribution of an extensive property, will be governed by this law. The formation of a hole or a certain free volume is the result of the redistribution of the polymer chains. To form a hole of a certain size, sufficient (thermal) energy is necessary. The amount of energy required will be linearly related to the volume of the hole (see § 2.3.6 and [10]). Hence the thermal energy distribution will be directly reflected in the hole-volume distribution.
The amount of energy to form a hole will largely depend on the polymer characteristics, from which the chain stiffness is the most important factor. In the glassy state stiffer chains will hinder tight packing, according to the 'spaghetti-model' (see figure 2.9). In the rubbery state the opposite is true: stiffer chains (less mobile) will not allow large density fluctuations, and thereby narrow the FVD.
When considering an *amorphous* glassy polymer the stress and thermal history co-determine the FVD, since these polymers are not in an equilibrium, unrelaxed state. Systems which have been frozen in farther from the equilibrium state will contain a larger amount of large holes. Nevertheless, the distribution in hole-sizes will still follow a Boltzmann distribution. Deviations from the distribution would indicate (local) ordering.

Following this reasoning a suitable relation for the distribution of the hole-sizes can be given:

$$N_i = A \cdot e^{-BV_i/kT} \tag{2.3}$$

In which $B \cdot V_i \equiv E_i$

and N_i *is* the number of holes with volume V_i. The factor B is a measure for the amount of thermal energy necessary to open up a hole of a certain size, to overcome the internal pressure in the matrix. It describes the slope or steepness of the distribution curve (see figure 2.13). B is a polymer and polymer condition dependent factor, incorporating chain stiffness and polymer history. A high chain stiffness, or for instance a rapid cooling from above the glass transition, will result in a less steep distribution curve, thus in a smaller B value. Bulky side-groups on the polymer chain will have the same effect. The 'frozen in' free volume below the glass transition temperature has a different origin than the free volume that arises from thermal motions of the chains. The frozen in holes are not mobile due to the restricted chain movement below T_g. This part of the free volume resembles the FVD of the rubbery state (see § 2.3.5, point 4), and hence can still be described by the Boltzmann type distribution. This extra free volume contributes to the diffusion process, which explains why polymers with more rigid chains tend to be more permeable.

The pre-exponential factor A is related to the amount of free volume at 0 K, hence the minimal amount of free volume in a given polymer; it is more or less a scaling factor to account for the total unoccupied volume of the system in its ground state.
In figure 2.13 the dependence of the distribution curve on B is depicted schematically, using arbitrary units and an identical total area (total free volume) under the curves.

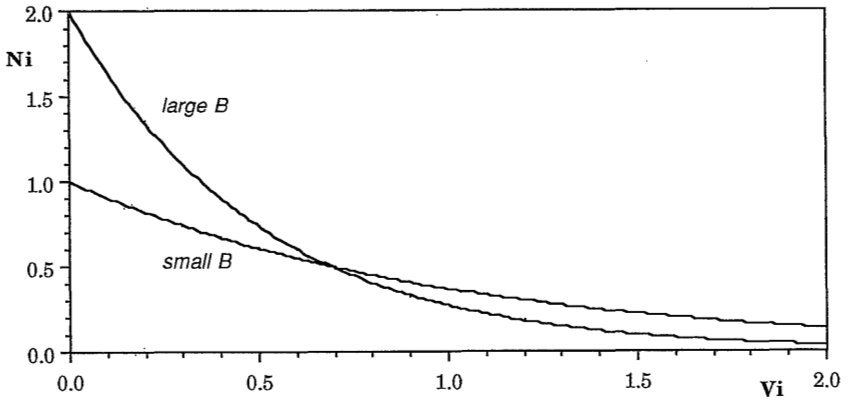

FIGURE 2.13: DEPENDENCE OF THE HOLE-VOLUME DISTRIBUTION N_I ON B

The total amount of empty space in the polymer can thus be taken up largely by small holes (large B), or can be spread over a wider range of hole sizes (small B).
The consequences for the movement of gas molecules are considerable: a wider distribution in hole sizes will allow a gas molecule of a certain size to use a larger part of the free volume for the diffusion process. This effect becomes immediately clear if we incorporate the size of the penetrant molecule in the graphs:

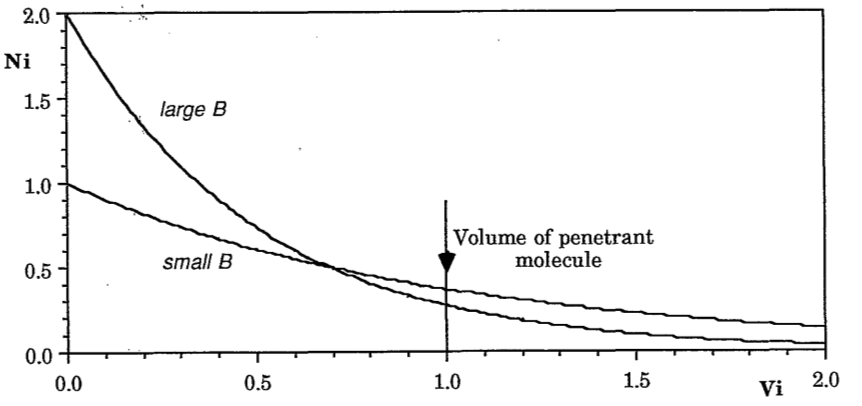

FIGURE 2.14: SIZE OF GAS MOLECULE IN RELATION TO THE FVD

This schematic figure clearly indicates that not all the free volume contributes to the diffusion, and that a minimum volume is necessary for a displacement. This minimum value depends on the size and the shape of the diffusing gas molecule.
The amount of available free volume will be higher in the case of a small value for B. Hence the rate of diffusion will be higher here, if other influencing parameters as CED are comparable for both cases.

2.3.5 Factors influencing the Free Volume Distribution

The distribution in the free volume is a function of a number of polymer related parameters (mainly primary and secondary structure), of the polymer history and state (residual stress, tension) and of the temperature. Only amorphous polymers (like the polyimides) will be considered here, since partial ordering or semi-crystalline polymers will complicate the model.

a. Effect of polymer chain structure

The primary structure constitutes the occupied volume of the matrix. This is also called the Van der Waals volume, and it can be calculated accurately using the refined atom-contribution method of Askadskii [22], see §2.3.2. Also from computer modelling (CAMM) the occupied volume can be determined.
A part of the free volume is the excluded volume. The distance between two chains can of course never be smaller than the *thickness* of the chain allows, and in this way a certain amount of excluded volume is created. The thickness of the chain is determined by the primary structure, see figure 2.15. By thermal motion a kind of 'elbow' volume is created which also contributes to the free volume.

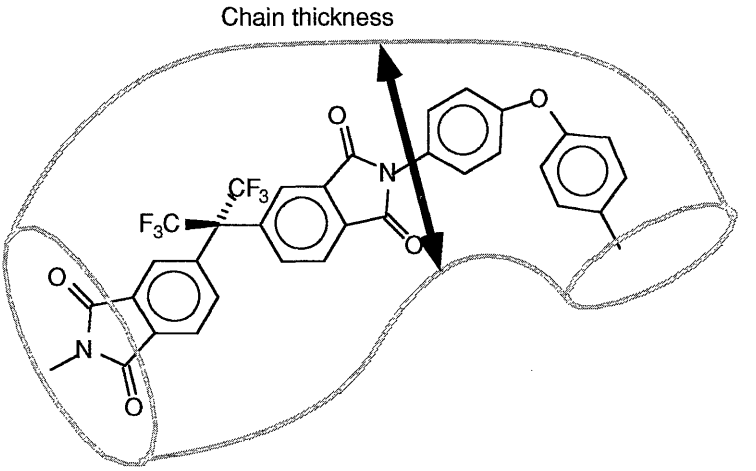

FIGURE 2.15: THE THICKNESS OF THE POLYMER CHAIN

Bulky side-groups will locally increase the chain thickness (as indicated in figure 2.15). Thicker chains will therefore tend to pack less efficiently due to a larger average inter-chain distance. The outline in figure 2.15 encloses the excluded volume of the polymer chain, incorporating the Van der Waals volume of the chain and the interstitial free volume.
If the packing density and the van der Waals volume are known, the total free volume can be calculated as will be shown in Chapter 3. This value is important, but gives no information about the distribution (factor *B*). It is linked to the pre-exponential factor *A*.
The occupied volume is slightly dependent on temperature, because of thermal motion of the atoms. We will ignore this effect since it is small compared to the increase in free volume due to thermal motions.

b. Effect of chain folding

The secondary structure, the chain folding, is mainly responsible for the formation of small holes near the chains, the interstitial free volume. This empty space, which is also present in crystalline domains in polymers, are too small to hold a gas molecule. Hence they will not contribute to the diffusion process. However, the free volume present in these interstices does constitute a large part of the total free volume, since there are a lot of hinges in the chains (see e.g. figure 2.15). The effect on

B is not readily clear, since it is not directly connected to the number of larger holes.

c. Effect of chain stiffness

For glassy polymers the stiffness of the main chain prevents ideal packing and optimal folding, which means that extra free volume will be created. A higher chain flexibility narrows the FVD, hence it will increase the factor B (cf. the spaghetti model presented in §2.3.1). In the rubbery state the effect is opposite: more flexible chains are more mobile, thereby *broadening* the FVD.

The factors determining the chain stiffness can be investigated with the aid of computer modelling. In Chapter 3 this technique will be used to explain the experimental data on *meta/para*-isomers. In Chapter 4 the computer modelling technique will be described in more detail.

d. Effect of thermal and stress history

Equation 2.3 shows that a higher temperature will broaden the distribution. By increasing the temperature more chain segments or parts of the chain will be able to rotate and dislocate, due to sufficient thermal energy. However, the temperature dependence has not been investigated further.

The effect of the sample history on B, which is especially important for amorphous glassy polymers, will be very strong. The non-equilibrium state of glassy polymers is the reason for this. When the glass transition temperature is passed, the state of the polymer is practically frozen in. The kinetics of this process (the rate of the temperature decrease) determines the amount of unrelaxed free volume. The chain motions become very restricted because the thermal energy is not sufficient to overcome rotational and translational barriers. Relaxation of the quaternary structure, and hence a reduction of the size of the larger holes that were formed, becomes almost impossible.

Figure 2.16 offers a general picture of the considerations presented.

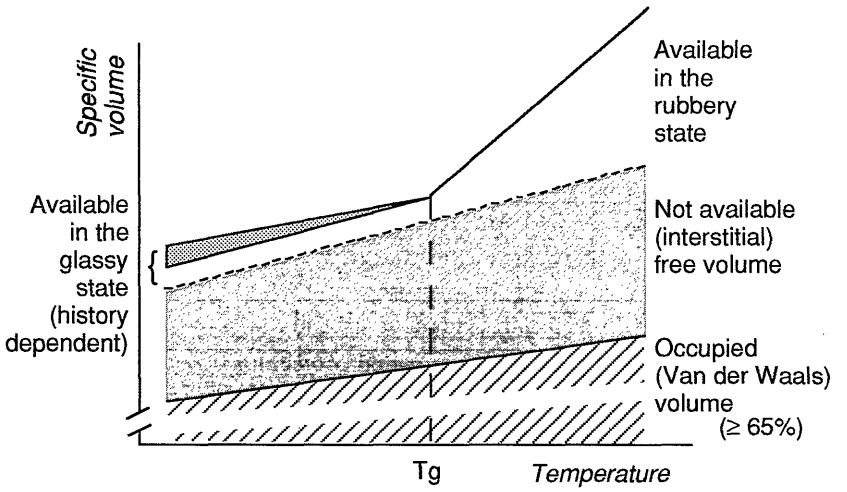

FIGURE 2.16: OCCUPIED AVAILABLE FREE VOLUME VERSUS TEMPERATURE.

The quaternary structure of a glassy polymer will thus closely resemble the state of the polymer around T_g, consequently it will have a FVD like the polymer at T_g. This also makes clear the dependence of the distribution on the cooling-rate or on annealing time, which is the time the polymer sample has been treated at a certain temperature not far from T_g.

If a polymer is cooled very fast from its rubbery state, freezing in of the matrix starts earlier in the process and a large amount of free volume is obtained (which may be decreased by relaxation). The matrix will have the state of the rubber at a relatively higher temperature, because the rate of relaxation is strongly temperature-dependent. Annealing has the opposite effect for the same reason.

The longer a polymer is in the glassy state, the further the quaternary structure will relax to its equilibrium state. This results into a closer packing of the matrix and a steepening of the FVD, represented by a larger value of B. A higher temperature (annealing) will enhance this process.

Stress imposed on the polymer, e.g. during membrane formation, also broadens the FVD; the cast film is fixed on the glass plate, and thereby cannot contract freely . Especially larger holes are formed by stress. The small, interstitial holes are not much effected by stress as long as the

chains are not extended. The resultant is again a smaller B value.
The effect of ordering due to oriented stresses has not been accounted for, the polymers were not subjected to orientational forces. Pongratz [14] has studied the effect of imposed stress on the diffusion.
At the moment no experimental method is available to measure accurately the important parameters which influence the FVD. Wide Angle X-ray Diffraction (WAXD), NMR-spin/fluorescent dye probing, and positron annihilation may be used to determine a 'mean' hole size, but this does not give (much) information on the FVD. An indirect method to determine the FVD is Computer Aided Molecular Modelling (CAMM). This method is difficult to apply to the type of aromatic polymers considered here, but has succesfully been employed for simple polymers like polymethylene, see Chapter 4.
In Chapter 4 CAMM will be used to create a model of the polymer matrix, and to spot the motion of CO_2 at a molecular scale through this matrix.

2.3.6 Cohesive Energy Density of the polymer matrix

The occasional opening of a tunnel in the matrix is necessary for the diffusion of a penetrant molecule. The motion in the matrix, the separation of polymer chains requires energy. The amount of this energy depends on the interaction forces between the polymer chains, reflected in the cohesive energy density (CED) of the polymer. The cohesive forces are the sum of all attractive forces, e.g. polar and Van der Waals interactions and hydrogen bonding, and the electrostatic interactions. A higher CED value means stronger inter-chain interactions, and obviously more energy will be needed to create a hole in the matrix.

Meares [10] related the activation energy for diffusion $E_{\mathbb{D}}$ directly to the cohesive energy density. He considered the tunnel that has to be opened up for a diffusional jump (see figure 2.7A) as a cylinder with the diameter of the penetrant molecule and the length equal to the jump length:

$$E_h = \frac{\pi}{4} d^2 \lambda \ CED \qquad [2.4]$$

E_h Energy of tunnel (or hole) formation

d Diameter of penetrant molecule (Lennard-Jones collision diameter)

λ Diffusional jump length

The opening of this volume, and thus the diffusional jump, requires an amount of energy that is directly related to the activation energy of diffusion, expressed per mole:

$$E_{\mathbb{D}} = \frac{\pi}{4} d^2 \lambda \ N_{AV} CED \qquad [2.5]$$

N_{AV} Avogadro's number

Chen and Edin [11] studied this relation in more detail. They investigated the diffusion of alkanes (and CO_2) through bisphenol-A-polycarbonate, and found a very good linear relation between the Lennard-Jones collision area (or d^2) and $E_{\mathbb{D}}$ (see figure 2.17).

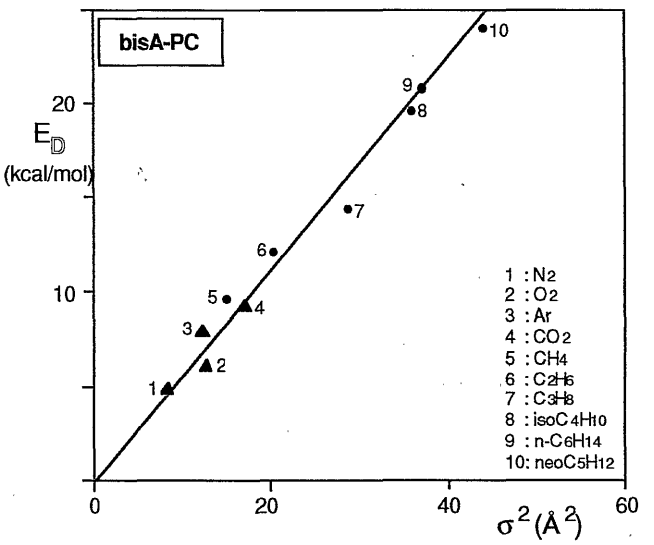

FIGURE 2.17: RELATION BETWEEN ACTIVATION ENERGY OF DIFFUSION AND THE SQUARE DIAMETER OF A PENETRANT MOLECULE [11]

It should be realized that for these experiments one polymer is used, and hence the CED in eq. 2.5 is a constant, which means that the jump length λ is equal for all the permeants, ranging from methane via neopentane to n-hexane; λ is thus a *polymer dependent* parameter. A possible molecular basis for the polymer dependent jump length will be given in §2.6.
As a first approach we assume that λ is constant for all the polyimides evaluated in one series. This assumption is justified if we consider that the jump length depends primarily on the chemical structure. We should keep in mind that the investigated polyimides have closely related structures.

2.4 Cohesive Energy Density and heat capacity jump ΔC_p

The linear relation between the permeability and ΔC_p can now be rationalized using the model described in the former paragraphs. A direct correlation between the activation energy of diffusion and the hole energy is apparent. But can this hole energy be related to the heat capacity jump at the glass transition temperature?
It was shown that the CED value is related to the magnitude of the hole energy E_h. Lee [28] showed that ΔC_p is linearly dependent on the cohesive energy density of polymers by the following relation:

$$\Delta C_p = 1.25 \cdot CED + 2.17 \text{ (cal/molK)} \qquad [2.6]$$

Even for a wide range of different polymers (from PE via Nylon-66 to PMA) a strikingly good agreement was found.
The physical background of the relation between CED and ΔC_p can be explained as follows. The movement of chains in the matrix involves segmental motion. For a hole to be opened up, a temporary redistribution of the free volume is necessary. A very similar process is taking place at the glass-rubber transition. This second-order change occurs at a temperature at which the main polymer chain has sufficient thermal energy to allow segmental mobility. This energy is needed to disrupt some intermolecular bonds [29], and this is reflected in both the magnitude of the T_g and that of ΔC_p. The glass transition process, like the opening of a

void, involves a change in the number of nonbonded nearest neighbors or a change in the intermolecular coordination number. The molecular mechanism of this transition is essentially local diffusion of chain segments in which the local free volume is redistributed, forming transient vacancies. This occurs without long-range perturbation of the matrix-structure [19,29].
The relation between the energy uptake for this transition and the hole formation energy is now apparent: the segmental motion for the creation of a void involves local chain separation, hence the breaking of intermolecular interactions. At T_g the same type of motion is involved. It should be realized that these effects do not originate from vibrational motion of side groups or local, rocking motion of the main chain backbone. These motions are responsible for subsidiary transitions at lower temperatures than T_g.

The number of segments that participate when a hole is formed depends on the primary structure: only geometrical parameters influence λ. It can be imagined that the jump length (at least to a first approximation) will be equal in the range of 6FDA-polyimides studied, as will be further described in Chapter 3 [30]. From these experiments it may be concluded that the size of the void to be opened for a diffusional jump, depends only on λ. Since λ will be very similar for the investigated 6FDA polyimides, this implies that E_h will only depend on CED, and hence on ΔC_p.

2.5 Diffusivity and heat capacity jump ΔC_p

From equations (2.4) and (2.6) the direct relation between E_h and ΔC_p becomes clear. We thus expect (following eq. 2.5) a linear relation between E_D and ΔC_p. If an almost constant sorption behavior is assumed within one class of polyimides, the linear relationship found between $\mathbb{P}$ and ΔC_p can be explained. A constant sorption behavior is not unlikely in structurally very similar polymers, and in § 3.5 it will be shown that for the 6FDA polyimides this is indeed the case.
One has to be cautious not to employ ΔC_p as a sole measure for the

diffusivity: many more parameters, like crystallinity, have a strong effect on the diffusivity *and* on the ΔC_p value.

2.6 Effect of the primary structure on E_h and diffusivity

There is still a need to elucidate the *molecular basis* for the relationship found.

The opening of the tunnel in the matrix is supposed to be the *rate-determining* step in the diffusional process. As shown, the size of the hole that has to be opened up depends on the size of the penetrant and on the jump length, the latter being a polymer dependent parameter.

If the matrix is considered on a molecular scale, it can be noticed that the primary structure severely restricts the number of possibilities of the stretch of the tunnel, thus of the jump length. To explain this, an enlarged view of the different sub-structures in the polymer matrix will be drawn (see figure 2.18).

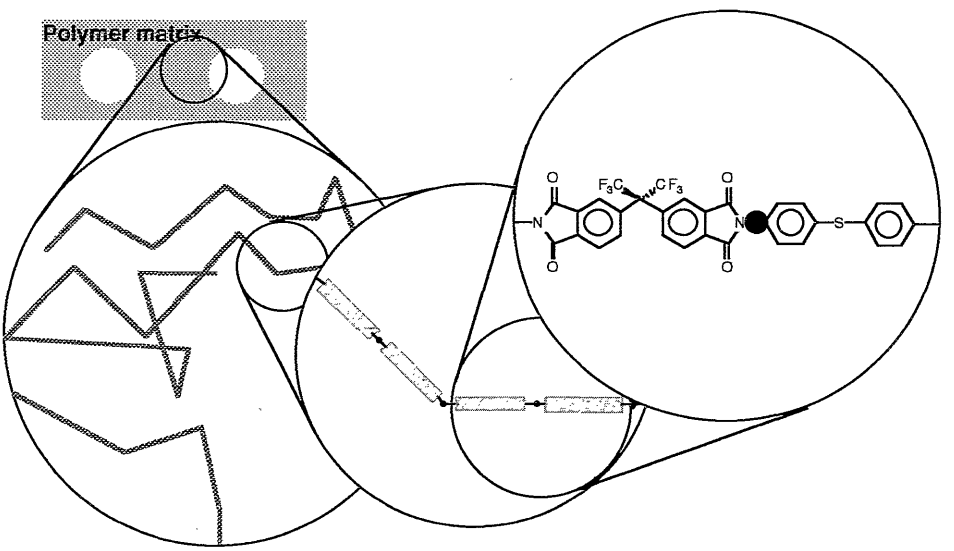

FIGURE 2.18: SCHEMATIC DRAWING OF THE PRIMARY, SECONDARY AND TERTIARY STRUCTURE

To open the tunnel a mobility of a few chain segments is required in a coordinated translational movement. This translation of a part of a chain in a rigid polymer occurs after bending of some parts in the chain. The chains are formed of rigid (e.g. aromatic) parts joined by more flexible bonds. Computer simulations have revealed which are the most flexible bending points in the polyimides. These so-called *pivot points* are indicated in figure 2.18 as black dots. Figure 2.19 gives a summary of computer simulation results of bending energies of three different 6FDA-polyimides. The energy difference for bending at a rigid and a flexible point differs by a factor of two. The probability of bending will largely depend on the energy needed, which means that the bending will preferably take place at the pivot points. The calculations will be explained in Chapter 4 [31].
It is not possible to create a hole of arbitrary length, since it has to be at least the size of an integer number of segments (which are linked together by the pivot points). The polymer determines the diffusional jump length, not the penetrant molecule. This fact is in agreement with the model postulated earlier, following the results of Chen and Edin [11]. The model also holds if the tunnel creation process is considered to take place in three dimensions: only an integral number of segments can move apart from each other to form the hole. Because many assumptions have been made this approach only holds for closely related polymers.

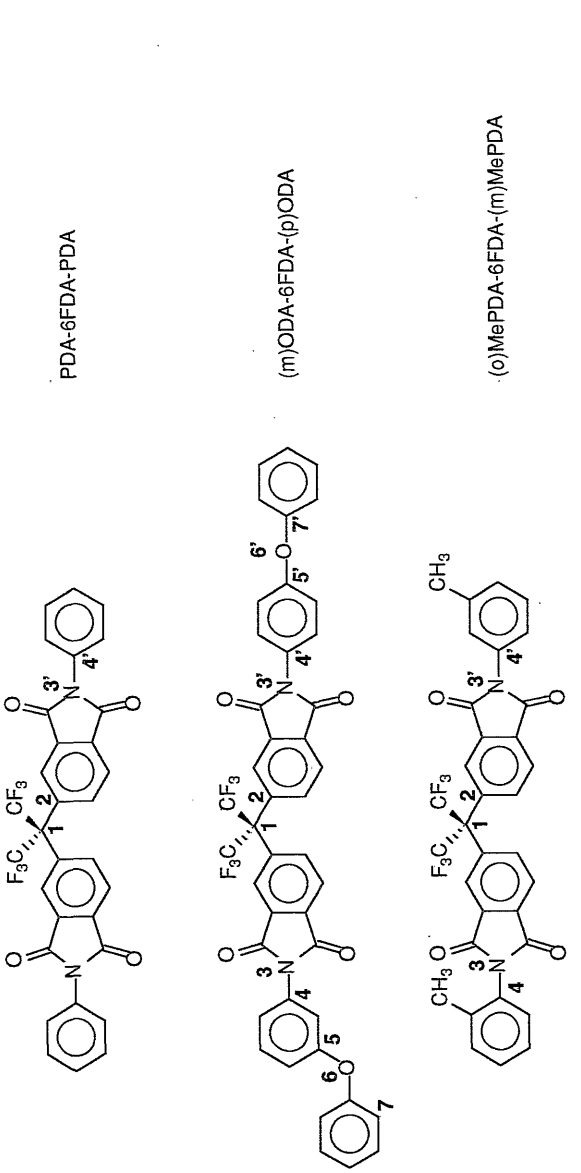

Force constants for bending of molecule on specified centre (in kcal.mol^{-1}deg^{-1})

Compound	1	2	3	3'	4	4'	5	5'	6	7	7'
PDA-6FDA-PDA	0.073	0.013	0.0061	-	0.0063	-	-	-	-	-	-
(m)ODA-6FDA-p(ODA)	-	-	0.0075	0.019	0.0066	0.0069	0.015	0.021	0.102	0.019	0.018
(o)MePDA-6FDA-(m)MePDA	-	-	0.0066/0.0087	0.0069	-	-	-	-	-	-	-

FIGURE 2.19: FORCE CONSTANTS FOR BENDING OF THE POLYMER MOLECULE AT SPECIFIC CENTRES

2.7 Conclusions

The permeability $\mathbb{P}$ of CO_2 in a homologous series of polyimides is found to be linearly related to ΔC_p, the jump in heat capacity at T_g. This observation may give more insight in the processes that actually govern the rate of diffusion of a gas through a polymer.
One of the more important points is that the diffusion proceeds in discrete jumps with diffusional jump length λ. This λ is a key parameter and from the given relation between $E_{\mathbb{D}}$ and ΔC_p it may be concluded that λ is constant for the polymers in one series.
Other parameters like the chain stiffness and the amount of free volume are very important. But as will be shown in Chapter 3, the overall free volume differs only a little within the homologous series investigated.

Literature

(1) Kim, T.H., Koros, W.J. and Husk, G.R., *J. Membr. Sci.*, **1989**, 46, 43

(2) Raucher, D. and Sefcik, M.D., in *Industrial Gas Separations*, Ch. 6, Whyte, T.E., Yon, C.M. and Wagener, E.H. (Editors), A.C.S. Symp. Ser. № 223, A.C.S., Washington, D.C. **1983**

(3) Frisch, H.L., *J. Phys. Chem.*, **1957**, 62, 93

(4) Salame, M., *Polym. Eng. Sci.*, **1986**, 26(22), 1543

(5) Sefcik, M.D., Schaefer, J., May, F.L., Raucher, D. and Dub, S.M., *J. Polym. Sci., Polym. Phys.*, **1983**, 21, 1041

(6) Vieth, W.R., Howell, J.M. and Hsieh, J.H., *J. Membr. Sci.*, **1976**, 1, 177

(7) Fujita, H., *Fortschr. Hochpolym.-Forsch.*, Bd.3, **1961**, 1

(8) Vrentas, J.S., Duda, J.L. and Ling, H.C., *J. Membr. Sci.*, **1989**, 40, 101

(9) Brandt, W.W., *J. Phys. Chem.*, **1959**, 63, 1080

(10) Meares, P., *J. Am. Chem. Soc.*, **1954**, 76, 3415

(11) Chen, S.P. and Edin, J.A.D., *Polym. Eng. Sci.*, **1980**, 20(1), 40

(12) Sanchez, I.C., *J. Appl. Phys.*, **1974**, 45(10), 4204

(13) Bonart, R, Owen, A.J. and Paulus, I., *Colloid and Polym. Sci.*, **1985**, 263, 435

(14) Pongraz, W., Ph.D. Thesis, University of Regensburg, Germany **1990**

(15) Kloczkowski, A. and Mark, J.E., *J. Polym. Sci., Polym. Phys.*, **1989**, 27, 1663

(16) Privalko, V.P., *Macromolecules*, **1973**, 6(1), 111

(17) Simha, R. and Boyer, R.F., *J. Chem. Phys.*, **1962**, 37, 1003

(18) Privalko, V.P. and Lipatov, Yu.S., *J. Macromol. Sci.-Phys.*, **1974**, B9(3), 551

(19) Peiffer, D.G., *J. Macromol. Sci.-Phys.*, **1978**, B15(4), 595

(20) Sheu, F.R. and Chern, R.T., *J. Polym. Sci., Polym. Phys.*, **1989**, B27, 1121

(21) Sykes, G.F. and St. Clair, A.K. *J. Appl. Polym. Sci.*, **1986**, 32, 3725

(22) Askadskii, A.A., in: *Polymer Yearbook 4*, Pethrick, R.A. and Zaikov, G.E. (Editors), Harwood Academic Publishers, N.Y., **1987**, pp. 93-106

(23) Hayes, R.A., U.S. Patents 4,717,394, **1988**, 4,838,900, **1989**

(24) Kim, T.H., Ph.D Thesis, University of Texas at Austin, USA, **1988**

(25) Husk, G.R., Cassidy, P.E. and Gebert, K.L., *Macromolecules*, **1988**, 21, 1234

(26) Choy, C.L. and Young, K., *Polymer*, **1978**, 19, 1001

(27) Guggenheim, E,A., in *"Boltzmann's distribution law"*, Interscience Publishers, Inc., New York, **1963**

(28) Lee, C.J., *Polym. Eng. Sci.*, **1987**, 27(13), 1015

(29) Kaelbe, D.H. in *"Physical Chemistry of Adhesion"*, Ch. 7 and 8, Wiley Interscience, New York, **1971**

(30) Smit, E., *et al.*, to be published

(31) Van Eerden, J., Karrenbeld, H. and Smit, E., unpublished results

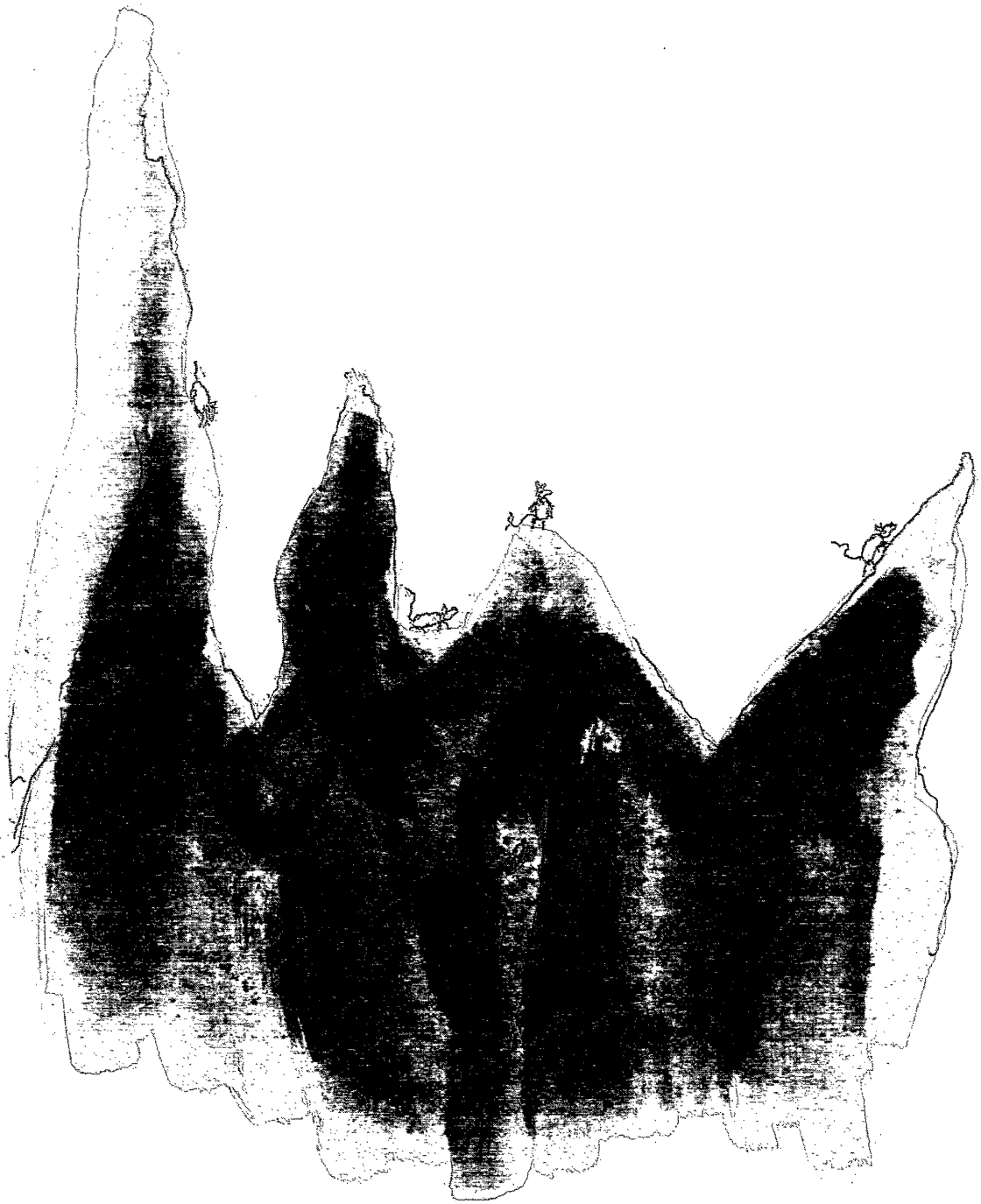

CHAPTER THREE
POLYMER STRUCTURE AND DIFFUSION

Elucidation of the molecular basis of the diffusion process

CONTENTS

3.1 Introduction

In this chapter a number of characterization methods will be described which may contribute to further elucidation of the relationship between the molecular structure of the polymer and the gas permeability and diffusivity. Homogeneous flat membranes are prepared of two series of polyimides, which are especially synthesized for this purpose, with systematic changes in the polymer backbone. In this way the effect of the primary and higher order structures on the permeability and diffusivity can be determined very accurately. The difference between the two types of polyimides lies in a relatively small change in the dianhydride part, which however may result in a dramatic change in separation performance.

Other polymer parameters of interest are the glass transition temperature and the heat capacity jump at this temperature, the density, the overall free volume and the Van der Waals (or occupied) volume. Differences in the free volume distribution are responsible for unexpected behavior between isomeric polymers.

In this Chapter we will occasionally use the computer aided molecular modelling (CAMM) method to explain some of the results.

3.2 Polyimide synthesis

The series of polyimides studied have systematic variations in the polymer backbone because different diamines which are combined with each of the two dianhydrides 6FDA and SiDA, see figure 3.1. The choice for these two series of polyimides was explained in Chapter 1.

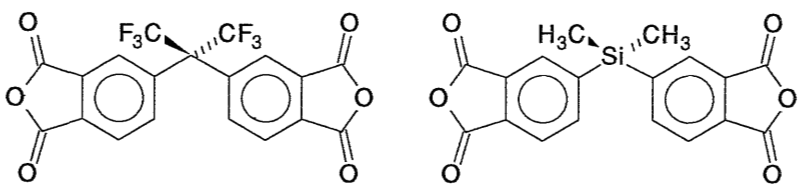

FIGURE 3.1: THE AROMATIC 6FDA AND SIDA DIANHYDRIDE MOIETIES

The dianhydride parts are very bulky and rigid, and dominate the polymer properties. Moreover, the use of these bulky dianhydrides leads to polymers soluble in common solvents which makes membrane preparation more accessible. The SiDA dianhydride was not available commercially, and was synthesized in our laboratory. The synthesis recipes and details on purification of the monomers are given in Appendix A. The chemicals used are listed in Appendix B.

3.2.1 Polymerization

Polyimide formation is a two-step process [1]: first a poly(amic acid) is formed from a dianhydride and a diamine by a polycondensation reaction. This reaction proceeds by the attack of the nucleophilic reagent, the diamine, on the electron-deficient carbonyl carbon of the dianhydride:

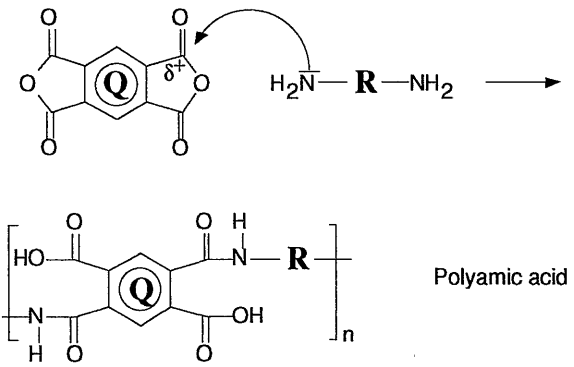

Since water is a very strong nucleophile, it should completely be excluded during the reaction.

Q signifies here the aromatic part in the dianhydride (see figure 3.1). **R** is the aromatic (or aliphatic) part of the diamine, for instance a *meta*-substituted phenyl in 3PDA:

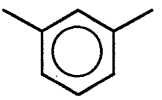

The chemical structures as well as the abbreviations used in this thesis are listed in Appendix C.

3.2.2 Imidization

The second step, the actual imidization, is a cyclo-dehydration reaction:

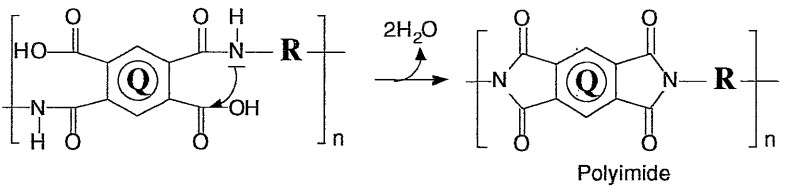

It is apparent that imidization during the polymerization reaction has to be prevented, because water is liberated during this step, resulting in chain termination or chain fission.
In order to shift the equilibrium of the imidization reaction to the right, water must be removed. Two techniques are used: a thermal and a chemical treatment. Generally the imidization is performed by a thermal treatment of the poly(amic acid). A typical procedure can be as follows: a 15% (w/v) solution of the poly(amic acid) in dimethylacetamide (DMAc) is cast on a glass plate and dried under a stream of nitrogen to obtain a homogeneous, tack-free film. This film is heated in an oven at various temperatures up to 300°C to remove the water formed during the imidization reaction. This procedure is carried out when the formed polyimides are insoluble, which is very often the case.
If the polyimides are soluble however, like the ones based on 6FDA and SiDA, a chemical imidization reaction is preferred. A mixture of acetic anhydride and a tertiary amine-base like pyridine acts as a water-removing agent:

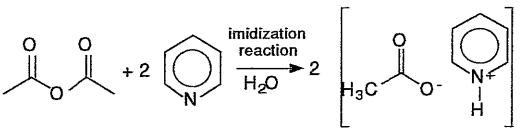

In this reaction path no cross-linking of the polymer will occur, which is an advantage if the polymer has to be processed after synthesis.

3.2.3 Characterization methods

Proton nuclear magnetic resonance (^{1}H-NMR) spectra were taken on a Varian EM 360A and a Brucker 200 spectrometer, with tetramethylsilane as internal standard. Infrared spectra were taken on a Perkin Elmer 1310 Spectrophotometer.
Inherent viscosities were obtained from 0.5% polyimide solutions in DMAc at 30°C (Ubbelohde-type measurements).
Differential scanning calorimetric (DSC) measurements were performed on a Perkin Elmer DSC-4 calorimeter at a heating rate of 20°C/minute. Samples were heated 30-40°C above T_g to eliminate sample history, quenched, and re-run. Analysis of the data was performed on the Perkin Elmer (TADS) Data station 4.
The density was measured in a calibrated gradient column, ranging from ρ=1.2 to 1.6 (a mixture of hexanol and tetrachloromethane). The accuracy of the column is ± 0.005 g/ml. The solvents were chosen to prevent swelling of the polymer samples.
Wide Angle X-Ray Diffraction (WAXD) spectra were taken on a Philips PW 1710, using copper radiation (Cu Kα, λ 1.5418Å) with a flat sample holder and a graphite monochromator. The intensity of 1 s counts in a continuous scan of 0.05° (2θ) per second was plotted against 2θ. Bragg's law was used to calculate the inter-chain distances from the reflection angles:

$$n\lambda = 2d \sin\theta \qquad (3.1)$$

where: n: order of the reflection
λ: wavelength X-rays
d: distance between reflective planes
θ: reflection angle

3.3 Results on synthesis and characterization

3.3.1 Synthesis results

The primary chemical structures of the polyimides which have been synthesized are listed in Appendix C. As can be seen from Table 3.1 polymerization is most successful for the aromatic diamines with a high electron density on the amine-group. The inherent viscosities of 0.5% polyimide solutions in DMAc are listed in this table. Strong electron withdrawing groups like sulfones (present in the diamines TSN, 3,3'-DDS and 4,4'-DDS) prevent the formation of a high molecular weight polymer at room temperature. The polymer weight is too low to form flexible films. It appeared as a rule of thumb that the inherent viscosity (as measured here) should be above 0.4 dl/g for film formation.
Also steric hindrance can prevent the formation of a high molecular weight, as is shown by the reaction of 6FDA with DAM:

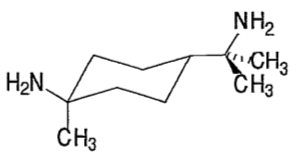

diamino-1,8-p-menthane

In this case the inherent viscosity was very low, less than 0.1 dl/g. The latter monomer was already mentioned recently in literature [2] for its inability to form polyamides. The explanation given was also steric hindrance.

3.3.2 Characterization results

The ^{1}H-NMR spectra of the polyimides are consistent with the chemical structure. IR data show that the imidization is complete: the absorption of the amide bonds (2865-3100, ca. 1655 and ca. 1540 cm^{-1}) are below detection limit, while the imide absorptions (ca. 1785 and 1720 cm^{-1}) are strongly present. A typical example is shown in Appendix D.

The glass transition temperatures of all 6FDA-polyimides are high, mostly well over 300°C, see table 3.1. This indicates the presence of a highly rigid polymer chain. The glass transition temperatures of the *meta*-substituted polyimides are always significantly lower than the corresponding *para*-isomers. This effect is very important, because a higher chain flexibility may result in a more efficient packing of the polymer matrix (cf. Chapter 2). As a consequence a higher packing density or, more probably, a narrower free volume distribution, may directly effect the permeability for gases in a negative way. The densities of the synthesized polymers are also given in Table 3.1.

All 6FDA-polyimides studied are completely amorphous, as shown by WAXD (an example is shown in Appendix E). The 'd-spacing', being the position of the maximum intensity of the amorphous X-ray scattering, ranges from 5.5Å (6FDA-3PDA) to 6.1Å (6FDA-TMe4PDA), see Table 3.1. These high values are often seen as an indication of the open matrix of these polymers [3-5]. Also the SiDA polymers are amorphous. The d-spacing ranges here from 4.7Å (SiDA-3,4'ODA) to 5.7Å (SiDA-TMe4PDA) (see Table 3.1), always lower than their 6FDA analogues. The d-spacings do not differ very much for the polymers in one class, except for the bulky TMe4PDA.

Table 3.1: Results of polymer synthesis

Polymer	Obtained inherent viscosity (dl/g)	Tg (°C)	Density (ml/g)	d-spacing (Å)
6FDA-4PDA	>0.8	357 (376*)	1.450 (1.458*)	5.7
6FDA-3PDA	0.61	-	1.46	5.5
6FDA-(4OMe)3PDA	>0.4	311-324	N.D.	-
6FDA-(4Me)3PDA	>0.4	331-334	1.410	-
6FDA-(5Me)3PDA	>0.4	-	1.41	-
6FDA-TMe4PDA	>1.2	425	(1.517**)	6.1
6FDA-MDA	1.3	305	1.39	-
6FDA-SDA	>0.7	297	1.45 (1.465*)	5.7
6FDA-44ODA	>0.6	304-307	1.420-1.423	5.6
6FDA-34ODA	>0.6	269	1.422	5.7
6FDA-6FiPDA (Sixef™-44)	0.90	323	1.477	5.9
6FDA-6FiPDA$(NO_2)_{0.5}$	0.80	295	N.D.	
6FDA-44DDS	0.20	320	N.D.	5.4[p]
6FDA-33DDS	0.21	264	N.D.	5.7[p]
6FDA-TSN	<0.1	(241)	(1.39**)	-
6FDA-15NDA	0.83	289	1.387	-
6FDA-DAF	>0.4	-	1.417	-
6FDA-DAM	<0.1	(267)	N.D.	-
6FDA-TMe4PDA$_1$/ODA$_1$	>0.4	360	N.D.	-
6FDA-TMe4PDA$_1$/ODA$_9$	>0.4	313	1.414	-
6FDA-TMe4PDA$_1$/MDA$_1$	0.46	359	N.D.	-
6FDA-TMe4PDA$_3$/33DDS$_1$	0.19	334	N.D.	-
6FDA-TMe4PDA$_1$/33DDS$_1$	0.30	316	N.D.	-
6FDA-TMe4PDA$_1$/33DDS$_9$	0.29	264	N.D.	-
6FDA-TMe4PDA$_1$/44DDS$_9$	<0.1	(323)	N.D.	-
SiDA-4PDA	0.38	324 (382*)	1.26	5.1
SiDA-3PDA	0.24	269	N.D.	-
SiDA-(4Me)3PDA	0.42	292	1.20	4.1[p]
SiDA-TMe4PDA	0.59	394	(1.38**)	5.7
SiDA-MDA	0.62	276	1.26	5.1
SiDA-SDA	0.27	251	N.D.	5.1
SiDA-44ODA	1.1	266	1.25-1.27	4.8
SiDA-34ODA	0.45	225	1.26	4.7
SiDA-15NDA	0.27		N.D.	-

*: Polymer heat treated (annealed for 2 hours or kept a short time ca. 20°C above T_g)
**: These polymers are probably swelling in the solvents of the density gradient column
[p]: powder; rest is as film
Two diamines in the abbreviation signify that a mixture was used, the ratios of the diamines is denoted in the subscript

From the density data listed in table 3.1, and the calculated Van der Waals volume of each polyimide (according to Askadskii [6], §2.3.2) the overall packing density K can be determined:

$$K = \frac{d_{measured}}{d_{calculated}} = \frac{d_{measured}}{M / N_A \cdot \sum_i \Delta V_i} \qquad (3.2)$$

The K values for the 6FDA- and SiDA-polyimides from which the densities are measured are listed in Table 3.2 respectively 3.3, calculated with the Van der Waals volume or the Van der Waals density.

Table 3.2: Densities, Van der Waals volumes and packing factors for 6FDA-polyimides

membrane	polymer	density [g/ml]	$V_{VdWaals}$ [ml/mole]	K
1,2	6FDA-3PDA	1.460	229.0	0.647
3,4,5	6FDA-4PDA	1.485	229.0	0.659
6	6FDA-4PDA	1.450	229.0	0.643
7,8	6FDA-TMe4PDA	1.517	269.0	0.713*
9,10	6FDA-44ODA	1.423	279.3	0.653
11	6FDA-44ODA	1.420	279.3	0.652
12	6FDA-44ODA	1.410	279.3	0.647
13,14	6FDA-34ODA	1.423	279.3	0.653
15	6FDA-MDA	1.390	284.2	0.651
16	6FDA-SDA	1.465	285.6	0.670
17,18	6FDA-4Me3PDA	1.410	239.0	0.635
19	6FDA-15NDA	1.387	256.5	0.626
20	6FDA-TMe4PDA(1)/44ODA(9)	1.414	278.3	0.650
23,24	Sixef 44™	1.477	313.9	0.624

*: uncertain, due to possible swelling effects

Table 3.3: Densities, Van der Waals densities and packing factors for SiDA-polyimides

membrane	Polymer	density [g/ml]	$\rho_{VdWaals}$ [g/ml]	K
1	SiDA-4PDA	1.26	1.958	0.644
4	SiDA-TMe4PDA	1.38	1.872	0.737*
7	SiDA-4Me3PDA	1.20	1.93	0.620
8	SiDA-44ODA	1.25	1.932	0.647
9	SiDA-44ODA	1.27	1.932	0.657
12	SiDA-34ODA	1.26	1.932	0.652
13	SiDA-34ODA	1.26	1.932	0.652
14	SiDA-MDA	1.23	1.890	0.651
17	SiDA-SDA	1.26	1.946	0.647

*: uncertain, due to possible swelling effects

The density of the 6FDA-polymers is very high, ranging from 1.39 (6FDA-MDA) to 1.52 (6FDA-TMe4PDA). The latter value has to be considered with caution, because of polymer swelling in the tetrachloromethane of the density gradient column. The high density values are undoubtedly due to the very high molecular weight of the hexafluorodianhydride moiety. The SiDA polymers, lacking the hexafluoro group, do not show such a high density, varying from 1.20 (SiDA-4Me3PDA) to 1.38 (SiDA-TMe4PDA). Again this last value is uncertain.
The packing factors are low for both series, compared to most other polymers [6].

3.4 Membranes

The gas permeation measurements are carried out with homogeneous flat sheet membranes. The preparation was as follows: A 15% (by weight) solution of polyimide in DMAc was filtered over a Millipore™ filter (1-3 µm) to remove any dust particles. Subsequently the solution was cast on a glass plate and dried under a stream of nitrogen to obtain a dense homogeneous membrane with a thickness of about 15µm. After release

from the glass plate by immersion in water the membrane was dried overnight in a vacuum oven at 150°C to remove residual solvent. Circular pieces were cut for use in the gas permeation set-up. From the *same* polymer film samples were taken for all the other physical measurements (T_g, ΔC_p, density, WAXD etc.). The thickness of the samples was determined by taking the average of about 20 measurements, randomly distributed. The error is about 5%.

3.5 Gas permeation measurements

From all membranes the gas permeability and diffusivity was measured with carbon dioxide and methane. The gases were obtained from Hoekloos (Netherlands), and have a purity of at least 99.5%.
A completely automized apparatus was used to measure the permeability and diffusivity. A precise description is given elsewhere [7]. A schematic representation is given in figure 3.2. The temperature of the measurement set-up can be adjusted.

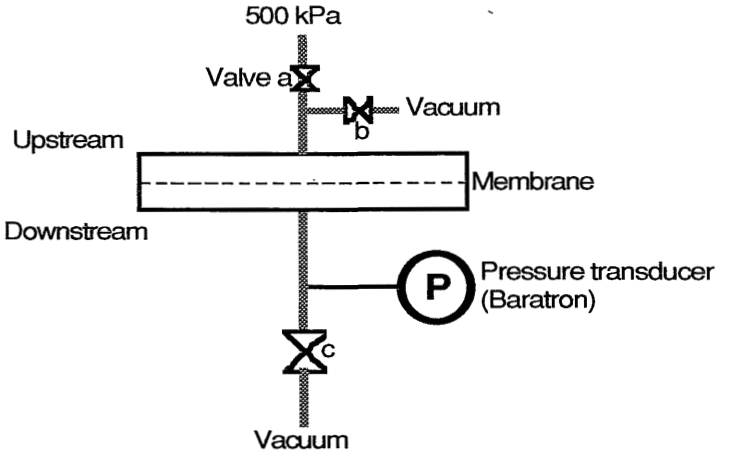

FIGURE 3.2: PERMEATION AND DIFFUSION MEASUREMENT SETUP

The measurements are performed in three steps:

a. Complete evacuation of the set-up and the membrane by applying vacuum (≤ 1 Pa) on both sides of the membrane for 4-5 hours. Valves b and c are open, a is closed. Any residual gas in the membrane will influence the measurement, as it will shorten the time-lag.
(A more detailed discussion of the mechanism of the time-lag method is given elsewhere [7])
b. After closing valves b and c, a is opened and at once a pressure of 500 kPa (5 Bar) of the desired gas is applied to the membrane. The pressure transducer, connected to a computer, reads out the pressure increase in a calibrated volume.
c. After the steady state flux has been reached, the set-up is degassed again.

The actual time-lag measurements typically last only 5-10 minutes, and the total measurement cycle is repeated at least 4 times for each determination.
A typical flux-time curve shows a transient state and a steady state part. From this measurement the time-lag θ can be determined as shown schematically in figure 3.3:

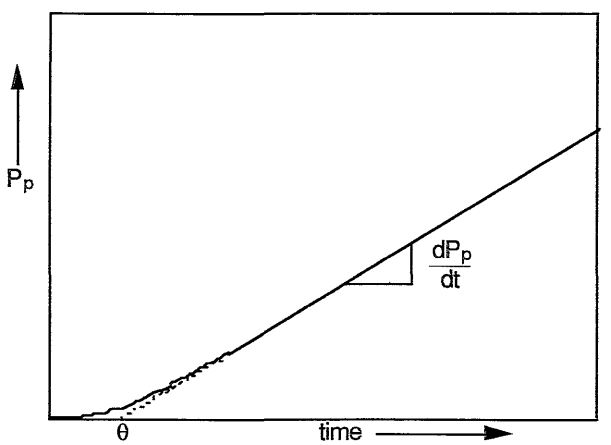

FIGURE 3.3: TYPICAL TIME-LAG PLOT

From the extrapolated curve to $P_p = 0$, the time-lag θ is obtained and the diffusivity $\mathbb{D}$ can be calculated according to [8]:

$$\mathbb{D} = \frac{\overline{d^2}}{6\theta} \qquad (m^2 s^{-1}) \qquad (3.3)$$

Here d is the averaged membrane thickness (in m), and θ the time-lag (in s). It can be argued that this relation, originally derived for rubbery polymers, can also be used for intimately related glassy polymers (at least to a first approximation).

From the slope of the steady state part, $\frac{dP_p}{dt}$, the permeability $\mathbb{P}$ can be calculated:

$$\mathbb{P} = \frac{1}{P_{feed}} \cdot \frac{V_d \cdot M_{gas} \cdot d}{\rho \cdot RT \cdot A} \cdot \frac{dP_p}{dt} \quad \left(m^3 m m^{-2} Pa^{-1} s^{-1}\right) \qquad (3.4)$$

P_{feed} feed pressure (Pa)
V_d downstream compartment volume (m^3)
M_{gas} molecular weight of the gas (kg/mole)
d membrane thickness (m)
ρ density of the gas (kg/m^3)
R gas constant (J/K·mole)
A area of the membrane (m^2)

In Tables 3.4 and 3.5 the results of the permeability and diffusivity measurements are tabulated for the 6FDA- and SiDA-polyimide series respectively. The accuracy of the diffusivity value is about 5 to 10 %, for the permeability about 2 %.

The ratios of the diffusivities and permeabilities of both gases gives the ideal diffusivity- resp. permeability-selectivity factor α. The ratio $\alpha_{\mathbb{P}}/\alpha_{\mathbb{D}}$ (denoted $\alpha_{\mathbb{S}}$) gives an apprehension of the sorption selectivity.

Table 3.4: Permeability and diffusivity of carbon dioxide and methane through 6FDA-polyimide membranes

membr. nr.	polymer	$\mathbb{D}$ CO_2 m^2s^{-1} $*10^{12}$	$\mathbb{P}$ CO_2 $m^3mm^{-2}Pa^{-1}s^{-1}$ $*10^{18}$ [1)]	$\mathbb{D}$ CH_4 m^2s^{-1} $*10^{12}$	$\mathbb{P}$ CH_4 $m^3mm^{-2}Pa^{-1}s^{-1}$ $*10^{18}$	$\alpha_{\mathbb{D}}$	$\alpha_{\mathbb{P}}$	α_S
1	6FDA-3PDA	0.749	89.4	-	-	-	-	-
2	6FDA-3PDA	0.950	109	0.076	1.7	12	65	5.2
3	6FDA-4PDA	-	-	0.067	3.7	-	-	-
4	6FDA-4PDA	1.34	179	0.12	4.9	11	37	3.3
5	6FDA-4PDA	8.62	547	-	-	-	-	-
6	6FDA-4PDA	1.83	180	-	-	-	-	-
7	6FDA-TMe4PDA	20.0	3000	2.1	83	10	36	3.8
8	6FDA-TMe4PDA	16.2	4000	1.9	134	9	30	3.5
9	6FDA-44ODA	2.45	209	-	-	-	-	-
10	6FDA-44ODA	-	-	0.076	2.8	-	-	-
11	6FDA-44ODA	2.43	158	-	-	-	-	-
12	6FDA-44ODA	0.767	91.7	-	-	-	-	-
13	6FDA-34ODA	0.667	68.5	-	-	-	-	-
14	6FDA-34ODA	0.948	88.6	-	-	-	-	-
15	6FDA-MDA	1.82	195	0.063	3.69	29	53	1.8
16	6FDA-SDA	0.623	72.4	-	-	-	-	-
17	6FDA-4Me3PDA	1.51	223	0.12	4.7	13	48	3.8
18	6FDA-4Me3PDA	3.00	367	0.19	6.6	16	55	3.5
19	6FDA-15NDA	3.28	548	0.30	15	11	37	3.4
20	6FDA-TMe4PDA$_1$/44ODA$_9$	2.26	220	-	-	-	-	-
21	6FDA-TMe4PDA$_1$/44ODA$_1$	4.05	833	0.28	16	15	53	3.7
22	6FDA-4OMe3PDA	2.98	319	0.14	4.8	21	66	3.1
23	Sixef™-44)	-	-	2.5	72	-	-	-
24	Sixef™-44)	5.94	626	-	-	-	-	-
25	6FDA-6FiPDA$(NO_2)_{0.5}$	7.34	708	-	-	-	-	-

[1)]: 1 $m^3mm^{-2}Pa^{-1}s^{-1}$ = $1.33 \cdot 10^7$ $cm^3cm\ cm^{-2}\ s^{-1}cmHg^{-1}$

The large difference between different samples of the same polymer (but a different synthesis batch) are caused by different sample histories. The large effect of sample history will again be shown in § 3.7.

Table 3.5: Permeability and diffusivity of carbon dioxide and methane through SiDA-polyimide membranes

membr. nr.	polymer	$\mathbb{D}$ CO_2 m^2s^{-1} *10^{12}	$\mathbb{P}$ CO_2 $m^3mm^{-2}Pa^{-1}s^{-1}$ *10^{18}	$\mathbb{D}$ CH_4 m^2s^{-1} *10^{12}	$\mathbb{P}$ CH_4 $m^3mm^{-2}Pa^{-1}s^{-1}$ *10^{18}	$\alpha_{\mathbb{D}}$	$\alpha_{\mathbb{P}}$	$\alpha_{\mathbb{S}}$
4	SiDA-TMe4PDA[1]	2.68	453	0.52	32.4	5.2	14	2.7
9	SiDA-44ODA[2]	0.055	10.9	0.047	8.65	1.2	1.3	1.1
15	SiDA-MDA	-	-	0.023	0.45	-	-	-

Remarks: [1]: Film cracked during measurement so no other experimental results have been obtained. Unfortunately there were no other defect-free membranes available and the polyimide did not re-dissolve in DMAc because of physical cross-linking (gel formation).

[2]: Because of the low values of the selectivity the membrane is probably not completely defect-free. Re-dissolving this polymer to make new membranes failed because of gel formation. Also an attempt to dissolve the polymer in an ultrasonic bath for several hours failed.

In the case of the SiDA polyimides rather brittle membranes are obtained, resulting in only very few data.

The 6FDA polyimides are all, as expected [3,4,9,10], highly permeable (taking into account that they are glassy polymers) and combine this with high selectivities. The SiDA polyimides have lower permeabilities, in the same order as PES and PSF.

The solubilities of the gases CO_2 and CH_4 in the polymers were not determined directly in this study, because the investigations were focussed on diffusivity and permeability. But from the calculated $\alpha_{\mathbb{S}}$ values for the 6FDA polyimides can be deduced that these polymers do not differ much in their sorption behavior. The mean sorption selectivity is 3.5. A comparable conclusion cannot be drawn in the case of the SiDA polyimides because of the lack of data, and the inaccuracy of the measurements.

3.6 Calorimetric measurements

The glass transition temperature T_g and the accompanying heat capacity jump ΔC_p were measured with *the same polymer films* as used for the gas

permeation measurements. This was done because the history of the polymer influences both the thermal and the gas permeability properties of the membrane. The crystallinity in the polymer is a factor that also influences $\mathbb{D}$ (thus $\mathbb{P}$) and ΔC_p, but wide angle X-ray diffraction (WAXD) did not show any crystallinity in the polyimides.
The magnitudes of the heat capacity jumps, as well as the calculated CED values (according to Lee [11]) are summarized in Tables 3.6 and 3.7. The volumetric CED is the molar CED divided by the molar volume of the bulk polymer: $V_{VdWaals}/K$.

Table 3.6: Heat capacity jump and CED in 6FDA-polyimides

membr nr.	polymer	MW $g.mol^{-1}$	ΔC_p $J.g^{-1}.K^{-1}$	molCED $J.mol^{-1}$	volCED $J.ml^{-1}$
1	6FDA-3PDA	516.4	0.265	67.7	0.296
2	6FDA-3PDA	516.4	0.226	56.7	0.248
3	6FDA-4PDA	516.4	0.139	31.4	0.137
4	6FDA-4PDA	516.4	0.080	15.0	0.065
5	6FDA-4PDA	516.4	0.098	20.7	0.090
7	6FDA-TMe4PDA	572.5	0.042	5.42	0.020
8	6FDA-TMe4PDA	572.5	0.041	5.12	0.019
9	6FDA-44ODA	608.5	0.181	44.1	0.196
10	6FDA-44ODA	608.5	0.168	50.2	0.180
11	6FDA-44ODA	608.5	0.140	40.7	0.146
12	6FDA-44ODA	608.5	0.193	59.4	0.213
13	6FDA-34ODA	608.5	0.209	64.3	0.230
14	6FDA-34ODA	608.5	0.202	61.9	0.222
15	6FDA-MDA	606.5	0.162	49.3	0.173
16	6FDA-SDA	624.5	0.206	63.0	0.221
17	6FDA-4Me3PDA	530.4	0.178	46.3	0.194
18	6FDA-4Me3PDA	530.4	0.171	44.2	0.185
19	6FDA-15NDA	568.5	0.108	28.2	0.110
20	$6FDA\text{-}TMe4PDA_1/44ODA_9$	604.9	0.141	41.0	0.147
24	Sixef 44™	742.5	0.090	28.9	0.092

Table 3.7: Heat capacity jump and CED in SiDA polyimides

membr nr.	polymer	MW $g.mol^{-1}$	ΔC_p $J.g^{-1}.K^{-1}$	molCED $J.mol^{-1}$	volCED $J.ml^{-1}$
1	SiDA-4PDA	424.5	0.203	61.7	0.183
2	SiDA-4PDA	424.5	0.067	20.4	0.060
3	SiDA-4PDA	424.5	0.039	11.9	0.035
4	SiDA-TMe4PDA	480.6	0.080	23.5	0.067
5	SiDA-3PDA	424.5	0.212	64.8	-
6	SiDA-3PDA	424.5	0.213	65.1	-
7	SiDA-4Me3PDA	438.5	0.178	55.2	0.151
8	SiDA-44ODA	516.6	0.139	46.3	0.127
9	SiDA-44ODA	516.6	0.169	62.6	0.154
10	SiDA-44ODA	516.6	0.203	67.6	0.185
11	SiDA-44ODA	516.6	0.257	85.6	0.234
12	SiDA-34ODA	516.6	0.162	60.9	0.149
13	SiDA-34ODA	516.6	0.195	73.3	0.179
14	SiDA-MDA	514.6	0.071	24.9	0.060
15	SiDA-MDA	514.6	0.092	32.3	0.077
16	SiDA-MDA	514.6	0.147	51.6	0.124
17	SiDA-SDA	532.6	0.127	48.5	0.115
18	SiDA-SDA	532.6	0.165	63.1	0.149

Comparing the glass transition temperatures (Table 3.1) with the values of the accompanying ΔC_p (and thus CED), it is evident that a higher T_g is attended by a lower CED. In the next paragraph this intriguing phenomenon will be discussed. There is no apparent CED correlation between the 6FDA and SiDA homologues.

The considerable error in the ΔC_p and concurrent CED values of different samples of the same polymer indicates the large dependence of these parameters on the sample history. This makes it (almost) impossible to give one specific ΔC_p or CED value for a particular polymer. When ΔC_p and CED are related to other parameters caution must be taken that the correlated values belong to the same sample.

3.7 Discussion: relating polymer properties and diffusivity data

In Chapter 2 a model was proposed relating permeability with specific polymer parameters to explain a dependence of $\mathbb{P}$ and $\mathbb{D}$ with ΔC_p. With the data from the extended polymer series we will now verify this model, and try to refine it.

The most striking relation between the two polymer series is found for the glass transition temperatures. The glass transition temperatures of the SiDA-polyimides are always about 46°C *lower* than their 6FDA analogues as can be seen clearly from figure 3.4:

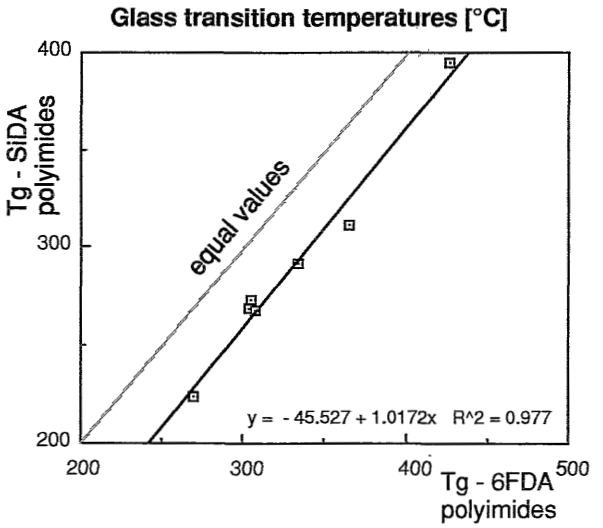

FIGURE 3.4: CORRELATION BETWEEN THE T_G'S OF ANALOGUES POLYIMIDES

A more flexible chain in the case of the SiDA polyimides will be the cause of the lower T_g. Since the difference in the primary structure is only the dimethyl silylene unit, the higher flexibility can be contributed to this moiety. This higher chain flexibility in return will be one of the major reasons for the lower permeability and diffusivity of the SiDA polyimides, as explained in Chapter 2.
It can be seen from the data in Table 3.1 that there is a dependence of T_g

and hence of the chain rigidity with the chemical structure. An increase in glass transition temperature in a closely related group of polymers is directly related to in an increase in chain rigidity, as stated by Privalko [12]. We will now look for the effect on $\mathbb{D}$ and $\mathbb{P}$.

Very intriguing in the two series of polyimides is the effect of *para*- versus *meta*-substitution in the main chain, i.e. 4,4'-ODA against 3,4'-ODA and 4-PDA against 3-PDA, both for the 6FDA- and the SiDA-dianhydride on $\mathbb{D}$ and $\mathbb{P}$ values (see table 3.8). It can be seen that the permeability and diffusivity of the *para*-substituted polymer are significantly higher.

This *para/meta* isomer effect has also been found by other researchers e.g. by Chern et al. [13] and Sykes [14] for other polymers. Some other polymer parameters which may be related to the chain rigidity are also listed in table 3.8. The ΔC_p values increase with a decrease in T_g in the case of the isomers and in addition this results in a reduced diffusivity and permeability.

Table 3.8: The *para/meta* isomer effect

Polymer	T_g (°C)	ΔC_p (J/gK)	V_f fraction	d-spacing (A)	$\mathbb{D}$ (CO_2) ($10^{12}m^2/s$)	$\mathbb{P}$ (CO_2) ($10^{16}m^3 \cdot m/m^2 \cdot Pa \cdot s$)
6FDA–44ODA	305	0.17	0.348	5.6	2.43-2.45	1.58-2.01
6FDA–34ODA	269	0.20	0.347	5.7	0.67-0.95	0.69-0.89
6FDA–4PDA	330	0.09	0.341	5.7	1.34-1.83	1.8
6FDA–3PDA	305	0.24	0.353	5.5	0.75-0.95	0.89-1.09
SiDA–44ODA	266	0.17	0.351	4.8	0.06	0.11
SiDA–34ODA	225	0.18	0.348	4.8	-	
PT 3p1m	318	<0.05	0.321	5.0	0.45	2.41
PT 1p3m	257	0.23	0.348	5.0	0.25	0.72
PC-PPh p	299	-	-	-	4.5	3.76
PC-PPh m/p	279	-	-	-	3.7	2.96
PC-PPh m	249	-	-	-	2.2	1.66

The polytriazole (PT) data are taken from ref. 15, the polycarbonate (PC) data from ref. 13.

There is no explicit relation between the isomer configuration and the overall free volume; V_f (= 1-K) is not significantly effected. Furthermore there is no relation between d-spacing and permeability. The effect on $\mathbb{D}$

and $\mathbb{P}$ must therefore be determined in the difference in *free volume distribution* between the *para*- and *meta*-isomers.
A molecular basis for this *para/meta* rigidity difference is based on the electronic structure of the polymer chain, see figure 3.5.

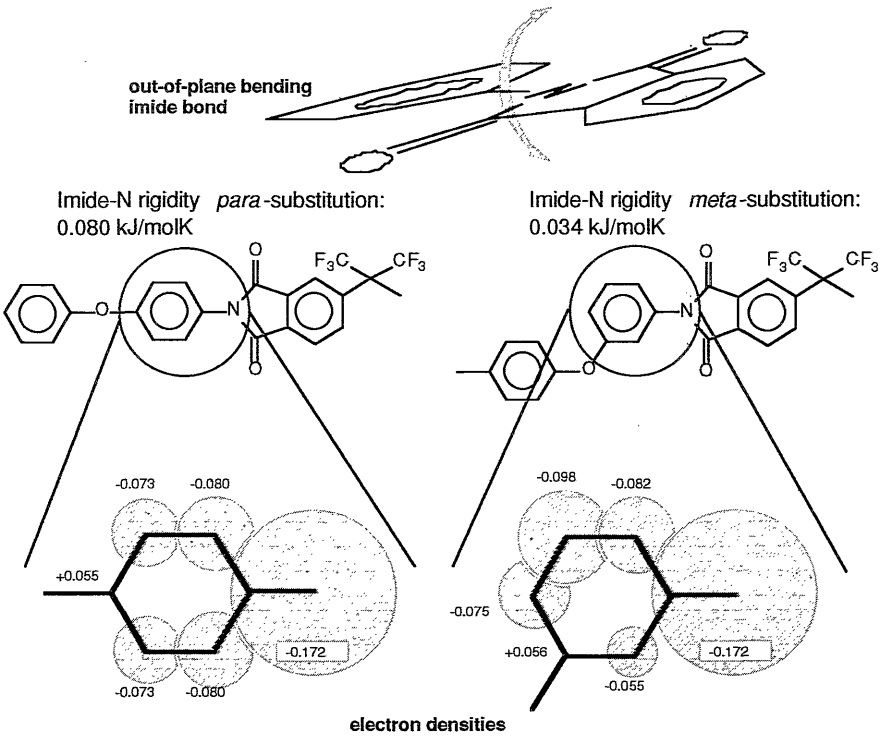

FIGURE 3.5: COMPARING LOCAL ELECTRON DENSITIES OF *PARA* AND *META* ISOMERS

(The electron distributions were derived from *tabulated* data embedded in the CAMM package Quanta CHARMm)
From figure 3.5 it can be seen that the *meta*-isomer has a lower electron density at the pivot point than the *para*-isomer. This will result in a lower electronic steric hindrance at this point. The pivot-point is the location where the chain will bend, thus determining to a large extent the chain rigidity. Even a small extra steric hindrance will thereby have a large effect on the overall chain rigidity, and thus on the parameters

that are associated with this rigidity such as glass transition temperature, free volume distribution and hence diffusivity.

The model proposed in Chapter 2 showed a linear relationship between the activation energy of diffusion and the value of the heat capacity jump. The experimental results are listed in Table 3.9 and represented in figure 3.6, in which $\log\mathbb{D}$ (linearly related to $E_{\mathbb{D}}$) is plotted against ΔC_p.

Table 3.9: Heat capacity jump and diffusivity data of CO_2 for 6FDA-polyimides

Nº	Polyimide	ΔC_p (J/gK)	$\mathbb{D}$ (m^2/s)
1a	6FDA-4PDA (unannealed)	0.098	$2.309 \cdot 10^{-12}$
1b	6FDA-4PDA (annealed 1 hour)	0.131	$1.759 \cdot 10^{-12}$
1c	6FDA-4PDA (annealed 2 hours)	0.163	$1.820 \cdot 10^{-12}$
2	6FDA-(4OMe)3PDA	0.098	$2.991 \cdot 10^{-12}$
3	6FDA-MDA	0.160	$1.491 \cdot 10^{-12}$
4a	6FDA-44ODA (unannealed)	0.140	$2.232 \cdot 10^{-12}$
4b	6FDA-44ODA (annealed 2 hours)	0.193	$7.670 \cdot 10^{-13}$
5	6FDA-34ODA	0.202	$9.520 \cdot 10^{-13}$
6	6FDA-SDA	0.206	$6.220 \cdot 10^{-13}$
7	6FDA-TMe4PDA$_1$/44ODA$_9$	0.141	$2.255 \cdot 10^{-12}$
8	6FDA-TMe4PDA$_1$/44ODA$_1$	0.069	$7.010 \cdot 10^{-12}$
9	Sixef™-44	0.090	$3.523 \cdot 10^{-12}$
10	Sixef™-44$(NO_2)_{0.5}$	0.065	$5.198 \cdot 10^{-12}$

The subscripts denote the ratio of each monomer or substituent in the copolymer

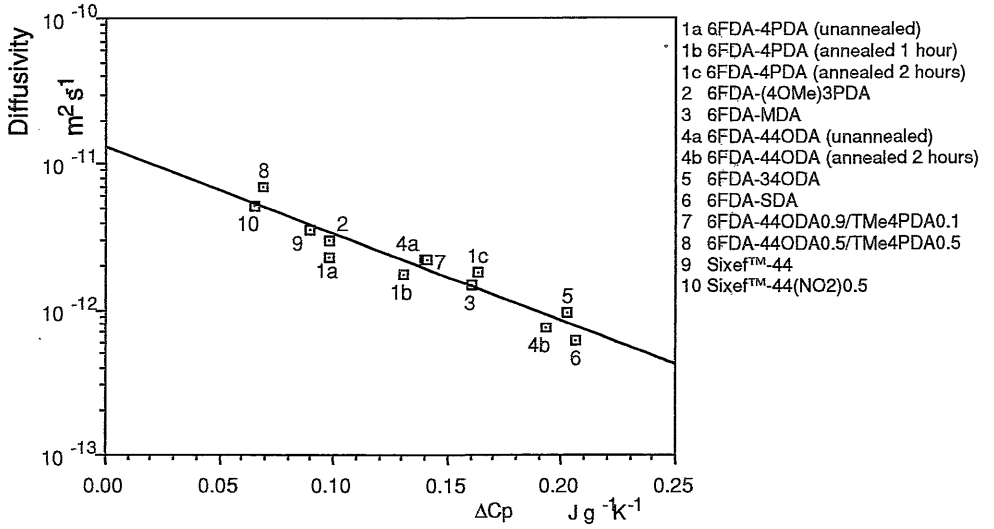

FIGURE 3.6: DIFFUSIVITY OF CO_2 AS A FUNCTION OF ΔC_p FOR A SERIES OF UNANNEALED AND ANNEALED 6FDA POLYIMIDES

From figure 3.6 the exponential correlation is clear. It can be seen that the more bulky polymers with 6FiPDA- (Sixef™-44) and TMe4PDA-diamine moieties have the higher diffusion coefficient. This can be related to the lower packing-ability. The *meta*-ODA isomer 5 has a lower $\mathbb{D}$ (and higher ΔC_p) than its *para*-ODA isomer 4a.

To study the effect of annealing of the polymer matrix in time one membrane (1b) was heated at 200°C for 2 hours and two (1c, 2b) at 300°C for 1 hour, and re-measured. The new data points fit on the line, showing that the heat capacity jump might indeed be a measure for the state of the polymer matrix, in relation to the diffusion process. The increase in ΔC_p is dependent on the extent of annealing, as can be expected. When the chain-movement is more restricted by annealing, the energy necessary to separate the chains (CED hence ΔC_p) will increase. As a consequence a lower diffusivity of the penetrant may be expected, which is indeed found.

Another alteration of the highly permeable 6FDA-6FiPDA was modification by nitration. This on-chain chemical modification up to 50% (i.e. one nitrate group per two repeat units (4 segments)) with a polar group

results in an increase in diffusivity and permeability, contrary to expectations: in most other polymers on-chain modification with a polar group results in a decrease in $\mathbb{D}$ and $\mathbb{P}$, and in an increased selectivity for CO_2/CH_4. The results for the modified polymer showed a reduced CO_2/CH_4 selectivity. This is possibly due to an even more reduced packing efficiency, which dominates over the effect of the increased intermolecular polar attractions.

When the 6FDA based polyimides are considered with the model as proposed in Chapter 2, we are now able to distinguish two different 6FDA series. The discrimination depends on the mean distance between the pivot points (see figure 3.7).

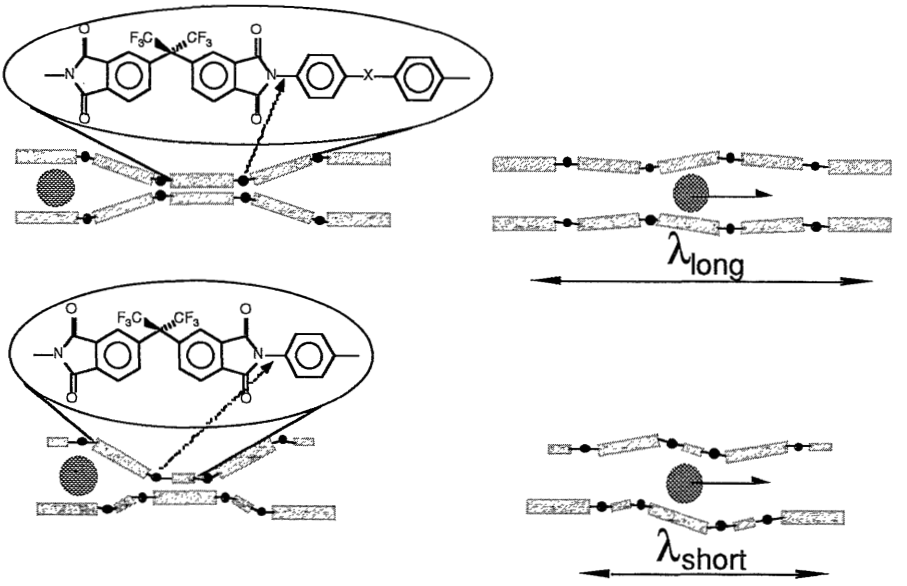

FIGURE 3.7: DEPENDENCE OF JUMP LENGTH ON THE PRIMARY STRUCTURE

This discrimination should give two series of polymers when the diffusivity is related to the hole forming energy, one for the 6FDA-polymers with a long (average) distance between two pivot points, and one for a shorter distance. The diffusivity in the latter class of polymers should depend

less strongly on the (volumetric) CED. The activation energy for diffusion depends linearly on CED, with λ as a proportional variable:

$$E_{\mathbb{D}} \sim \lambda \cdot CED$$

Since $$\mathbb{D} = \mathbb{D}_0 \cdot \exp(E_{\mathbb{D}}/RT)$$

it follows that $$\log\mathbb{D} \sim \lambda \cdot CED \qquad (3.5)$$

When the diffusion coefficient of CO_2 in the polyimides is plotted against the *volumetric* CED, which is the molar CED divided by the molar volume of the bulk polymer ($V_{vdWaals}/K$), figure 3.8 is obtained:

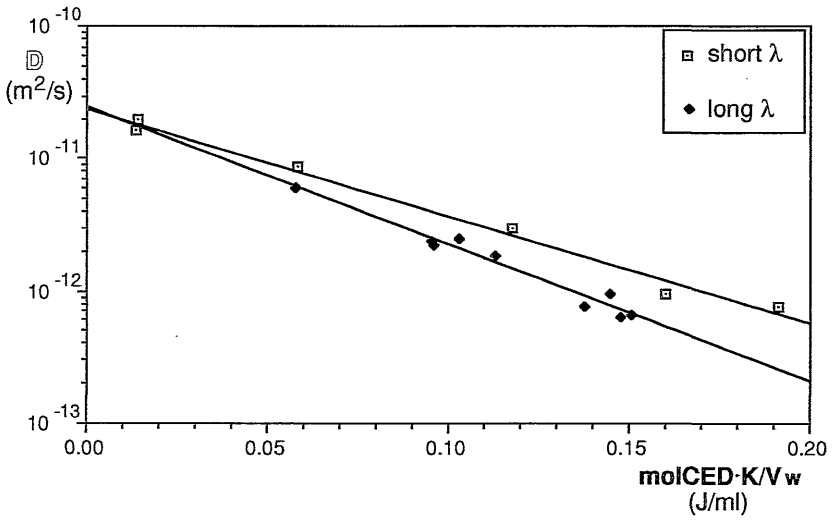

FIGURE 3.8: DIFFUSION COEFFICIENT AS A FUNCTION OF THE CED FOR VARIOUS JUMP LENGTHS

As expected two series are formed. In the group with the larger mean λ the dependence of $\log\mathbb{D}$ on the volume CED is indeed stronger. However it must be noticed that the accuracy in the values of the (vol)CED and the diffusivity are almost in the same order as the maximum difference.

3.8 Conclusions

The molecular model of the diffusion process, introduced in Chapter 2, is successful in rationalizing the dependence of the diffusivity on the cohesive energy density of the polymer. The now presented extended model incorporates the polymer structure factor that determines the diffusional jump length λ. In addition, there is a direct link between this λ value and the primary structure of the polymer.
However it will be clear that the model presented so far cannot explain all diffusivity and permeability related phenomena. It is not yet clear why the relation holds for closely related polymers such as the 6FDA polyimides, whereas it will not be valid when structurally different polymers are considered (e.g. PES and PSF). This may probably be associated with the relatively large differences in the free volume distribution between polymers of different classes. The small distribution in the packing densities (Table 3.2) and in the calculated sorption selectivity α_S for 6FDA polyimides (Table 3.4) are strong indications of a great similarity of the matrix structures in this class of polymers. This is essential in the model used to explain the permeability-ΔC_p relation.

With the help of computer modelling a more thorough transport model will be presented in the next chapter.

Literature

(1) Sroog, C.E., *J. Polym. Sci.: Macromol. Rev.*, **1976**, 11, 161

(2) Trumbo, D.L., *J. Polym. Sci., Polym. Chem.*, **1988**, A26, 2859

(3) Kim, T.H., Koros, W.J. and Husk, G.R., *J. Membr. Sci.*, **1989**, 46, 43

(4) Stern, S.A. Mi, Y.; Yamamoto, H. and St.Clair, A.K., *J. Polym. Sci., Polym. Phys.*, **1989**, B27, 1887

(5) Hellums, M.W., Koros, W.J., Husk, G.R. and Paul, D.R., *J. Membr. Sci.*, **1989**, 46, 93

(6) Askadskii, A.A., in: *Polymer Yearbook 4*, Pethrick, R.A. and Zaikov, G.E. (Editors), Harwood Academic Publishers, N.Y., **1987**, pp. 93-106

(7) E. Smit *et al.*, to be published

(8) Felder, R.M. and Huvard, G.S., in: *Methods of Experimental Physics*, vol. 16c, Academic Press, N.Y., **1980**, Chapter 17

(9) Hayes, R.A., U.S. Patents 4,717,394, **1988**, 4,838,900, **1989**

(10) Hoehn, H.H. and Richter, J.W., U.S. Patent 3,899,309, **1975**

(11) Lee, C.J., *Polym. Eng. Sci.*, **1987**, 27(13), 1015

(12) Privalko, V.P., *Macromolecules*, **1973**, 6(1), 111

(13) Sheu, F.R. and Chern, R.T., *J. Polym. Sci., Polym. Phys.*, **1989**, B27, 1121

(14) Sykes, G.F. and St. Clair, A.K. *J. Appl. Polym. Sci.*, **1986**, 32, 3725

(15) Hensema, E.R. and Boom, J.P., personal communications

APPENDIX A
SYNTHESIS

A.1 Synthesis of SiDA

The SiDA monomer is not commercially available. A generally accepted route to synthesize SiDA is given by Pratt and Thames [1]. We followed this route with some modifications. These modifications will be marked.

The synthesis of SiDA consists of four steps:

- Preparation of the lithiated aromatic (*o*-xylene type) parts of the monomer.
- Bridging two aromatic parts with dimethyl silane.
- Oxidizing the benzylic methyl groups
- Cyclo-dehydrating the formed tetracarboxylic acid to the dianhydride

A.1.1 Reaction of 4-bromo-o-xylene with n-butyl lithium (halogen-metal interchange)

Remark: 4-bromo-*o*-xylene, which is used as a starting material in the synthesis of SiDA, is only available in a purity of 75-80%. The other component present is 3-bromo-*o*-xylene. In order to get a reasonable yield and purity of the reaction product, a distillation step was introduced. Since the boiling points of both isomers are about the same at atmospheric pressure, a vacuum distillation with an isolated (Dewar-type) Vigreux column was employed to obtain sufficiently pure 4-bromo-*o*-xylene. It has been attempted to determine the purity of the product by NMR spectroscopy, but because of the complexity of the spectrum this proved to be impossible. It can however be concluded that the only products in the mixture are 4-bromo-*o*-xylene and 3-bromo-*o*-xylene.
To a stirred solution of 185.1 g (1 mole) 4-bromo-*o*-xylene in 500 ml anhydrous ether 400 ml (1 mole) 2.5 M n-butyl lithium solution in hexane at 0°C is added from a dropping funnel. The reaction set-up is kept under a stream of dried nitrogen, considering that the strongly basic n-BuLi reacts very fast and exothermic with water, if exposed to air. After all the n-BuLi has been added, the solution is stirred for 5 hours at ambient temperature.

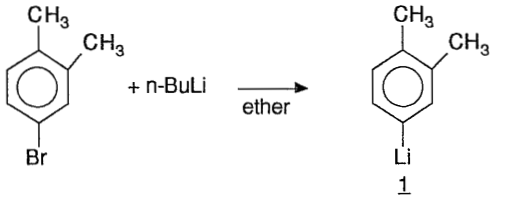

1

FIGURE A1: LITHIATION REACTION

The product, 1, is not purified but directly used in the next step.

A.1.2 Reaction of 4-Li-o-xylene with dichlorodimethylsilane

To the above reaction mixture 60.6 ml (0.5 mole) dichlorodimethylsilane is added drop-wise. The solution is stirred overnight before the precipitated LiCl is removed by suction filtration and the ether is removed by evaporation. After distillation 90.4 g (68 %) of 2 is obtained, boiling point 120-124°C (0.29 mm Hg), which solidifies on cooling, m.p. 51-54°C.

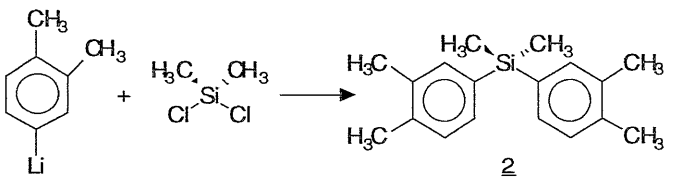

FIGURE A2: SILYLATION REACTION

One recrystallization from ethyl acetate gives pure 2, m.p. 54-56°C. (lit.: 54.5-55.5°C).

A.1.3 Aqueous $KMnO_4$-pyridine oxidation of 2

26.8 g (0.1 mole) 2 is dissolved in 400 ml pyridine and 110 ml water. In small portions 145 g (0.92 mole) $KMnO_4$ is added while stirring and heating to a slow reflux. The solution is refluxed for one hour at 120°C before 10 ml methanol is added to destroy any unreacted potassium permanganate.

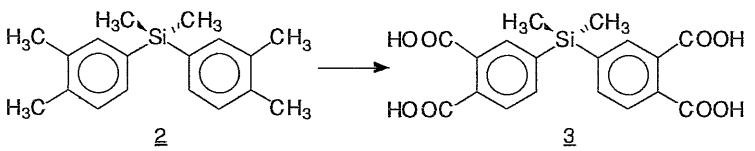

FIGURE A3: OXIDATION REACTION

After suction filtration of the MnO_2 followed by washing with boiling water, the mixture is acidified with concentrated hydrochloric acid of pH = 1. Then, contrary to the prescription of Pratt and Thames [1], the reaction mixture was extracted continuously overnight with ethyl acetate. This resulted in a much higher yield of crude tetracarboxylic acid 3 (after distilling off the ethyl acetate). Without the extraction step only 1-2 g of product can be collected. The crude tetracarboxylic acid 3 is not purified but dehydrated directly as described below.

A.1.4 Dehydration of 3 to form SiDA

18.2 g 3 is slowly refluxed for 1 hour with 60 ml acetic anhydride at 70°C, taking care to prevent degradation by overheating. The solvents are removed by vacuum distillation, and crude SiDA is collected.

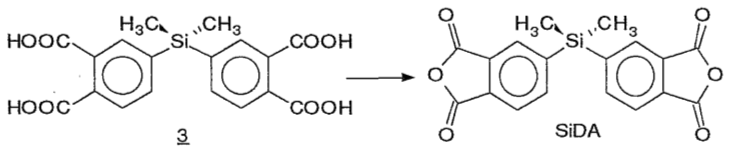

FIGURE A4: ANHYDRIDIZATION REACTION

The SiDA is purified by recrystallization from boiling toluene, m. p. 179-180.5°C (lit. 180.5-181°C). The overall yield is very low: 13%, while Pratt and Thames [1] claim 45%.

A.2 Synthesis of the polyimides

(Chemical structures and abbreviations are listed in Appendix C)
The polymer preparation was carried out in two steps: the formation of a poly(amic acid) by polycondensation of a dianhydride and an aromatic diamine. This poly(amic acid) was then *chemically* imidized to a polyimide. Both reactions will be discussed in more detail below.
The dianhydrides were stored under an absolutely dry atmosphere and used without further purification. In general the diamines were recrystallized at least once from 2-propanol. 4-Methoxy-1,3-diaminobenzene ((OMe)3PDA) and 2,7-diaminofluorene (DAF) were used as received. 1,4-Diamino-2,3,5,6- tetramethylbenzene (TM4PDA), 3-aminophenyl sulfone (3,3'DDS) and 4-aminophenyl sulfone (4,4'DDS) were recrystallized from 1-pentanol, and subsequently rinsed with n-hexane. 4-Aminophenyl ether (4,4'ODA) and 4,4'-methylene dianiline (MDA) were recrystallized twice from 1-pentanol. 1,8-Diamino-*p*-menthane (DAM) was vacuum distilled before use and stored under dry nitrogen. *o*-Toluidine sulfone (TSN), 4-aminophenyl sulfide (SDA) and 3,4'-aminophenyl ether (3,4'ODA) were used without further purification.
Solvents were used as received. *N,N*-dimethylacetamide (DMAc) was vacuum distilled from calcium hydride before use in the polymerizations. The solvent was stored under nitrogen on Linde 4Å molecular sieves. Pyridine was distilled from KOH, acetic anhydride was vacuum distilled before use. Both were stored under dry nitrogen prior to use.

A.2.1 Polymerization: poly(amic acid)

The poly(amic acid) was prepared at a final concentration of 10-15% by the slow addition of the dianhydride in an exact stoichiometric amount to a stirred diamine solution, or a mixture of diamines, in DMAc. The polymers were synthesized at a 1-5 gram scale. Because the synthesis of SiDA had afforded only a small amount of product (approximately 10 g), as little SiDA as possible was used during the polymerizations. For every reaction roughly 1 g SiDA was used.
The reaction was performed in a thoroughly dried system. During the reaction the mixture was kept under an atmosphere of dry nitrogen. The solution was stirred for 2-24 hours, with optional additional heating to 70°C. The inherent viscosity of the polymers was determined *after* imidization.

A.2.2 Imidization: chemical cyclodehydration

Since the polyimides based on 6FDA and SiDA are all soluble in a variety of common solvents, chemical imidization is preferred for these polymers (see § 3.2.2). A very beneficial result is that polyimides thus formed are not cross-linked. The conversion by chemical imidization is usually over 98%.
The poly(amic acid)s are imidized chemically by the addition of 5 equivalents of pyridine and 2.5 equivalents of acetic anhydride to the polymerization mixture and stirring for 2-3 hours at room temperature. The solution is then poured into a large excess of ethanol in a blender. Subsequently the product is washed two times, and dried to produce a white to yellowish polyimide as a powder or as threads. The yield was generally over 95%.

Literature

(1) Pratt, J.R. and Thames, S.F., *J. Org. Chem.* **1973**, 38(25), 4271

APPENDIX B
CHEMICALS USED

Abbreviation	Full name	CAS-number	Supplier	Purity
Dianhydride				
6FDA (electronic)	5,5'-(2,2,2-trifluoro-1-(trifluoromethyl)-ethylidene)-bis-1,3-isobenzofuranedione	1107-00-2	Hoechst Celanese Summerville NJ (USA)	>99%
Diamines				
3PDA	1,3-diaminobenzene	108-45-2	Aldrich, Steinheim (BRD)	>99%
4PDA	1,4-diaminobenzene	106-50-3	Aldrich	
DAF	2,7-diaminofluorene	525-64-4	Aldrich	
TMe4PDA	1,4-diamino-2,3,5,6-tetramethyl-benzene	3102-87-2	Janssen Chimica Beerse (Belgium)	
44ODA	4,4'-oxydianiline	101-80-4	Merck, Darmstadt(BRD)	97%
34ODA	3,4'-oxydianiline	--	Wakayama Seika Kogyo Wakayama (Japan)	
MDA	4,4'-methylenedianiline	101-77-9	Merck	97%
TSN	o-toluidinesulfon	--	Wakayama Seika Kogyo	
SDA	4,4'-thiodianiline	--	Wakayama Seika Kogyo	
4Me3PDA	1,3-diamino-4-methylbenzene	95-80-7	Aldrich	98%
15NDA	1,5-diaminonaphtalene	2243-62-1	Aldrich	98%
Commercial polyimide				
Sixef™-44	--	--	Hoechst Celanese	
Miscellaneous				
4-Bromo-o-xylene		538-71-1	Aldrich	~75%
Dichloro dimethylsilane		75-78-5	Aldrich	>98%
n-Buthyl lithium (2.5M in hexanes)		109-72-8	Aldrich	

APPENDIX C

MOLECULAR STRUCTURES OF THE POLYMERS

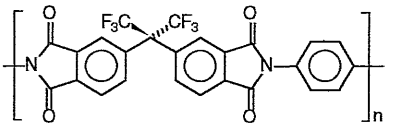

6FDA-4PDA

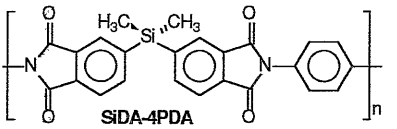

SiDA-4PDA

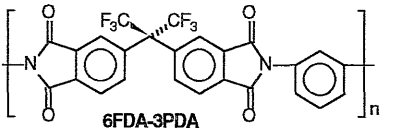

6FDA-3PDA

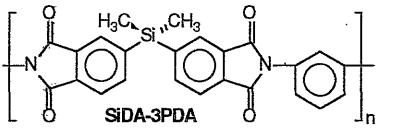

SiDA-3PDA

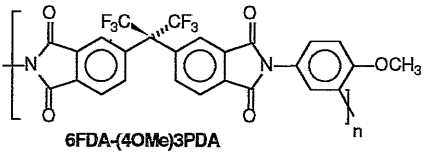

6FDA-(4OMe)3PDA

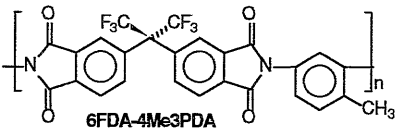

6FDA-4Me3PDA

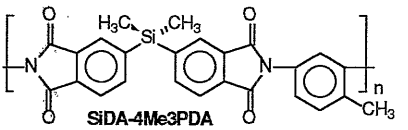

SiDA-4Me3PDA

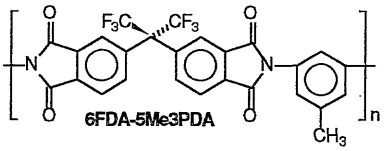

6FDA-5Me3PDA

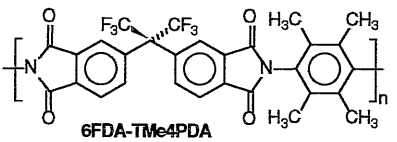

6FDA-TMe4PDA

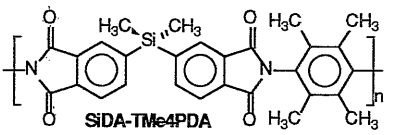

SiDA-TMe4PDA

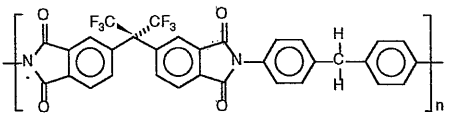

6FDA-MDA

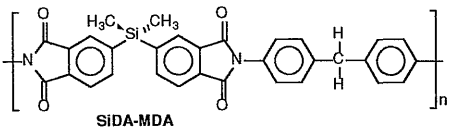

SiDA-MDA

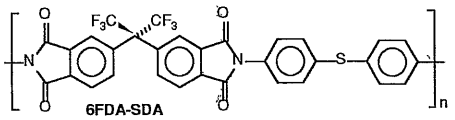

6FDA-SDA

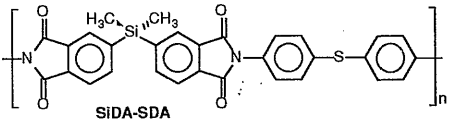

SiDA-SDA

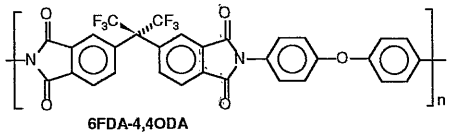

6FDA-4,4ODA

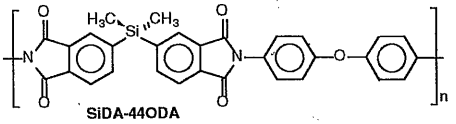

SiDA-44ODA

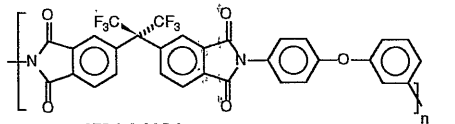

6FDA-3,4ODA

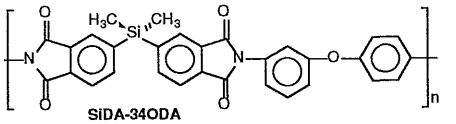

SiDA-34ODA

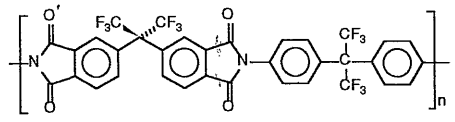

6FDA-6FiPDA (Sixef™-44)

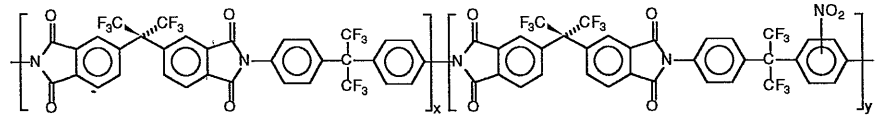

6FDA-6FiPDA(NO_2)$_{0.5}$

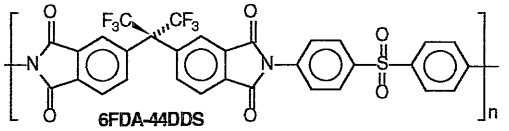

6FDA-44DDS

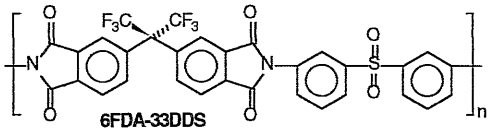

6FDA-33DDS

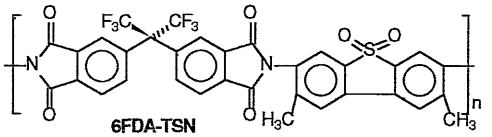

6FDA-TSN

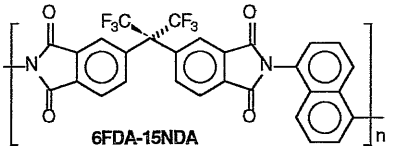

6FDA-15NDA

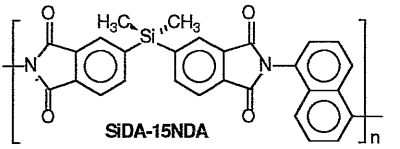

SiDA-15NDA

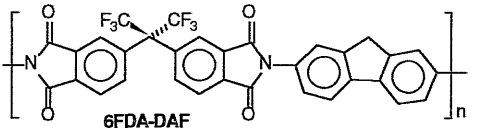

6FDA-DAF

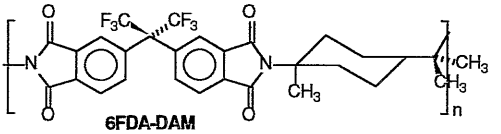

6FDA-DAM

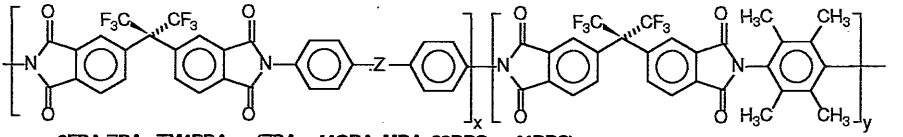

6FDA-ZDA$_x$-TM4PDA$_y$ (ZDA = 44ODA, MDA, 33DDS or 44DDS)

APPENDIX D

TYPICAL IR SPECTRUM OF A POLYIMIDE FILM

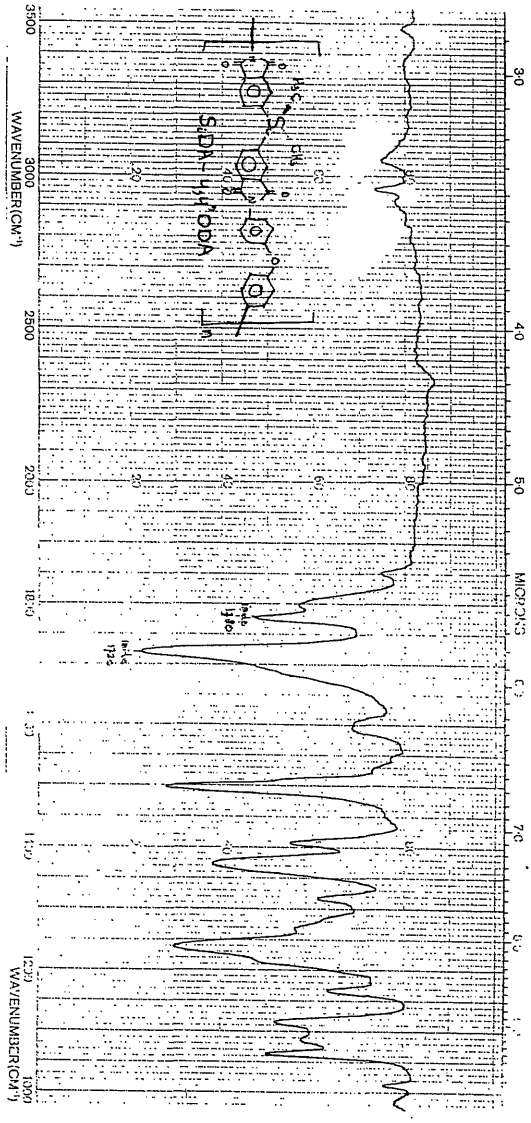

APPENDIX E

TYPICAL WAXD SPECTRUM OF A POLYIMIDE

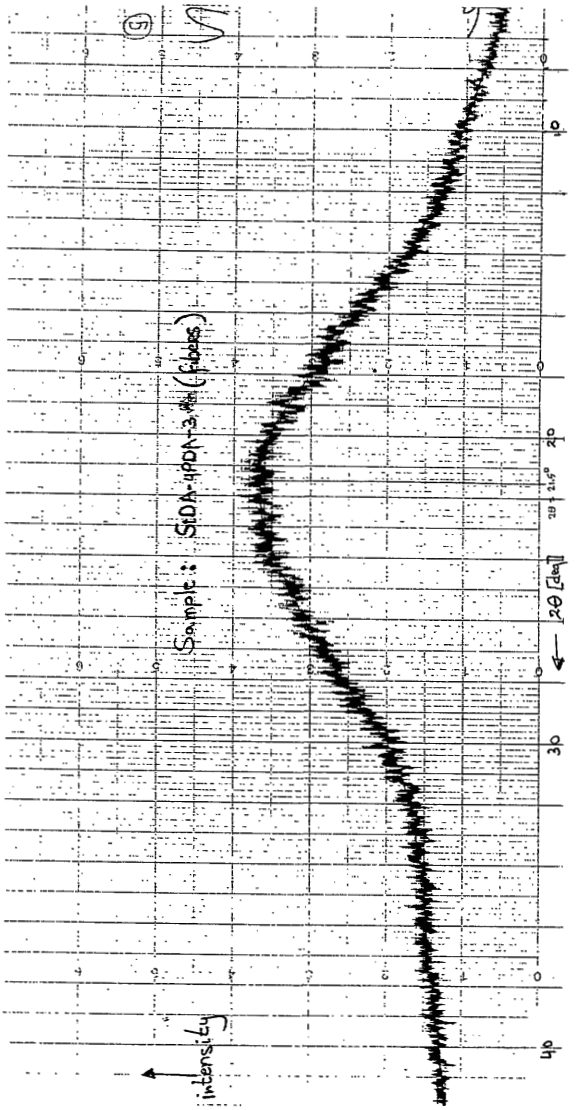

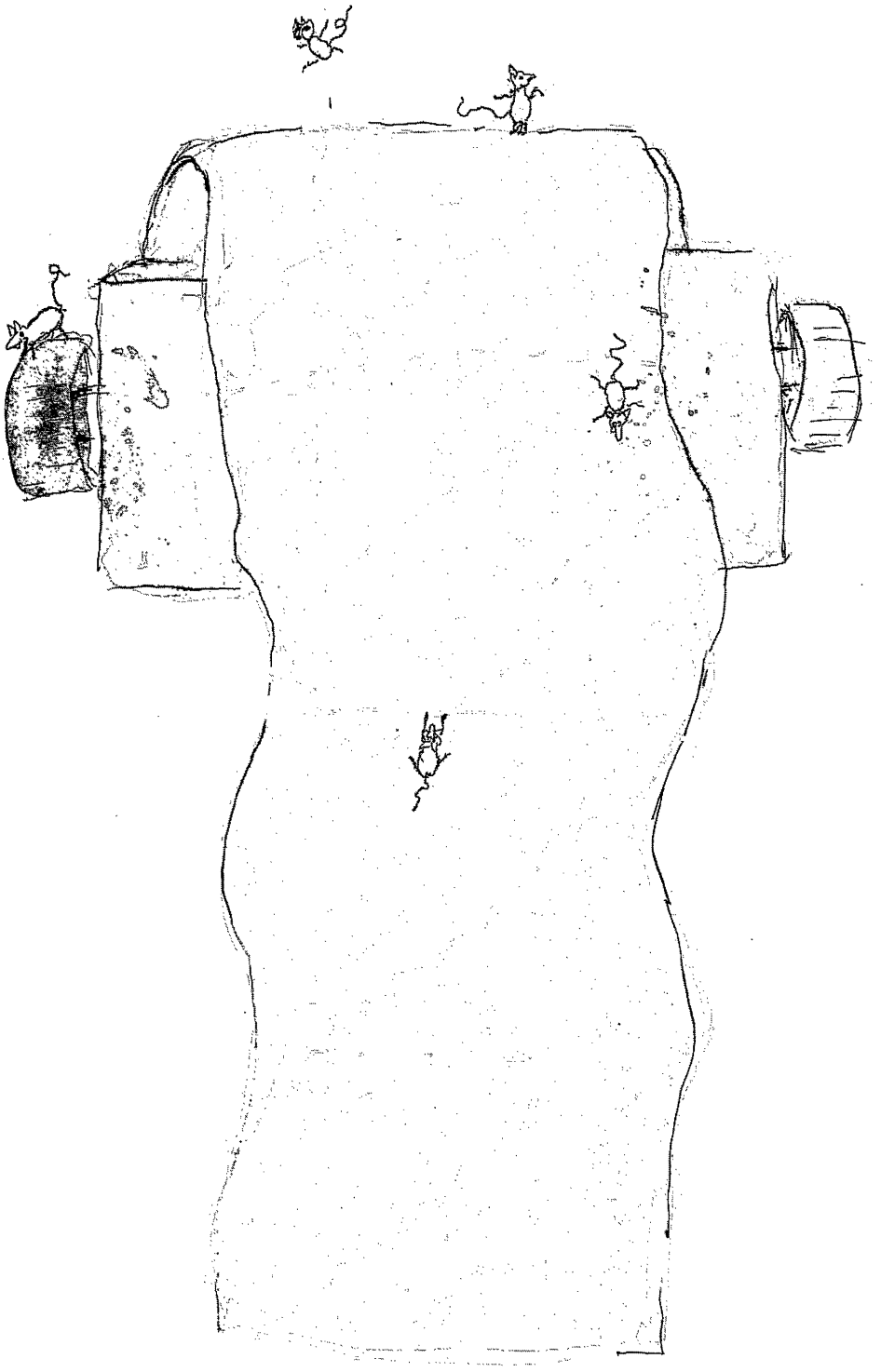

CHAPTER FOUR

AN ADVANCED MATRIX MODEL FOR THE DIFFUSION OF GASES THROUGH POLYMERIC MEMBRANES

Computer aided molecular modelling

CONTENTS

4.1 Introduction to Computer Aided Molecular Modelling

The permeation and diffusion behavior of gases through polymers cannot be completely described by the models mentioned so far. A major problem is that we are unable to consider the processes on a molecular level. However, recently Computer Aided Molecular Modelling (CAMM) is being used more frequently to obtain that information. CAMM is the most recent and most advanced method available at present to simulate a polymer matrix. Molecular dynamics (MD) simulations can give insight in the diffusion process in such a detail as was previously unattainable. MD may be used to predict the *macroscopic* properties resulting from *inter-atomic* interactions [1].

The technique is available in our department and in cooperation with other researchers (Berendsen and Sok from the University of Groningen, the Netherlands, and H. Takeuchi from Mitsubishi Corp., Yokohama, Japan) an amorphous polymer matrix box has been created, and the diffusion of CO_2 through that box was simulated. In this way we were able to simulate the highly complex 6FDA-polyimides which have been synthesized in our group (cf. Chapter 2 and 3). This means that computed results could be compared with the actual diffusion measurements.

For the MD calculations we used the GROMOS program [2]. It makes use of a force-field consisting of a sum of the bonded and non-bonded interactions between the atoms in the system to be studied:

$$E_{tot} = E_{bond} + E_{angle} + E_{dihedral} + E_{improper} + E_{VdW} + E_{electrostatic} \qquad (4.1)$$

The *bonded* interactions describe the interactions between covalently linked atoms (see also figure 4.1):

$$E_{bond} = \Sigma^1/_2 k_{bond} (r-r_0)^2 \qquad (4.2)$$

$$E_{angle} = \Sigma^1/_2 k_{angle} (\Theta-\Theta_0)^2 \qquad (4.3)$$

$$E_{dihedral} = \Sigma k_{dihedral} (1+\cos(n\Phi-\delta)) \qquad (4.4)$$

$$E_{improper} = \Sigma^1/_2 k_{improper} (\Psi-\Psi_0)^2 \qquad (4.5)$$

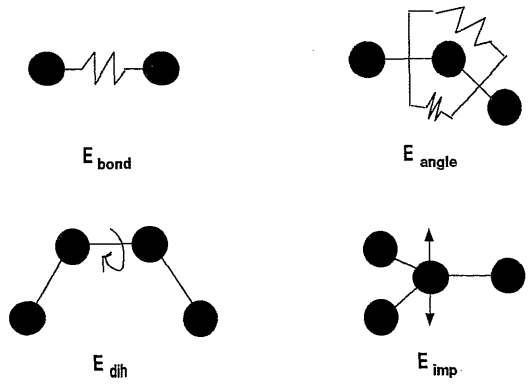

FIGURE 4.1: FORCE-FIELD USED IN THE MD CALCULATIONS: BONDED INTERACTIONS

The non-bonded atoms are taken to exhibit pairwise Van der Waals and electrostatic interactions (see also figure 4.2):

$$E_{VdW} = \Sigma C_{12} (r_{1,2})^{-12} - \Sigma C_6 (r_{1,2})^{-6} \quad (4.6)$$

$$E_{electrostatic} = \Sigma(q_1 q_2 / (4\pi\varepsilon_0 r_{1,2})) \quad (4.7)$$

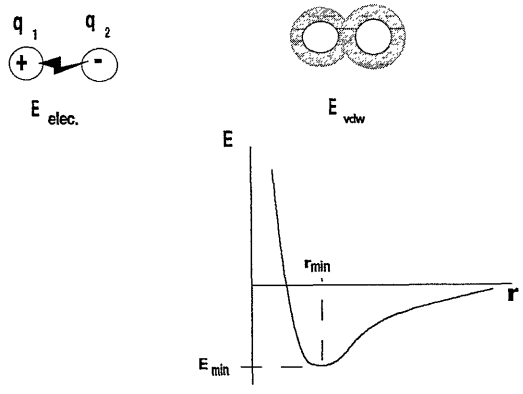

FIGURE 4.2: FORCE-FIELD USED IN THE MD CALCULATIONS: NON-BONDED INTERACTIONS

CAMM packages (like GROMOS) use only static charges on atoms, which can be a limitation as will be shown later (§ 4.6).

From the entire system a topology-file is created, incorporating all bonds, angles, the (improper) dihedrals and the nonbonded interaction pairs within the cutoff-range. The parameters describe through the force-field the energy of the system. Integration of Newton's equations of motion over time using all forces gives the time-evolution of the system, in the pico-second (ps, 10-12 s) range.
The amorphous box created by the method to be described in § 4.3, making use of this force field, and is used to perform molecular dynamics calculations to simulate CO2 diffusive motion (§ 4.4). It can also be used to estimate a free volume distribution, see § 4.2 (we have not yet performed these laborious calculations ourselves).

4.2 Free volume distribution determination with CAMM

The overall free volume, the free volume distribution and the CED are important parameters that determine the rate of diffusion of a penetrant molecule through a polymer matrix.
In the last four decades it has been shown that diffusivities of penetrants in polymers, and other properties like stress-relaxation and viscoelastic behavior, can be correlated with the polymer free volume [3-5]. However, we think that the *free volume distribution* is even more important. A first improvement in looking at free volume distribution effects is to consider the volume instead of the diameter of the penetrant [6].
The determination of the free volume and, even more difficult, the free volume distribution still is a basic problem. In Chapter 2 a kind of Boltzmann model was given for the determination of the FVD, but the results from this model have not been verified yet. It is not possible to measure the FVD accurately, but CAMM may be a promising computational alternative.
The most frequently used modelling polymer in literature is polymethylene (PM, a polyethylene metaphor), in which the atoms in the CH_2 units are united (for the sake of simplicity) to one "quasi" atom with the characteristic properties of the methylene unit. The reason for this approach is that this polymer is very easy to model, and the results of the calculation can be compared with experimental data for polyethylene.

After constructing a polymer matrix, which can be accomplished in several ways, the free volume and free volume distribution calculations can be performed. One way to resolve the free volume distribution is by probing the box with spherical penetrant molecules of different sizes. The spheres are placed randomly in the box, and those positions on which the sphere does not disturb the polymer structure are counted as contribution to the FVD. The fractional available space available to each sphere of a certain size is plotted against its volume. Different researchers have found perfect exponential free volume distributions for the *rubbery state* of various polymers using this method [6,7]. An example is shown in figure 4.3 (PDMS, from [7]).

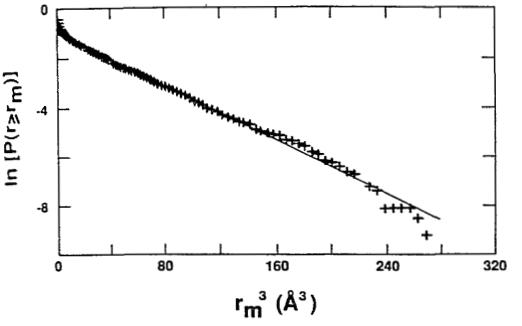

FIGURE 4.3: PROBABILITY $P(R \geq R_M)$ VERSUS R_M^3 IN PDMS; FROM [7]

We consider this as a strong evidence for the applicability of the Boltzmann-type FVD-model (Chapter 2), although no FVD determinations have been performed so far on glassy polymers.

Another elegant method to estimate the FVD is being developed by Takeuchi [8] and will soon be published. The FVD computation in a simulated polymer matrix is performed by gradually increasing the Lennard-Jones size of the atoms of the chains. At some critical point the atoms touch (which can easily be determined) and interconnected free volume elements are separated, smaller holes are formed. These holes reflect the structure of the matrix in the starting configuration, thus the distribution of free volume elements.

An important parameter in determining the FVD is the chain stiffness, which directly influences the (dynamics of the) free volume. One way to simulate different rigidities in the same polymer is to change a main-chain bond torsional potential and thus E_{angle}, $E_{dihedral}$ and $E_{improper}$ (eq. 4.3-4.5). It is also possible to change only a main-chain bond angle. The overall effect on the chain rigidity is the same, as was shown by Takeuchi *et al.* [8]. They studied the model system PM well above T_g, with infinite chain length, and varied the equilibrium angle θ_0 between the methylene units: 100°, 109.5° (tetrahedral, reference), 130° and 150°. A larger bond angle results in more stretched chains, thus less intermolecular shielding. The chains can be more easily brought together, resulting in a shorter inter-chain separation and thus a reduced diffusion, even if the overall free volume remains the same (which is the case). As θ_0 is increased, the packing becomes more tight (narrower FVD). This is an indication of an increasing chain stiffness in the case of *rubbers*: less flexible chains cause the dynamics of the free volume elements to slow down, see also §2.3.4. When the chain is more flexible the free volume distribution is wider in the rubbery state. Also the average chain spacing is increased [8-10], and diffusion proceeds faster. Trohalaki *et al.* also noticed such an effect, although without attributing it to the chain stiffness [7]. By changing the Si-O-Si bond in model PDMS from its normal 37° to 70°, thereby artificially stretching the chain, the distribution of the free volume narrowed. For glassy polymers the picture reverses, a contrary trend which can also be found in experimental data on rubbers and glassy polymers. For example, the introduction of a bulky side group tends to *increase* $\mathbb{D}$ (and $\mathbb{P}$) in glassy polymers whereas a *decrease* can be observed in rubbers. The diffusion in the rubbery state depends more strongly on the dynamics of the polymer, and in the glassy state it depends more strongly on the local structure of the matrix. This can be explained by the difference in relaxation times of chain elements in the two states: the motion of a glassy polymer chain is orders of magnitude slower than that of the penetrant molecule, whereas they are more on the same level in rubbers (a liquid-like system). Rigby and Roe reported [11] that the self diffusion coefficient of the polymer chain almost vanishes below T_g, whereas above T_g it is only 7-9 times smaller than that of the penetrant molecules.

4.3 Simulation of the polymer matrix

In order to study the diffusional jump process in detail, Molecular Dynamics (MD) calculations were performed inside 6FDA-4PDA and 6FDA-44ODA matrices using CO_2 as gas. Our aim is to investigate by simulation the jump model proposed in the previous chapters. The motion of CO_2 in a simulated polyimide box (see figure 4.4) might provide us some helpful information.

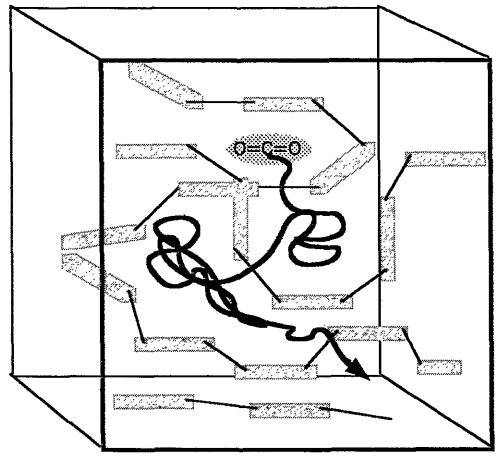

FIGURE 4.4: PENETRANT MOTION IN A SIMULATED POLYMER MATRIX BOX

The diffusion simulation consists of several parts:

1. Parametrization of the force-field that determines the dimensions and energetic constraints of the polymer chains
2. Creation of an amorphous 'box' of sufficient size to estimate relevant parameters, and to examine the degree to which the box is amorphous.
3. Simulation of the diffusion of a small penetrant molecule through this polymer box.

It is important to determine the energetic constraints in an isolated polymer chain of one of our polyimides, because this directly influences the ease of chain- and matrix deformation. This in turn influences the diffusivity, as explained in § 2.6.

4.3.1 Simulation of the primary and secondary structure

The CAMM package used (GROMOS) does not have all parameters for the bond- and atom-types that occur in our polyimides. Van Eerden [12] has estimated the parameters for the imide–ring by *ab initio* calculations. Intra-molecular dimensions have been verified by X-ray data from 6FDA and SiDA crystals [13]. The calculated structure of these monomers and the crystal structure were in very good agreement.

In Chapter 2 (figure 2.19) the calculated out of plane bending energies for the different possible *pivot-points* were listed. The calculation of the bond-flexibilities was performed by bending these bonds in small increments in a computer model of a trimer or pentamer (e.g. 34ODA-6FDA-44ODA) out of the plane, as shown in figure 4.5:

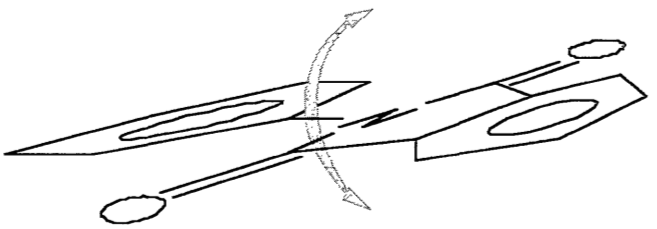

FIGURE 4.5: OUT-OF-PLANE BENDING OF A BOND FOR THE ESTIMATION OF THE FLEXIBILITY

Total energy calculations (of minimized structures) as a function of the improper dihedral angle were thus performed. The resulting curve was fitted to a third-order polynomial, of which the second term is the overall force constant:

$$E = k_3(Y - Y_0)^3 + \boxed{k_2(Y - Y_0)^2} + E_0 \qquad (4.8)$$

very small — flexibility — $E(Y_0)$

The imide bond between the N atom and the phenylene ring turns out to be the most flexible 'point' in the polymer chain, as was indicated in figure 2.19, Chapter 2. It should be mentioned that the electron densities on the atoms (atomic charges) are not calculated, but were put in the computer model as parameters.

The electron density near the imide bond in the *meta-* isomer is lower and thus the electronic steric hindrance will be smaller, resulting in a more flexible bond. Since it is also the pivot-point in the chain, it has a large influence on polymer properties. The consequences of this result for the model proposed in Chapter 2 were discussed in Chapter 3.

4.3.2 Creation of the polymer box

A commonly used method to create a random box of molecules is based on a self-avoiding random walk [14], but at higher densities (as in our polymers) this Monte-Carlo method fails.
We created the polymer matrices by employing the method also used by Berendsen and Sok [1,2], i.e. the reduction in size of a box with a very tenuous polymer filling to its final, actual density. A problem when simulating bulk polymer matrix formation is the time scale: in reality the formation of e.g. a membrane takes several hours, so the time for relaxation of the chains is in the order of 10^3-10^4 s. The time scale for computer simulation is in the order of pico seconds (10^{-12}-10^{-10} s). Hence it will be impossible in a straight-forward box-size reduction experiment to involve all possible chain relaxations. This will result in an unrealistic matrix, as indicated by the impossibility to reach the bulk density. Thus a *mathematical trick* has to be used, to take the main obstacle, the direct contact of the polymer chains and the impossibility to relax away from this frictional contact on such a short time scale. This non-relaxable contact would result in a premature freezing of the matrix.
The trick that has been applied is to use molecules with a temporarily replacement of the normal Van der Waals (Lennard-Jones 6-12) potential for intermolecular interaction by a so-called *soft-core* repulsion. We thus allow close contacts between atoms, and the individual chains can even traverse each other: the thermal motion can overcome the repulsion.

Hence:

$$E_{softcore} = V_{max}(1-(r/r_{min})^2)^2 \quad \text{and for } r<r_{min} \qquad (4.9)$$

$$E_{softcore} = 0 \quad \text{for } r \geq r_{min}$$

where $V_{max} \approx kT$, i.e. the maximum repulsion energy is in the order of kT.

This is visualized in figure 4.6:

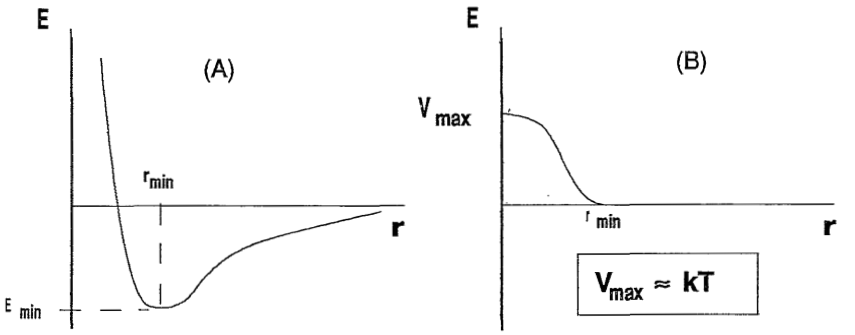

FIGURE 4.6: LENNARD-JONES 6-12 POTENTIAL (A) VERSUS SOFT-CORE POTENTIAL (B)

Also the electrostatic potential is neglected during the reduction of the size of the box. Since now the premature freezing of the matrix is prevented no complex relaxation processes occur during the matrix formation, and also no minimization during the volume reduction is necessary. In this way the simulation process is clearly accelerated.
The box which has been simulated contains 5 randomly orientated polymer chains of 11 monomer segments each (also with random folding, as far as strain permits), e.g.:

PDA-6FDA-PDA-6FDA-PDA-6FDA-PDA-6FDA-PDA-6FDA-PDA

The box has periodic boundary conditions to prevent surface effects, which means that parts that may leave the box on one side re-enter on the opposite side. Also the non-bonded interactions stretch through the box walls. At the start of the simulation process the size of the box is such that it has about 1% of the bulk density of the polymer. The density has been gradually increased up to the experimental value by reducing the size of the box, see figure 4.7.

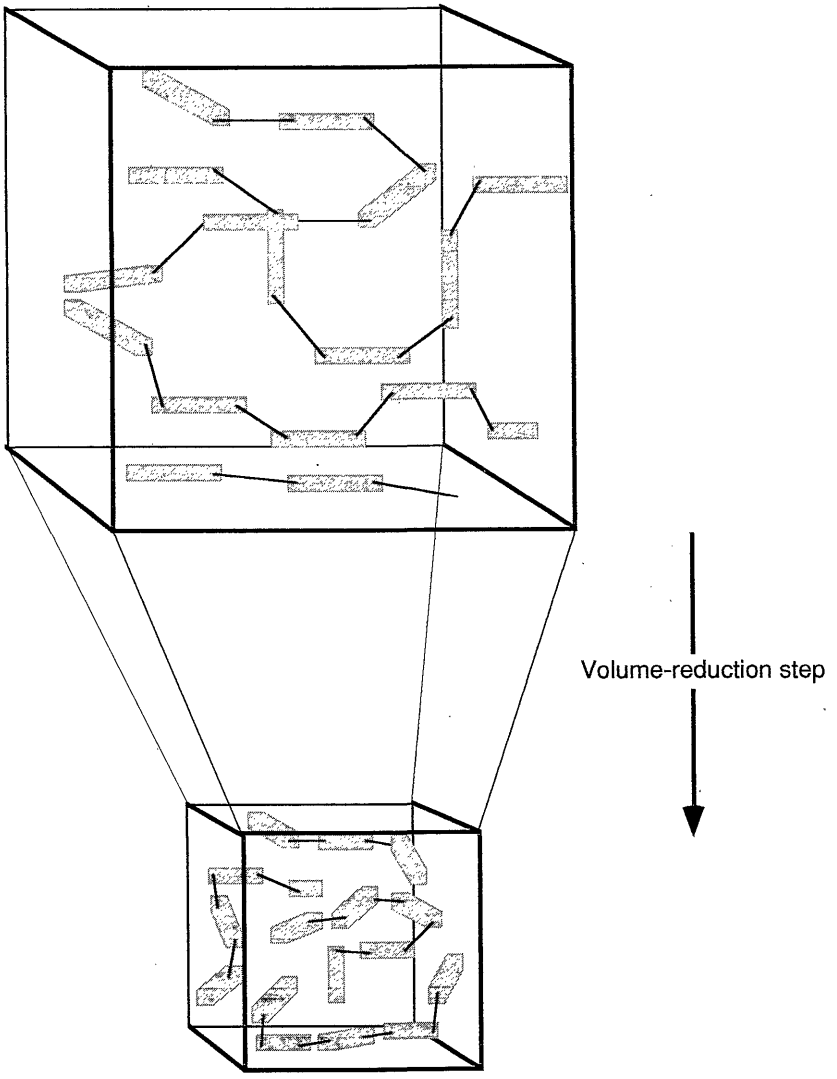

FIGURE 4.7: SHRINKING OF THE POLYMER BOX

After each small reduction step the box is 'shaken' by molecular dynamics procedures to achieve a relaxation of the polymer matrix. All significant bending-possibilities and rotational degrees of freedom are taken into consideration in the creation of the matrix. To get a realistic matrix simulation a large number (10,000) of reduction steps are necessary.

Since the box consists of approximately 1200 atoms, and thus many thousands of interactions (over 50,000, mostly non-bonded), the calculations are very time-consuming.

The result of the simulation with a final soft-core potential between the chains is not realistic, of course, and after the bulk density (or a somewhat higher value) is reached, the normal Lennard-Jones and electrostatic potentials are again introduced. Subsequently the system is equilibrated normally. This results in a limited moving apart of the chains, but not to a significant increase of the box volume. The resulting matrix should resemble the real polymer state. Both have an intimately intertwined structure, and are well-relaxed. The generated systems, consisting of 5 polymer chains, were cubic simulation boxes with periodic boundary conditions. The box edge after shrinking was about 25Å.
The distribution of the free volume in the box could now have been calculated as mentioned in § 4.2, but this elaborate computation has not yet been carried out due to lack of time.

In order to check the amorphous character of the boxes (6FDA-polyimides are completely amorphous), a test for parallel ordering of (segments) of the polymer chains was performed. The pair distribution function:

$$P_2 = \frac{1}{2}\left(3\langle \cos^2 \psi \rangle - 1 \right) \qquad (4.10)$$

was used to evaluate possible intermolecular alignments [14].
With only 5 chains in the box merely checking the *overall* chain ordering would give only 10 angles, resulting in an insufficient statistical significance. Therefore we divided every chain into sub-units (one 6FDA and one 4PDA or 44ODA unit, see figure 4.8).

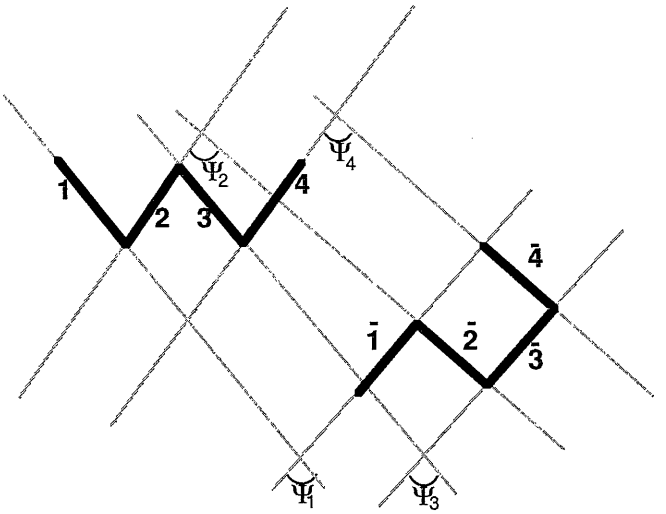

FIGURE 4.8: TEST FOR PARALLEL ORDERING OF CHAIN SEGMENTS IN THE POLYMER BOX

In this way 40 angles are considered. The result of the test for the polymer boxes is a P_2 value of about 0.02 ± 0.01. This low value indicates that the boxes are almost completely amorphous: perfect random ordering would yield $P_2 = 0$.

4.4 Modelling of the diffusion process by Molecular Dynamics

One, respectively 10, CO_2 molecules are placed into the boxes of 6FDA-4PDA and 6FDA-44ODA at random positions. The CO_2 molecule is considered as a stiff rod, and it is kept *nearly* straight: 179°. The deviation was necessary due to the program-routine that keeps the molecule from bending. In consecutive MD runs at 25°C the diffusive motion of the penetrant is simulated. *All possible interactions and chain motions were taken into account during the simulation of the diffusion process.*
When the path of a CO_2 molecule is followed **diffusional jumps** can actually be observed, as was predicted by the model (see Chapters 2 and 3). Figure 4.9 gives the motion of a CO_2 molecule as a function of time.

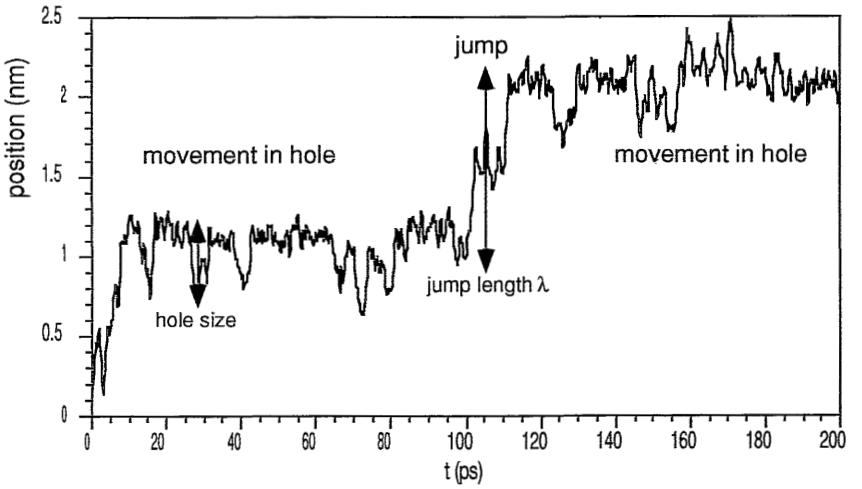

FIGURE 4.9: MOTION OF A CO_2 MOLECULE IN A 6FDA-4PDA POLYMER MATRIX

During the first 100 ps of the simulation the gas molecule is 'bouncing' at a high frequency inside a hole of about 5Å. Then it moves within a very short time over a distance of approximately 10Å, a *diffusional jump*. Next it moves inside a confined space again. This simulation process is depicted schematically in figure 4.10.

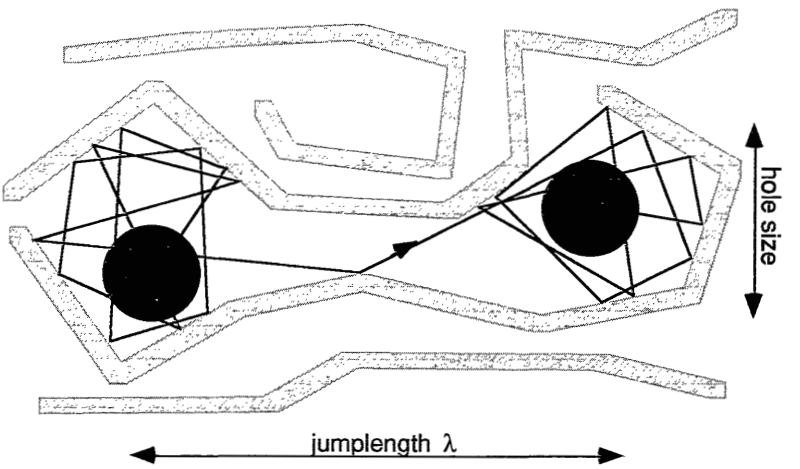

FIGURE 4.10: CONFINED MOVEMENT AND JUMP MOTION INSIDE THE MATRIX

The tunnel as shown in figure 4.10 is only temporary large enough to let the CO2 molecule pass. The polymer chains are moving also, but at a much slower rate.

To view only the total displacement with regard to the starting point does not yield all details of the motion, see figure 4.11:

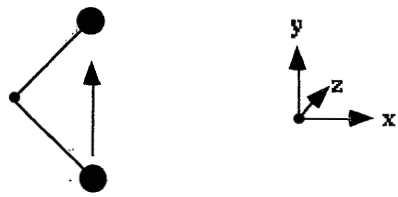

FIGURE 4.11: MOTION WITHOUT EFFECTIVE DISPLACEMENT IN THE X AND Z DIRECTION

Therefore we must consider the migration in all three dimensions. In this way more jumps are revealed as can bee seen in figure 4.12.
The same procedure was followed for 6FDA-44ODA. The results for one of the CO_2 molecules are shown in figures 4.13 (total movement) and 4.14 (movement in the three directions).

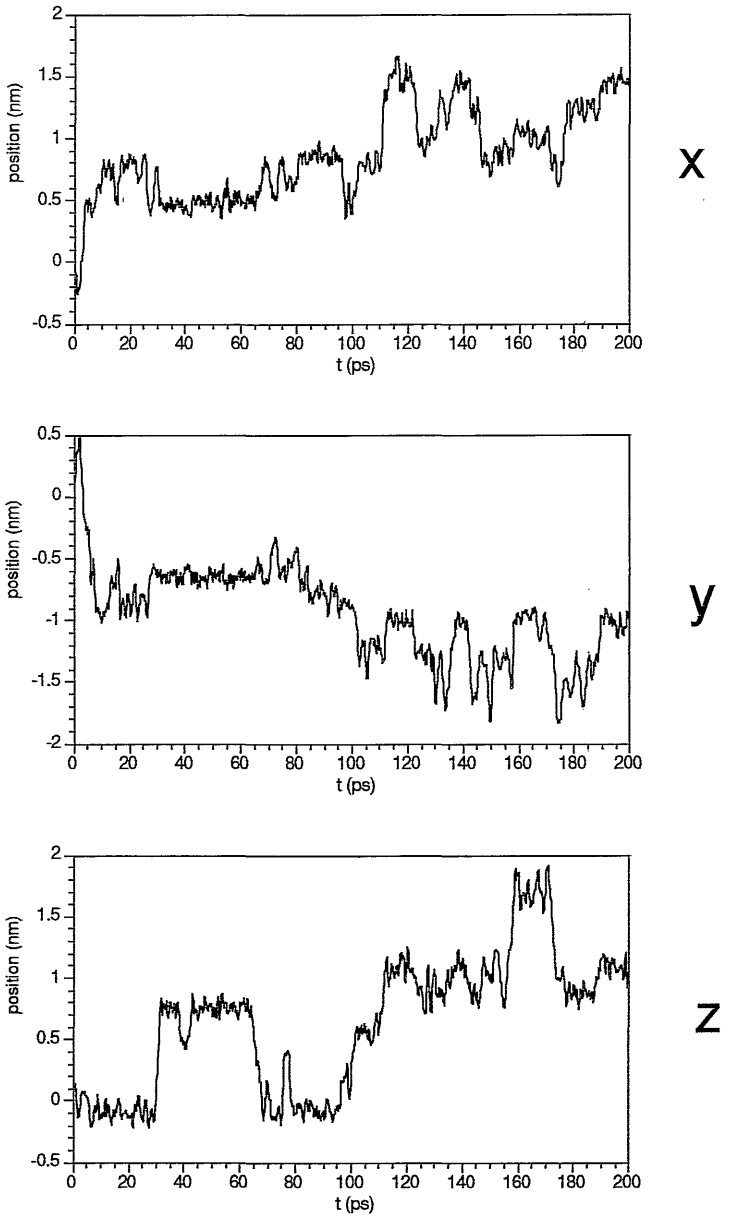

FIGURE 4.12: DISPLACEMENT OF CO_2 IN THREE DIRECTIONS IN 6FDA-4PDA

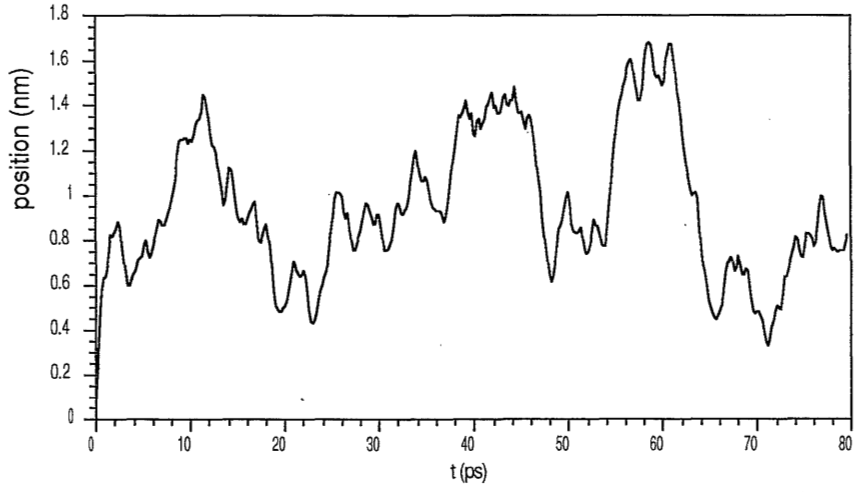

FIGURE 4.13: MOTION OF ONE OF THE CO_2 MOLECULES IN A 6FDA-44ODA POLYMER MATRIX

In the case of the 6FDA-44ODA matrix the jumping behavior seems less explicit. First it should be remarked that the total simulation time is only 80 ps. Secondly the more complex primary structure of the polymer may result in a more complex hole-distribution, resulting in a more complex motion of the gas molecule. However, in figures 4.13 and 4.14 leaps of over 13Å are visible, indicating true jumps.

From the coordinates of the centre of mass of the CO_2 molecules the selfdiffusion coefficient can be calculated using the Einstein relation:

$$\mathbb{D} = \lim_{t\to\infty} \frac{\langle r^2 \rangle}{6t} \tag{4.11}$$

where (averaging over all gas molecules and t_0)

$$\langle r^2 \rangle = \langle | r(t_0+t)-r(t_0) |^2 \rangle \tag{4.12}$$

For the two investigated systems the results are shown graphically in figures 4.15 and 4.16.

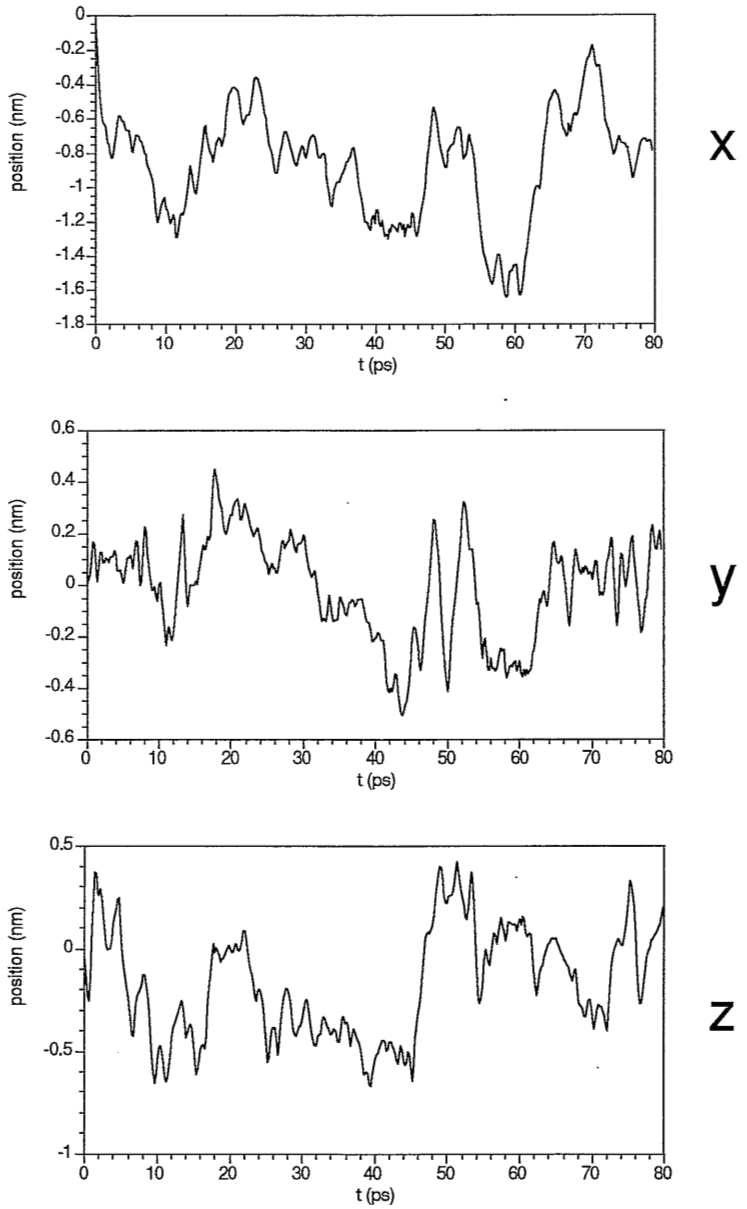

FIGURE 4.14: DISPLACEMENT OF CO_2 IN THREE DIRECTIONS IN 6FDA-44ODA

The limiting value represents the selfdiffusion coefficient of CO2 in the polymer box.

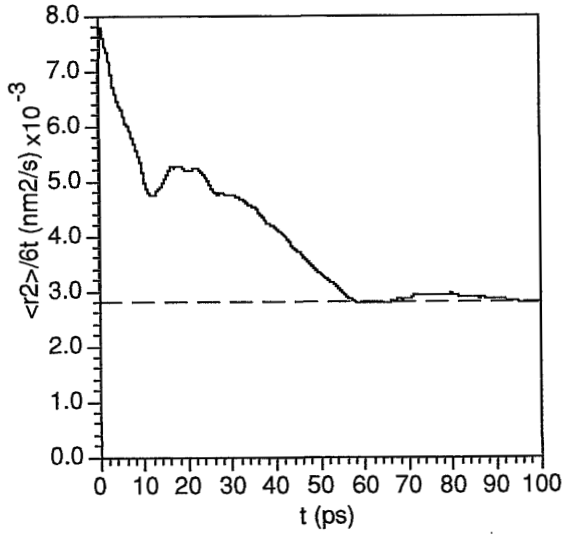

FIGURE 4.15: QUADRATIC DISPLACEMENT FROM ORIGIN VERSUS TIME IN 6FDA-4PDA

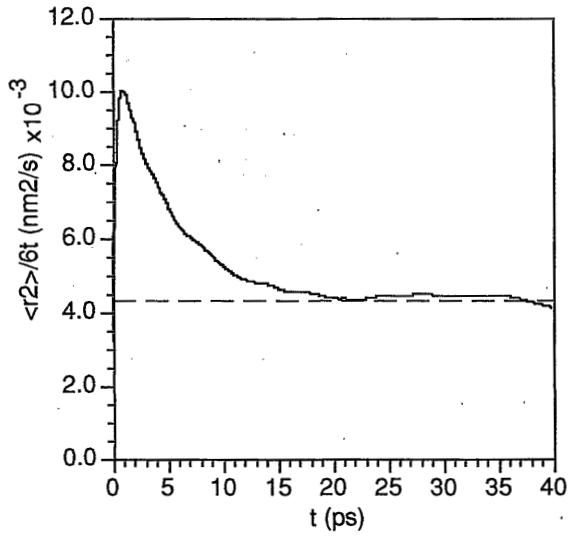

FIGURE 4.16: QUADRATIC DISPLACEMENT FROM ORIGIN VERSUS TIME IN 6FDA-44ODA (AVERAGE OF 10 CO_2 MOLECULES)

The resulting diffusion coefficients thus are:

$\mathbb{D} = 2.7 \cdot 10^{-9}$ m^2s^{-1} for 6FDA-4PDA measured: $2.31 \cdot 10^{-12}$ m^2s^{-1}

$\mathbb{D} = 4.3 \cdot 10^{-9}$ m^2s^{-1} for 6FDA-4,4ODA measured: $2.23 \cdot 10^{-12}$ m^2s^{-1}

The overshoot at the start of the simulation is caused by the fact that the gas molecule can only move *away* from its origin in the beginning of the run. As the simulation proceeds backward motion becomes possible also.

4.5 Discussion on the MD diffusion calculations

The jump of a gas molecule should be accompanied by a levelling of the barrier imposed by the polymer chains that form the boundary between two holes. This was indeed found by Takeuchi [8]: he noticed a temporary tunnel formation between two holes, and the gas molecule taking advantage of this situation by rapidly moving from one hole to the other. This is in accordance with our model. The motion of the polymer chains is thus the rate limiting factor in the diffusive motion of the gas molecule.
Hiwatari and Odagaki (unpublished results, see [8]) have discovered similar jumping behavior of penetrant molecules in a polymer box. They found a square displacement of the gas molecules in time, and defined the process as follows:

" 1. Residence time: during this period the molecule is trapped
2. Flying time: during this period the molecule makes a large jump

The distributions of the residence time and the flying time have very important physical meaning, especially for the diffusion and *the glass transition*". This is essentiality the same model used in Chapters 2 and 3 (from Meares).
No meaningful conclusion about the mean jump distance can be given from the small amount of jumps found so far. Nonetheless it seems that the jump length in the 6FDA-44ODA is larger (up to 13Å) than in the 6FDA-4PDA box (up to 10Å). This would be in accordance with the "classic" model as proposed in Chapter 3, that incorporates the mean distance between the pivot points.
The diffusivity values are about *three orders of magnitude* higher than

the experimental values. Takeuchi [8,9,16] and others also noticed in rubbery polymers a deviation, although smaller. They attributed this to incorrect, small packing density fluctuations caused by the free chain ends or to the crystallinity in the real sample. Sefcik *et al.* [17,18] noticed in ^{13}C-NMR rotating frame relaxation experiments a large difference between the effective (diffusion) and apparent (NMR) mobility of CO_2 in glassy polymers. This seems to indicate that the gas molecules move rapidly, but ineffectively inside holes in the matrix.

We assign the difference to an inaccuracy in the simulated matrix model. The short chains (5 units, 11 segments) have a relatively high amount of end groups: 18% instead of less than 2% for real polymers. This too high amount of end groups contributes very strongly to the unsatisfactory diffusion coefficient. The mobility of these "loose" ends is much higher than that of the middle of the real chain. This has also been found by others but the effect was not always recognized. Trohalaki *et al.* [7] measured the free volume as a function of the degree of polymerization (number of segments) of polydimethyl siloxane and polymethylpropyl siloxane (see Table 4.1).

Table 4.1: Free volume fraction as function of the degree of polymerization (DP)

DP	PDMS	PMPrS
10	0.0746	0.0610
15	0.0885	0.0622
20	0.118	0.0895
25	0.129	0.109

This table shows clearly that the highly mobile ends are effective in filling the holes in the matrix: the larger the fraction of free ends, the higher the packing density. The chain ends will definitely influence the state of the polymer: the more free ends, the more rubbery (even fluid-like) the polymer will be. The same is true for actual polymers: only a sufficiently high degree of polymerization will allow glass formation. This should have a large effect on the diffusion of gas molecules: the diffusion will be enhanced by the relatively much more mobile chain. Takeuchi

noticed this chain length effect: if a PM chain was enlarged from 20 units to an infinite number, the free volume increased from 0.344 to 0.386 (+12%) [16]. But more interesting is the observation that the relaxation time of internal rotations increase by 50%, and the self-diffusion coefficient of the chain decreased from $0.22 \cdot 10^{-5}$ to $8 \cdot 10^{-8}$ cm^2/s, a factor of *28*. This means that the overall chain mobility is significantly reduced when the chain length is increased.
We think that especially for glassy polymers this result is very important.

4.6 Conclusions

Although CAMM is a new technique, it seems to be a very powerful addition to "classical" methods to elucidate the molecular basis of physicochemical processes. However, the results show some inconsistencies such as the too high diffusivity which have to be cleared. The calculated diffusion coefficients must be scaled to achieve the same order as the measured values. The question remains: what are these scaling factors, and where do they originate from. Especially in the glassy polymers which we have investigated it was shown that the deviations are very large, a factor of about 1000.
We think that the relatively large amount of end-groups may be responsible for this anomaly. Although we have not yet investigated this fully, we assume that our system is not really in the glassy state, but at least locally (near the chain ends) in the rubbery state. The highly mobile chain ends create large density fluctuations, thereby facilitating the formation of tunnels for the penetrant. A determination of the self diffusion coefficient of the chains should give a definite answer.
Also the simulation-time is too short in our experiments. Only the jumps seem to contribute to the effective diffusion coefficient, hence a large number of jumps is necessary in order to use the Einstein equation for the calculation of the diffusion coefficient.
Another problem with our system is that modelling packages only use

static electric charges. But, as mentioned in Chapter 2, CO_2 is a non-polar but highly polarizable gas. This may have large interactions with its surroundings, dependent on the selected polymer, an interaction not accounted for in our model. It is plausible that the dipole on CO_2 induced by the polar chains reduces its mobility, as long as the matrix is not plasticized by the penetrant. Simulation experiments with non-polarizable gases such as N_2 or CH_4 are therefore necessary.

Literature

(1) Sok, R., personal communications and pre-prints

(2) Van Gunsteren, W.F. and Berendsen, H.J.C., *Groningen Molecular Simulation Library*, **1987**.

(3) Doolittle, A.K., *J. Appl. Phys.*, **1951**, 22, 1471

(4) Fujita, H., *Fortschr. Hochpolym.-Forsch.*, **1961**, 3, 1

(5) Vrentas, J.S. and Duda, J.L., in *Encyclopedia of Polymer Science and Engineering*, 2nd ed.; Kroschwitz, J., Ed., Wiley, N.Y., **1986**, Vol. 5, p. 36

(6) Shah, V.M., Stern, S.A. and Ludovice, P.J., *Macromolecules*, **1989**, 22, 4660

(7) Trohalaki, S., DeBolt, L.C., Mark, J.E. and Frisch, H.L., *Macromolecules*, **1990**, 32, 813

(8) Takeuchi, H., personal communications and pre-prints

(9) Takeuchi, H., Roe, R.J. and Mark, J.E., accepted for publication in J. Chem. Phys., August 20, 1990

(10) Takeuchi, H. and Okazaki, K., *J. Chem. Phys.*, **1990**, 92(9), 5643

(11) Rigby, D. and Roe, R.J., *J. Chem. Phys.*, **1987**, 87, 7285

(12) Van Eerden, J., unpublised results

(13) Harkema, S., Karrenbeld, H., Smit, E., and Feil, D., to be published

(14) Clarke, J.H.R. & Brown, D., *Molec. Sim.*, **1989**, 3, 27

(15) Weber, T.A. & Helfand, E., *J. Chem. Phys.*, **1979**, 71, 4760

(16) Takeuchi, H., *J. Chem. Phys.*, **1990**, 93, 4490

(17) Sefcik, M.D., Shaefer, J., May, F.L., Raucher, D. and Dub, S.M., *J. Polym. Sci., Polym. Phys.*, **1983**, 21, 1041

(18) Sefcik, M.D. and Shaefer, J., *J. Polym. Sci., Polym. Phys.*, **1983**, 21, 1055

SUMMARY

When new, better polymeric materials are to be developed for use as gas separation membranes, knowledge of the underlying principles of the separation process is essential. Much research is spent on the elucidation of the mechanism by which gas molecules sorb into and move through a polymer. Models were developed to describe the macroscopic behavior of the polymer in gas separation processes. The most widely used is the dual mode sorption model. To gain further insight in the mechanism the *microscopic* behavior, i.e. at a molecular scale, has to be considered.
This thesis deals with one aspect of this last topic: the diffusion of gases through the polymer matrix, viewed at a molecular scale. In Chapter 1 the uses and possibilities of gas separation membranes are briefly explained, and the research objectives are given as well as the justification of the choice of the polymers.
Then a molecular model of the diffusion process is created. First by using "classical" methods (Chapters 2 and 3), followed by *computer aided molecular modelling* (CAMM, Chapter 4).

In Chapter 2 the finding of a remarkable relation between the heat capacity jump at the glass transition temperature of a polymer and the permeability for CO_2 in a series of novel polyimides necessitated a model that describes the process at a molecular level. The ideas of Brandt and Meares are used. A model of the polymer matrix is build as being the sum of four levels of organization of the polymeric chains: the chemical/electronic structure, the chain folding, the chain packing and the non-equilibrium state of the matrix. This last level incorporates the excess free volume. A Boltzmann-type of distribution of the free volume in the matrix over small and larger holes is proposed. The diffusion of a gas molecule can be described by a jumping mechanism, moving from hole to hole. Temporary tunnels have to be created by the polymer chains to let the gas molecule perform the jumps. Thus the rate of diffusion of the gas molecule is restricted by the rate of movement of the chains. This

polymer dependent diffusion process can explain the found relation.
In Chapter 3 the synthesis of two polyimide series for the study is described. The series are based on 6FDA- and SiDA-dianhydride moieties as constant structural units. From the experimental data an exponential relation between the cohesive energy density (CED) of the polymer and the diffusion coefficient of the gas can be ascertained. An important parameter in this relation is the diffusional jump length. The validity of the model given in Chapter 2 could thus be examined.
To further refine the molecular model a more detailed look into the matrix is necessary. Since this is physically impossible, a computer model of the matrix was created, and the diffusion process was simulated (Chapter 4). CAMM is also used in Chapter 3, to explain the unexpected behavior of *meta*- versus *para*-isomeric polymers. The *meta*-isomers appear to have more flexible chains, resulting in a narrower free volume distribution and thereby in a lower permeability and diffusivity.
The movement of a CO_2 molecule inside the computer model of the polymer matrix shows a clear jumping behavior, as could be expected from the "classical" model. However, the thus calculated diffusion coefficient is three orders of magnitude higher than the measured value. A possible explanation can be found in the relatively large amount of free end-groups in the computer model. These mobile free ends result in an overall higher mobility of the polymeric chains. Since the chain mobility restricts the diffusivity of the gas molecule (cf. Chapters 2 and 3), this factor could account for the large discrepancy.
A new computer model is thus essential.

SAMENVATTING

Bij het ontwikkelen van nieuwe, betere polymeren voor gebruik als gasscheidingsmembranen is kennis van het mechanisme van de scheiding onontbeerlijk. Er wordt veel onderzoek verricht naar het mechanisme van de sorptie van een gasmolecuul in, en de beweging door een polymeer. Er zijn modellen ontwikkeld om het macroscopische gedrag van polymeren bij gasscheiding te beschrijven. Het meest gebruikte is het 'dual-mode sorption' model. Om meer inzicht te krijgen in het mechanisme moet echter het *microscopische* gedrag, dat wil zeggen op moleculaire schaal, worden bestudeerd.
Dit proefschrift beschrijft één aspect van dit laatste onderwerp: de diffusie van gassen door de polymere matrix op moleculaire schaal.
In Hoofdstuk 1 worden kort het gebruik en de mogelijkheden van gasscheiding met membranen uiteengezet. Verder wordt er het doel van het onderzoek beschreven, evenals een verantwoording voor de keuze van de polymeren.
Een moleculair model van het diffusieproces wordt opgebouwd, eerst met behulp van "klassieke" methoden (Hoofdstukken 2 en 3), daarna door middel van *computer aided molecular modelling* (CAMM, Hoofdstuk 4).

In Hoofdstuk 2 maakt de gevonden relatie tussen de warmtecapaciteitssprong op de glasovergangstemperatuur van een polymeer en de permeabiliteit voor CO_2 het noodzakelijk om een model te creëren dat het proces op een moleculaire schaal beschrijft. De ideëen van Brandt en Meares worden gebruikt. Een model van de polymere matrix wordt opgebouwd als de som van vier niveau's van polymere keten organisatie: de chemische/electronische structuur, de ketenvouwing, de ketenpakking en de niet-evenwichtstoestand van het polymeer. Dit laatste niveau bevat ook het overmatige vrije volume. Een Boltzmann-type verdeling van het vrije volume in de matrix (over de kleine en de grotere gaten) wordt voorgesteld. De diffusie van gasmoleculen door de matrix kan worden beschreven als een sprongsgewijze beweging van holte naar holte. Een

tunnel tussen beide holtes moet daartoe tijdelijk door de polymeerketens worden gevormd. De diffusiesnelheid van het gasmolecuul wordt aldus beperkt door de bewegingssnelheid van de polymeerketens. Deze *polymeerafhankelijke* diffusie kan de gevonden relatie verklaren.
In Hoofdstuk 3 wordt de synthese van twee polyimide series beschreven. De series zijn gebaseerd op 6FDA- en SiDA-dianhydrides als vaste structuureenheden. Uit de experimentele gegevens volgt een exponentiële relatie tussen de cohesieve energiedichtheid (CED) van het polymeer en de diffusiecoëfficiënt van het gas. Een belangrijke parameter in deze relatie is de diffusie-spronglengte. Dit is een sterke aanwijzing dat het voorgestelde moleculaire model juist is.
Om het model verder te verfijnen is een meer gedetailleerde kijk in de matrix noodzakelijk. Omdat dit niet direct mogelijkis, is een computermodel van de matrix gecreëerd (Hoofdstuk 4). CAMM is ook in Hoofdstuk 3 gebruikt om het onverwachte gedrag van *meta*- versus *para*-isomeren van een polymeer te verklaren. Het blijkt dat de polymeerketens in de *meta*-isomeren flexibeler zijn, wat als gevolg heeft dat de vrije volumeverdeling nauwer wordt. Dit resulteert in een lage permeabiliteit en diffusiecoëfficiënt.
Het volgen van een CO_2 molecuul door de gesimuleerde polymere matrix laat duidelijk een sprongsgewijze beweging zien, als was verwacht op grond van het "klassieke" model. Echter, de aldus berekende diffusiecoëfficiënt is een factor 1000 hoger dan de gemeten waarde. Een mogelijke verklaring is de relatief te hoge concentratie aan vrije eindgroepen in het computermodel. Aangezien deze mobiele groepen de algehele beweeglijkheid van de keten sterk verhogen, en de gas diffusie beperkt wordt door de ketenbeweeglijkheid (zie Hoofdstukken 2 en 3), zal dit een onrealistisch hoge diffusie-coëfficiënt opleveren.
Een nieuw computermodel is dus noodzakelijk.

WIE IS EVERT?

Evert Smit is op 11 juli 1961 geboren te Delft. Aan de dr. Aletta Jacobs scholengemeenschap te Hoogezand haalde hij in 1978 het HAVO diploma, en in 1979 het VWO diploma. In datzelfde jaar begon hij aan de Rijksuniversiteit Groningen met de studie scheikunde. In 1982 haalde hij het kandidaatsexamen S1. Eind 1982 zette hij zijn studie voort aan de Katholieke Universiteit Nijmegen, waar hij op 27 februari 1987 het doctoraalexamen scheikunde (hoofdrichting organische chemie bij prof. Tesser) behaalde. Op 1 februari 1987 trad hij in dienst als medewerker onderzoek aan de Universiteit Twente bij de vakgroep van prof. Smolders, in het kader van een BRITE project. Het vervolg op dit project (eerste geldstroom), de studie naar het moleculaire mechanisme van de gasdiffusie door een polymeer membraan, staat beschreven in dit proefschrift. Op 1 mei 1991 trad hij in dienst als medewerker onderzoek in tijdelijke dienst (post-doc) bij dezelfde vakgroep.